Surface Structure determination by Synchrotron X-ray Diffraction

I. K. Robinson
University College, London
and Diamond Light Source

ICTP School on Synchrotron Radiation
May 25th, 2006

Important Contributions from

Sanjit Ghose	Urbana
Peter Bennett	Arizona
Franz Himpsel	Wisconsin
Jia Wang	Brookhaven
Ratko Adzic	Brookhaven
Ben Ocko	Brookhaven
Sebastien Boutet	Urbana
Marie-Claire St Lager	CNRS
Pierre Dolle	CNRS
Maurizio deSantis	CNRS
Robert Baudouing-Savois	CNRS
X16A, X22A	NSLS
BM32	ESRF

Menu of Topics

- Crystal Truncation Rods
- Au quantum nanowires on Stepped Si
- Reconstruction of Pt(110)1x5
- Facetting of Cu(115) to Cu(104)
- Au ‘physisorption’ on Si(111)7x7
- Deep subsurface strain in Pt(111)/CO
- GSAXS and C-GSAXS new methods

Origin of Truncation Rods

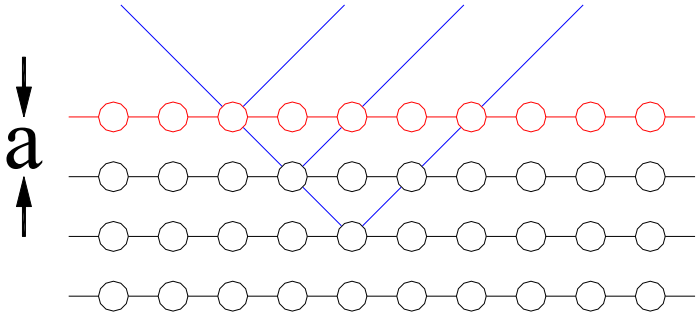

$$F_{CTR} = \sum_{n=0}^{\infty} A_n$$

$$= \sum_{n=0}^{\infty} f_L \; e^{inqa}$$

$$= \frac{f_L}{1 - e^{iqa}}$$

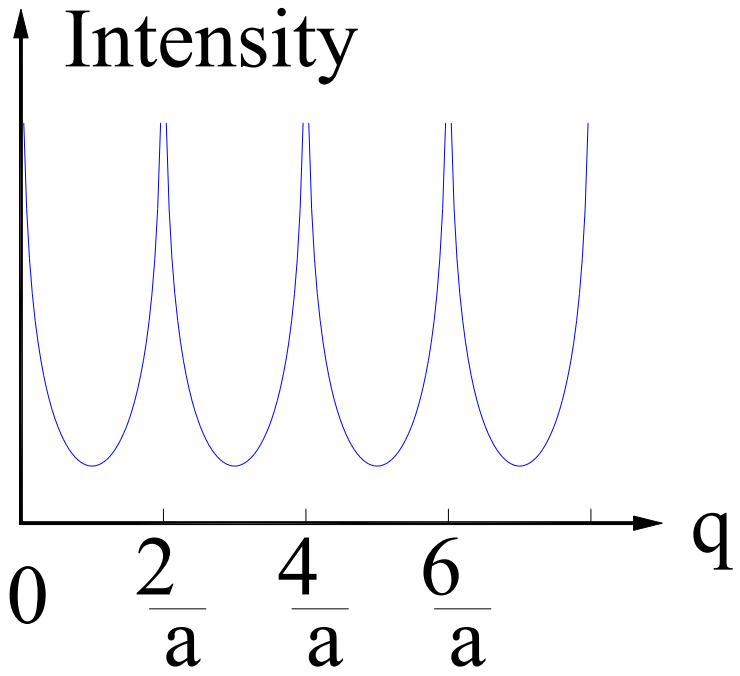

CTR as Convolution

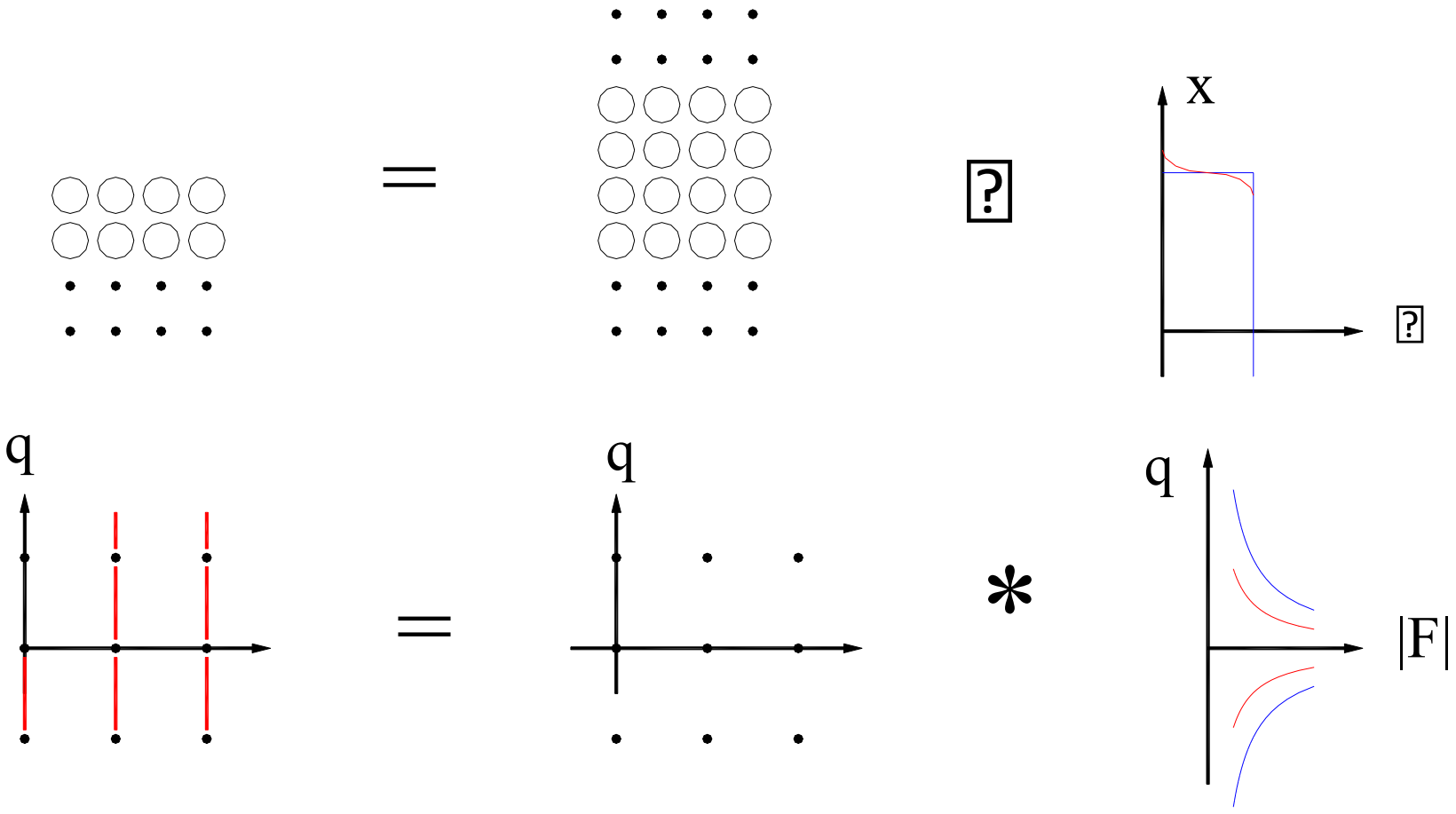

Surfaces and Interfaces

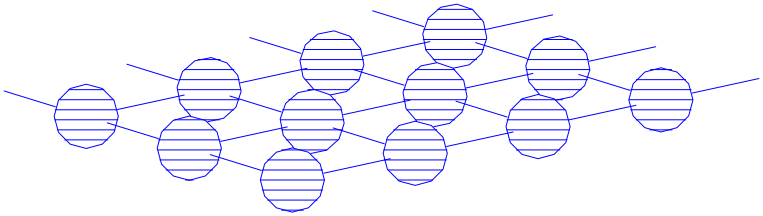

Isolated monolayer

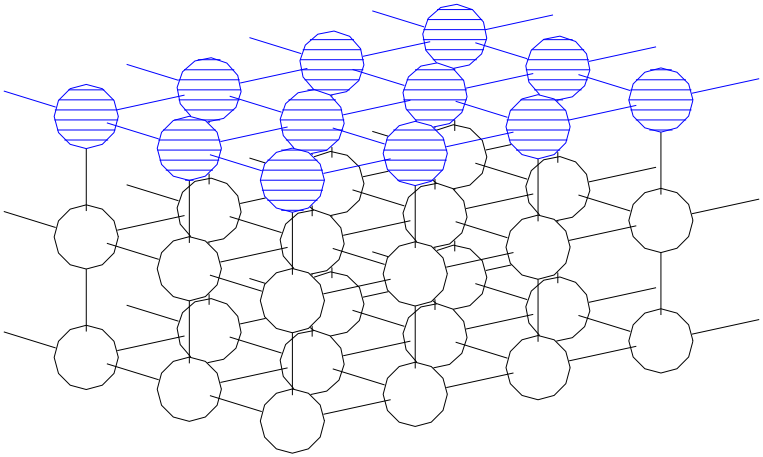

Surface of Crystal

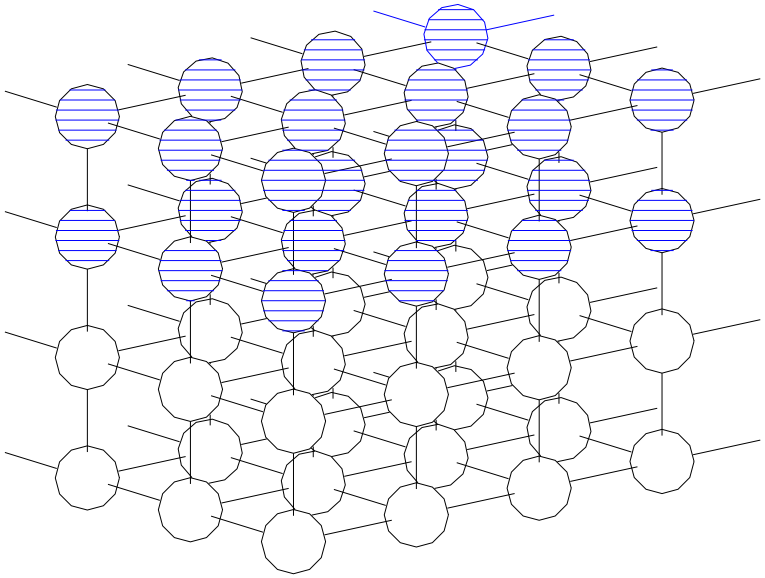

Crystal-Crystal Interface

Diffuse Scattering from Si Wafer

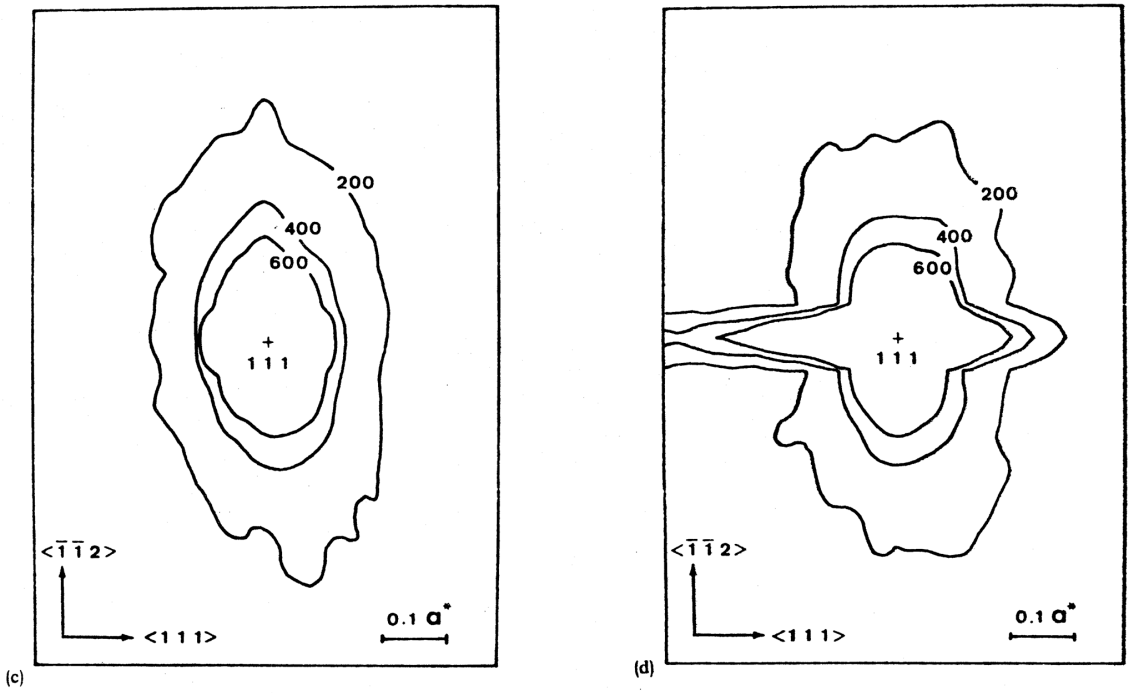

Unpolished wafer 40 microns removed

N. Kashiwagara, J. Harada and M. Ogino, J. Appl. Phys 54 2706 (1983)

Diffraction as a Surface Integral

Die äußere Form der Kristalle in ihrem Einfluß auf die Interferenzerscheinungen an Raumgittern

Von M. v. Laue

Annalen der Physik [5] 26 55 (1936)

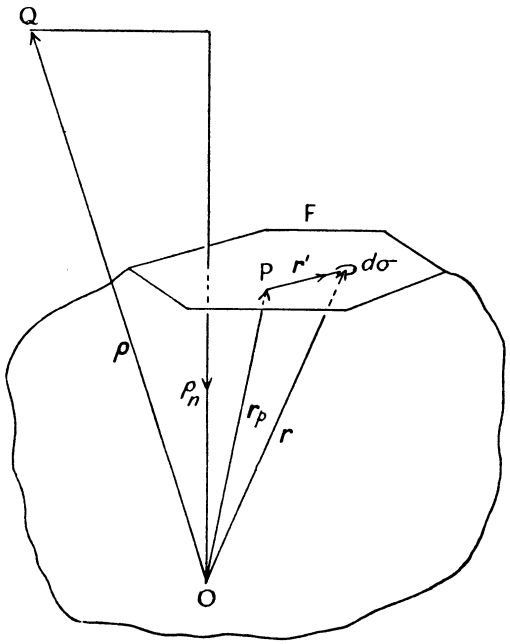

FIG. 200

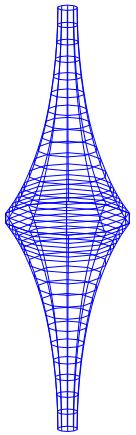

"Stacheln"

CTR is Sensitive to Surface Structure

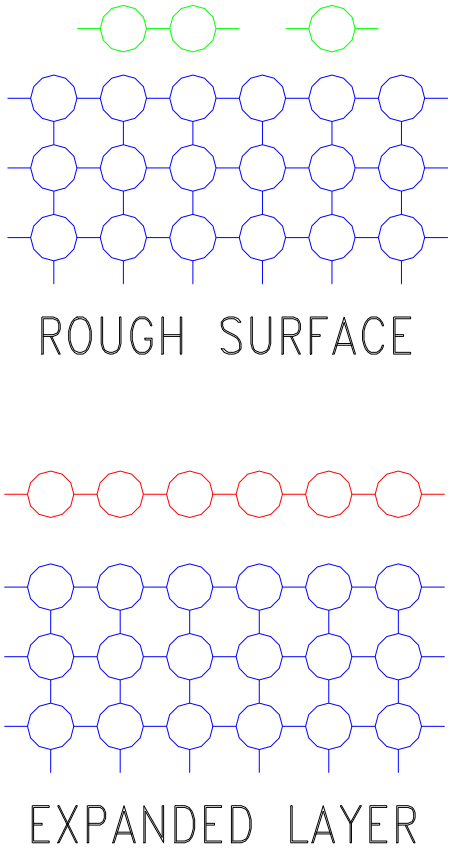

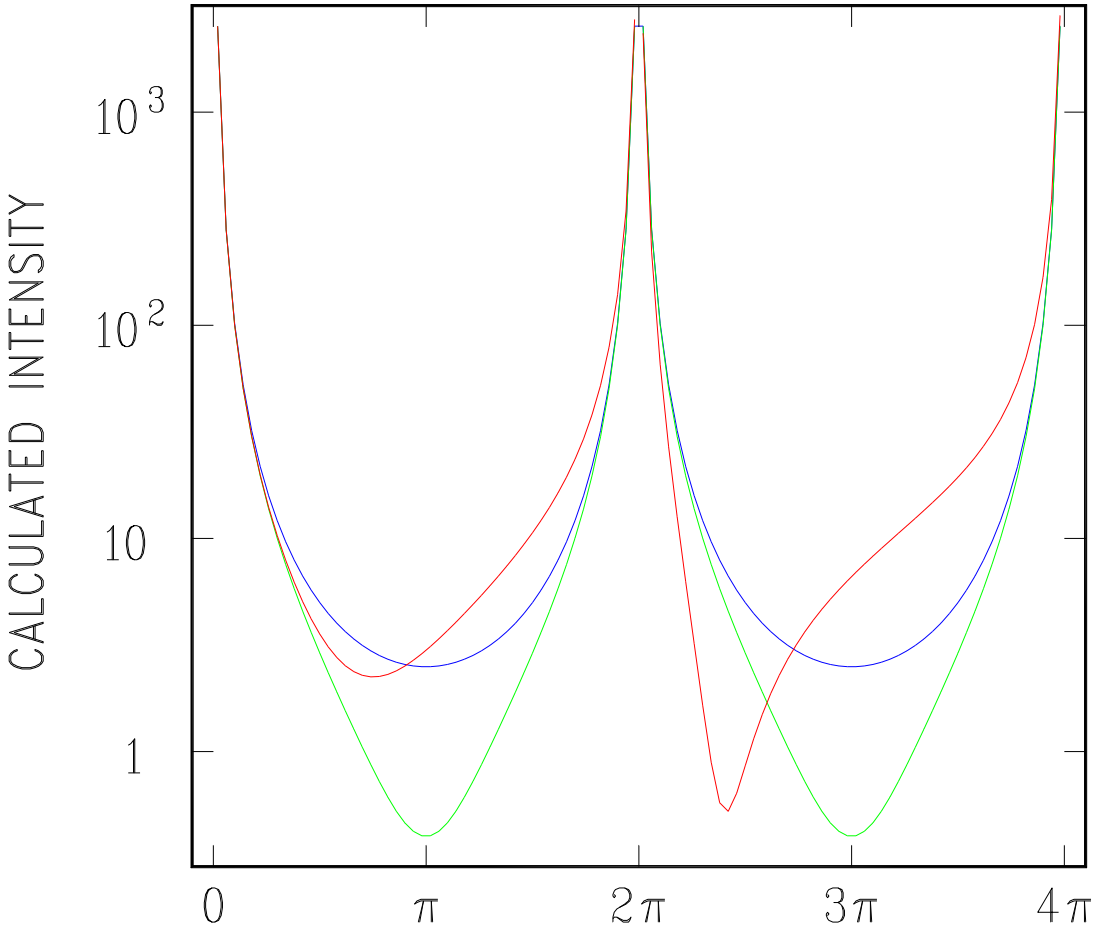

X16A Surface X-ray Diffraction

operating since 1987 ...

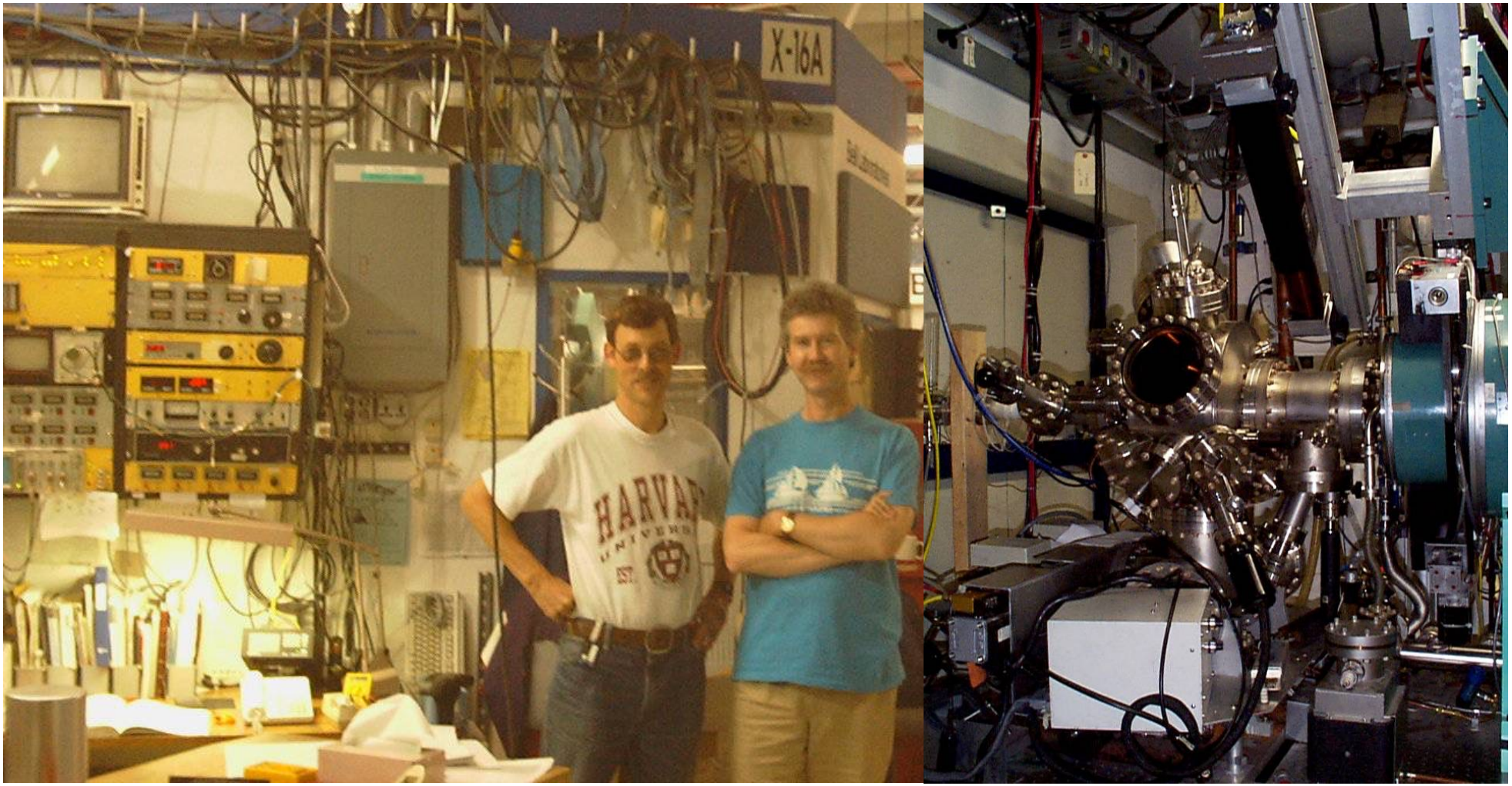

Menu of Topics

- Crystal Truncation Rods
- Au quantum nanowires on Stepped Si
- Reconstruction of Pt(110)1x5
- Facetting of Cu(115) to Cu(104)
- Au ‘physisorption’ on Si(111)7x7
- Deep subsurface strain in Pt(111)/CO
- GSAXS and C-GSAXS new methods

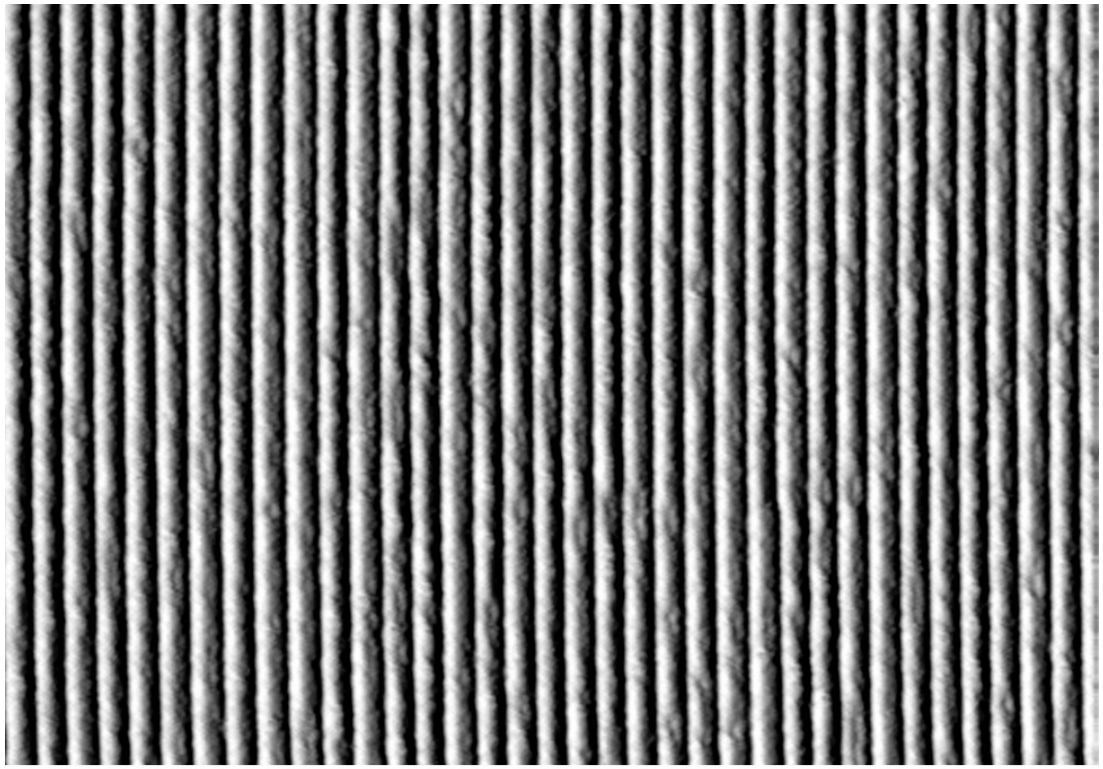

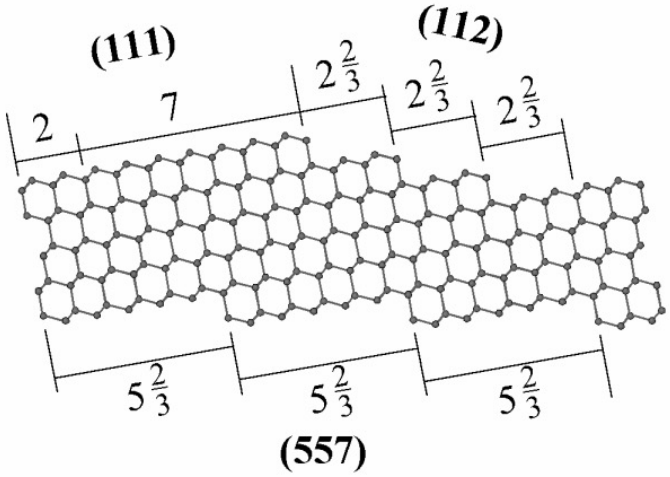
(111)
(112)
2
7
$2\frac{2}{3}$
$2\frac{2}{3}$
$2\frac{2}{3}$
$5\frac{2}{3}$
$5\frac{2}{3}$
$5\frac{2}{3}$
(557)

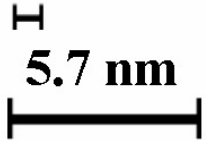
5.7 nm

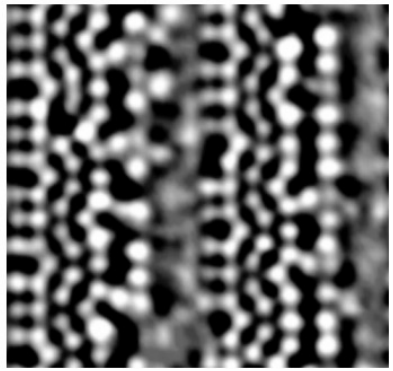

Crystallography of Stepped Surfaces

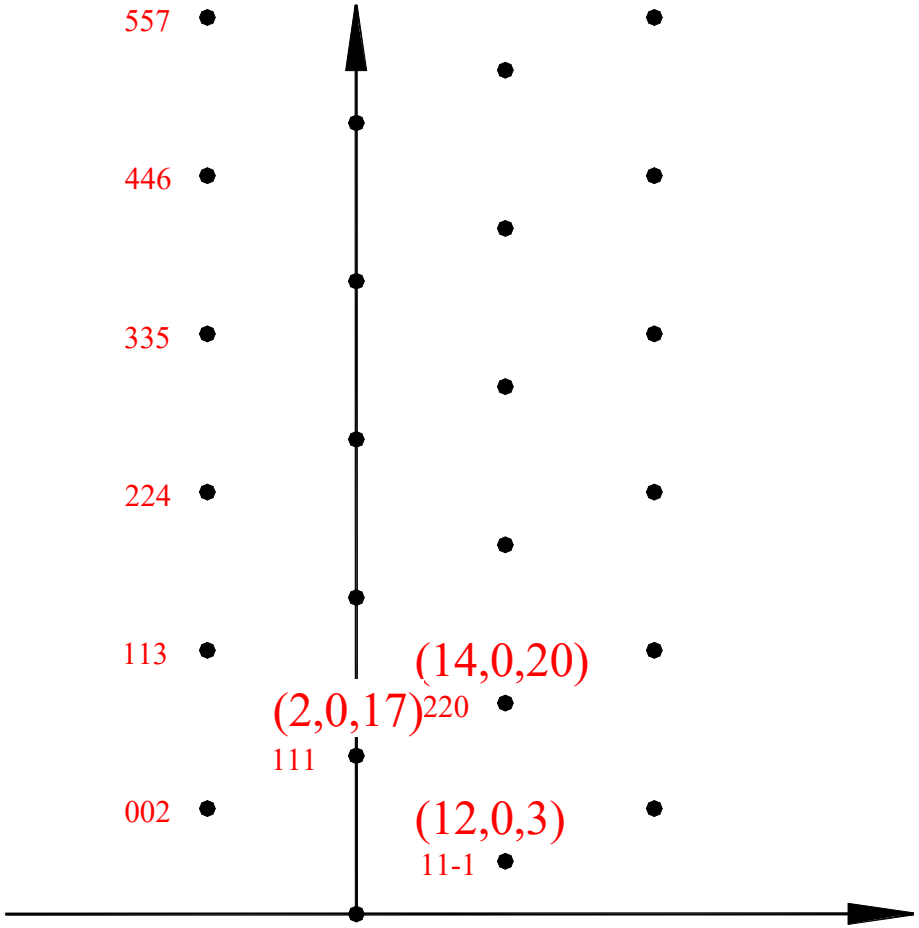

Silicon (111)

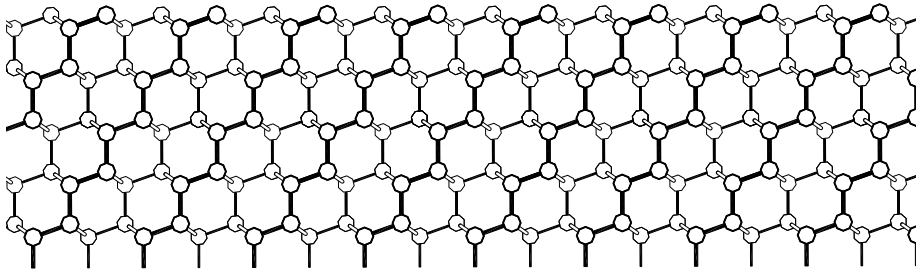

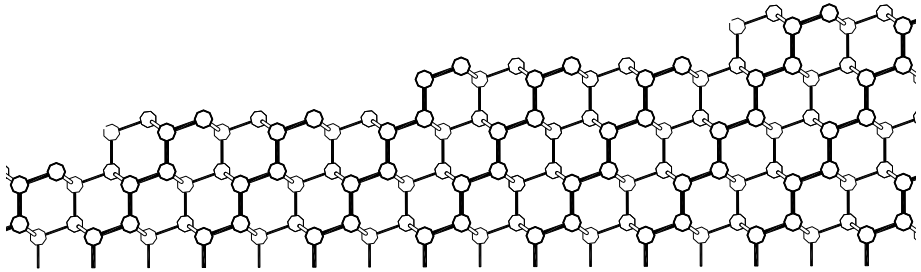

Si(557) surface

ıool on SR

Alignment is Straightforward

```
CALCULATED PARAMETERS:
          A           B           C       ALFA    BETA    GAMMA
REC:  0.164431    1.63392    0.116412   90.06   90.03   89.93
DIR:   38.2118    3.84548     53.9736   89.94   89.97   90.07
          H    K     L     TTH      TH      PHI      CHI      ALP      CTS    ERROR
OR 1 = 12.0  0.0   3.0  21.938 112.920   50.308   -1.137    3.841    22456  0.0027
OR 2 = -5.0  1.0   7.0  20.284  97.018  307.482   -2.259    9.179    20719  0.0018
OR 3 = 14.0  0.0  20.0  26.411 113.142   40.844   -1.290   26.483    13639  0.0009
OR 4 = 12.0  2.0   3.0  43.135 110.470    4.520   -2.092    4.313    12772  0.0009
Lambda = 1.20913 A, wv = 5.19647, Energy = 10.2542 keV (FIXED)
Five-Circle Mode using alm = 2 and bem = 2:
```

Centered Orthorhombic unit cell contains two steps.

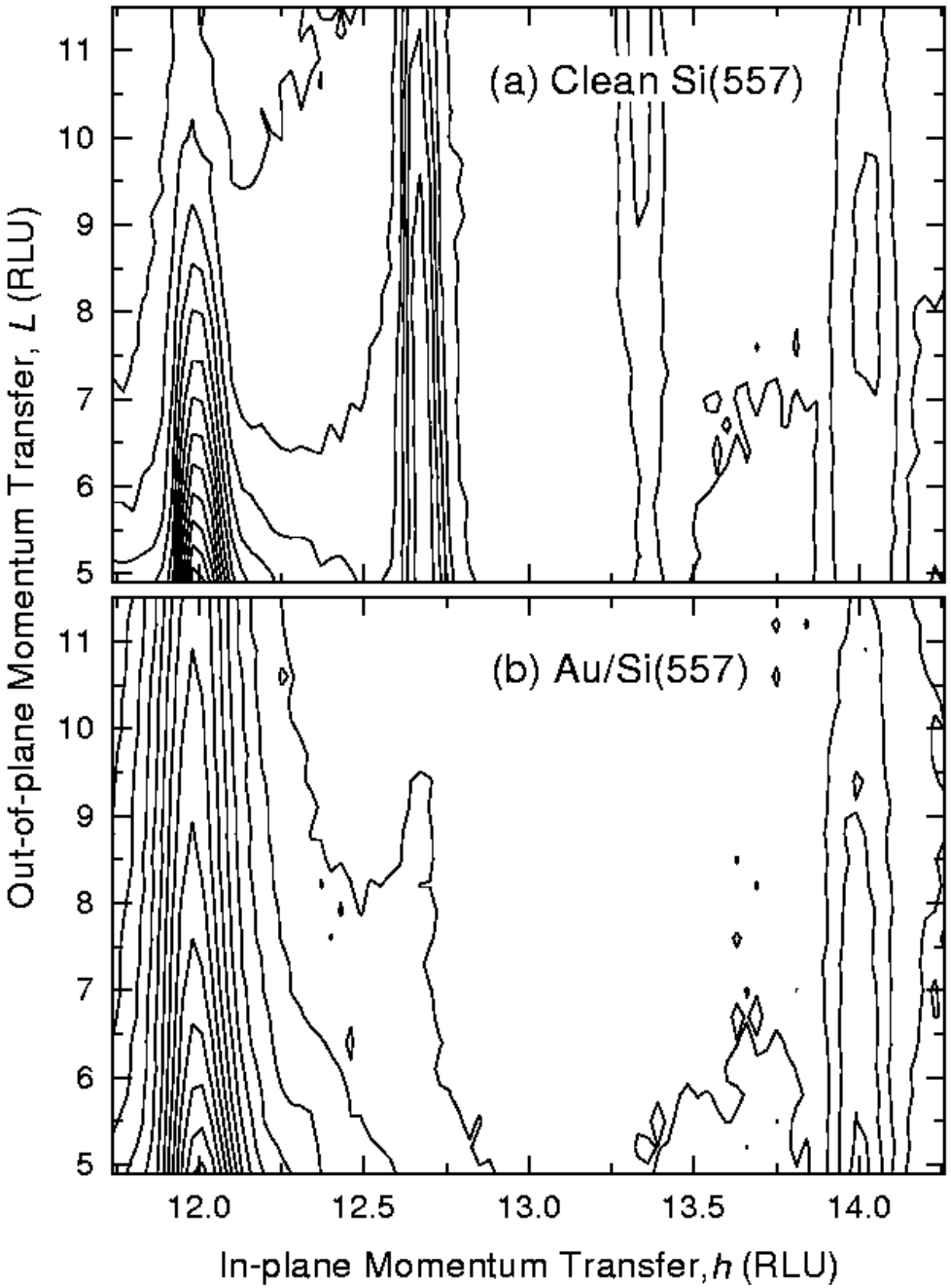

3×1 clean surface

1×1 surface with 0.2ML Au at 600C

STM of Si(557)/Au

R. Losio, et. al., Phys. Rev. Lett. 86 4632 (2001)

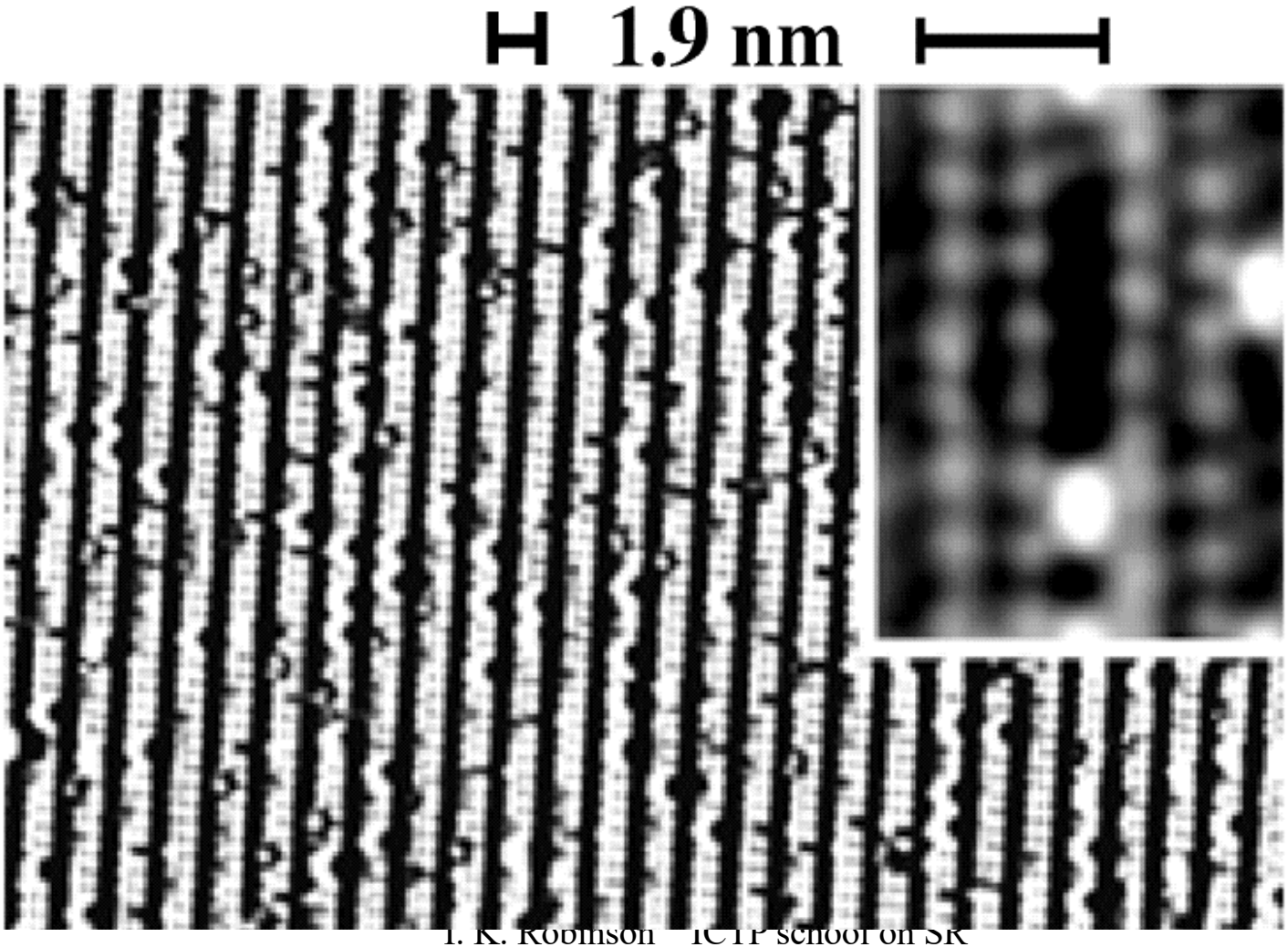

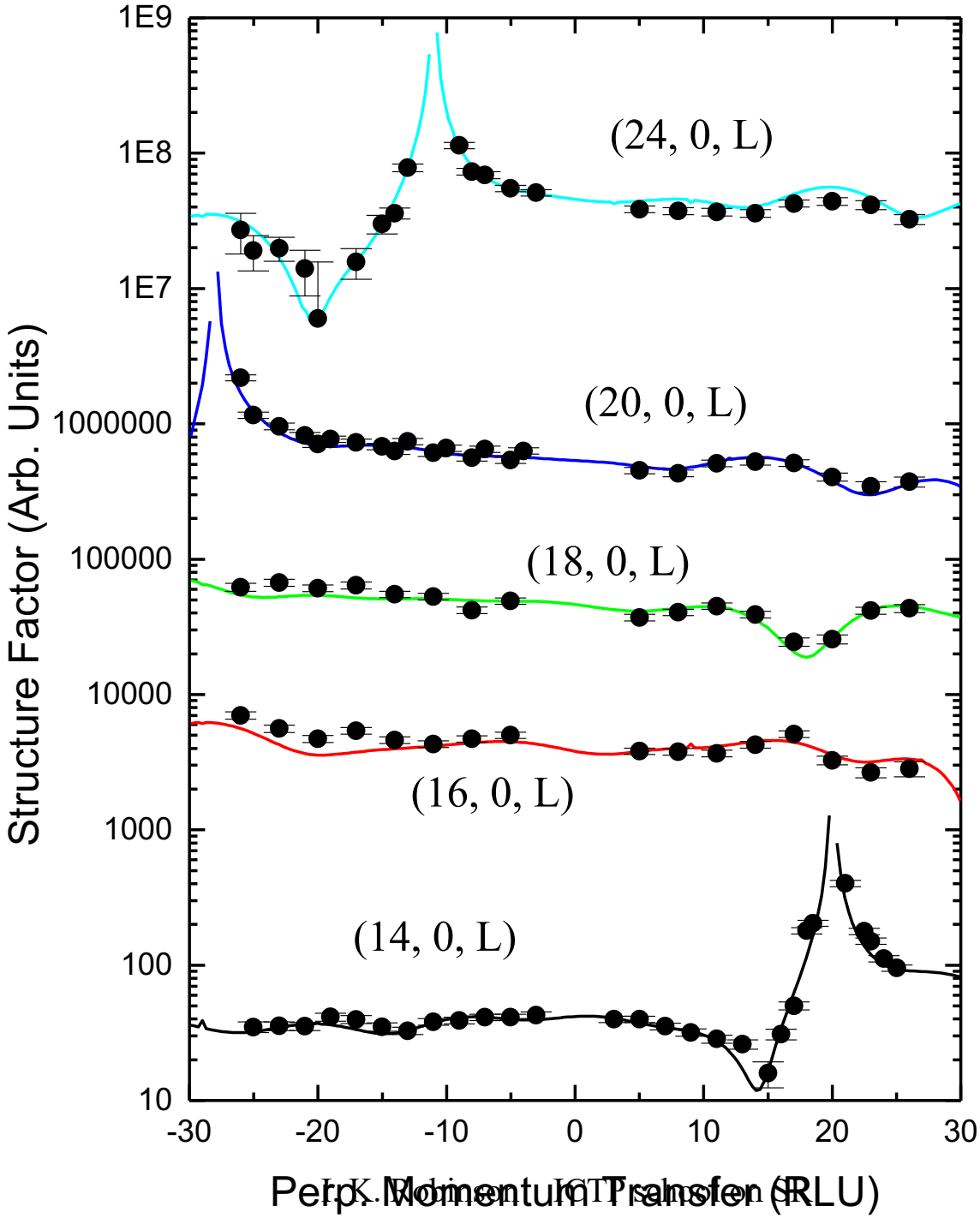

1E9
1E8
1E7
1000000
100000
10000
1000
100
10
-30
-20
-10
0
10
20
30
Structure Factor (Arb. Units)
Perp. Momentum Transfer (RLU)
(24, 0, L)
(20, 0, L)
(18, 0, L)
(16, 0, L)
(14, 0, L)

Phasing by a Single Heavy Atom

H. B. Dyer, Acta Cryst. 4 42 (1951)

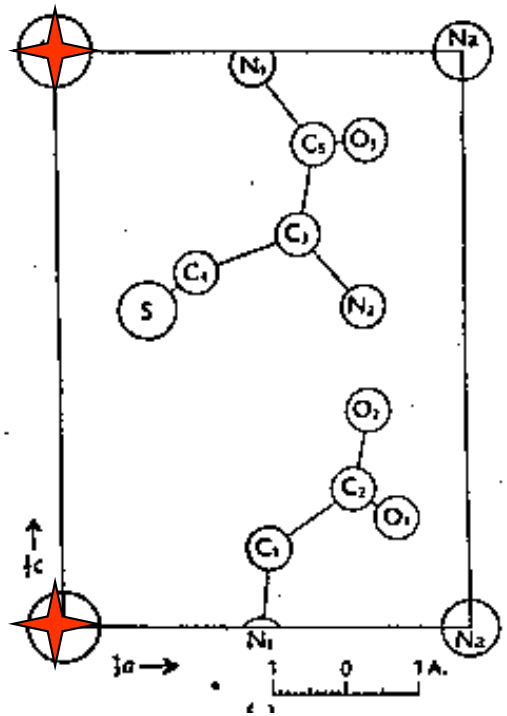

Cysteinylglycine sodium iodide

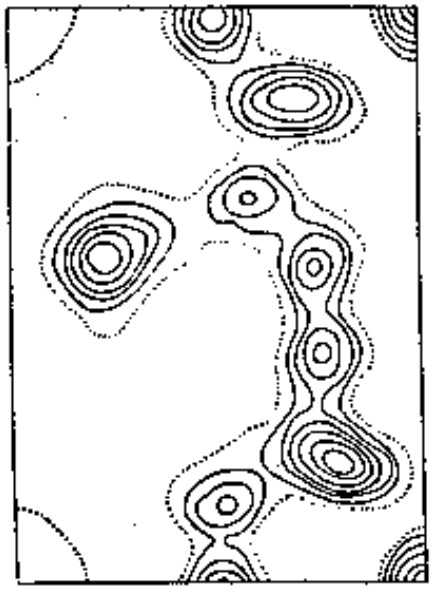

Patterson

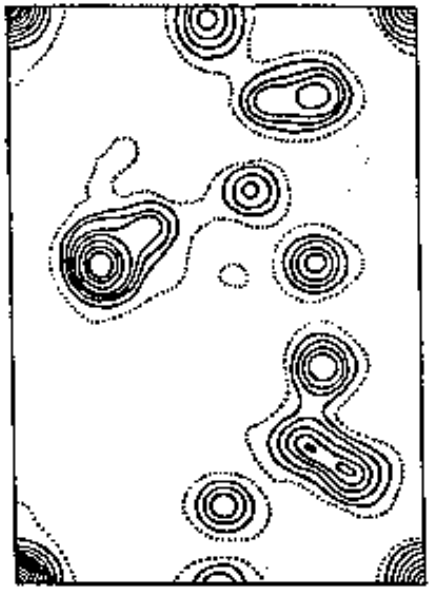

Electron density

X-Z Patterson of Au/Si(557)

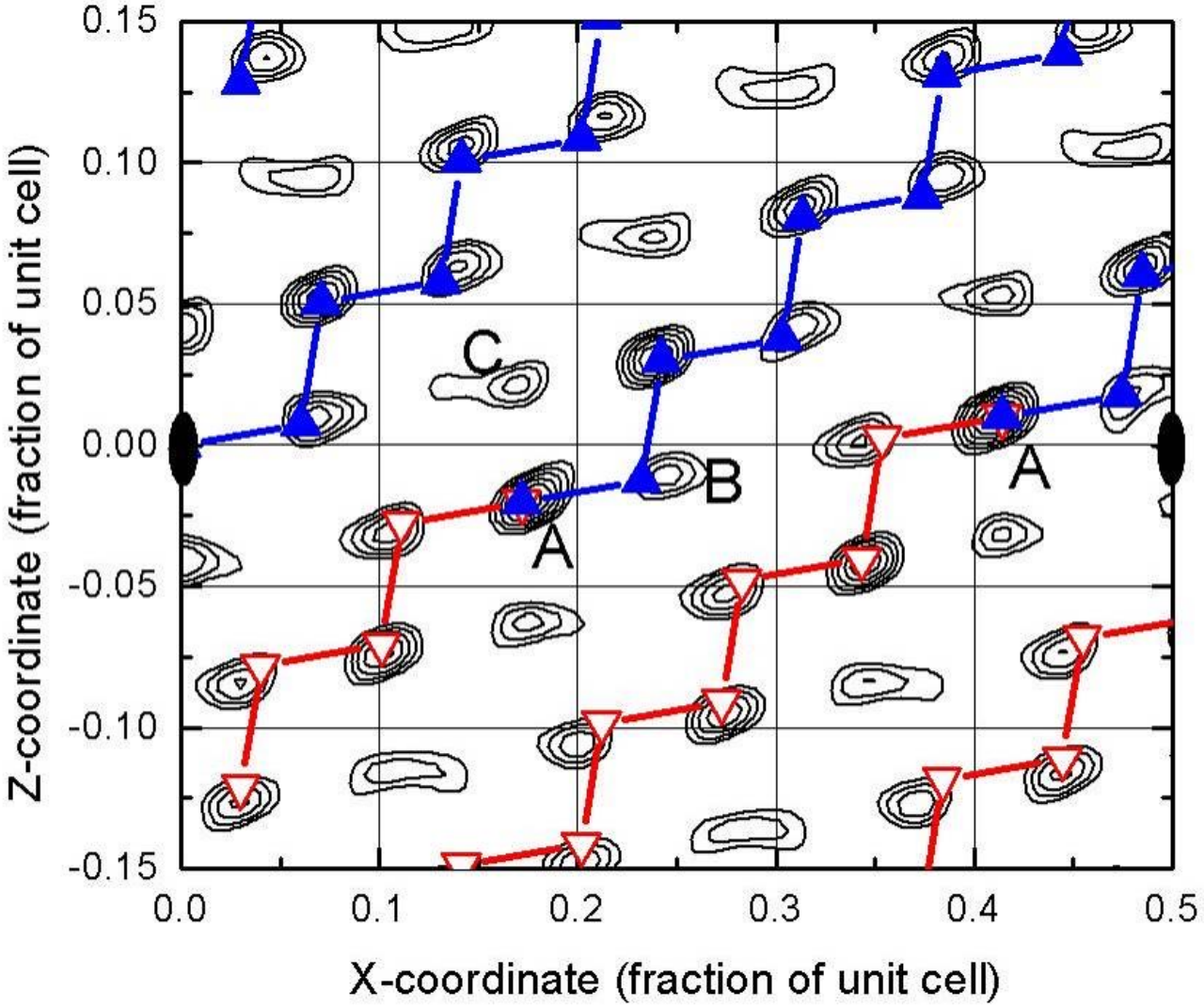

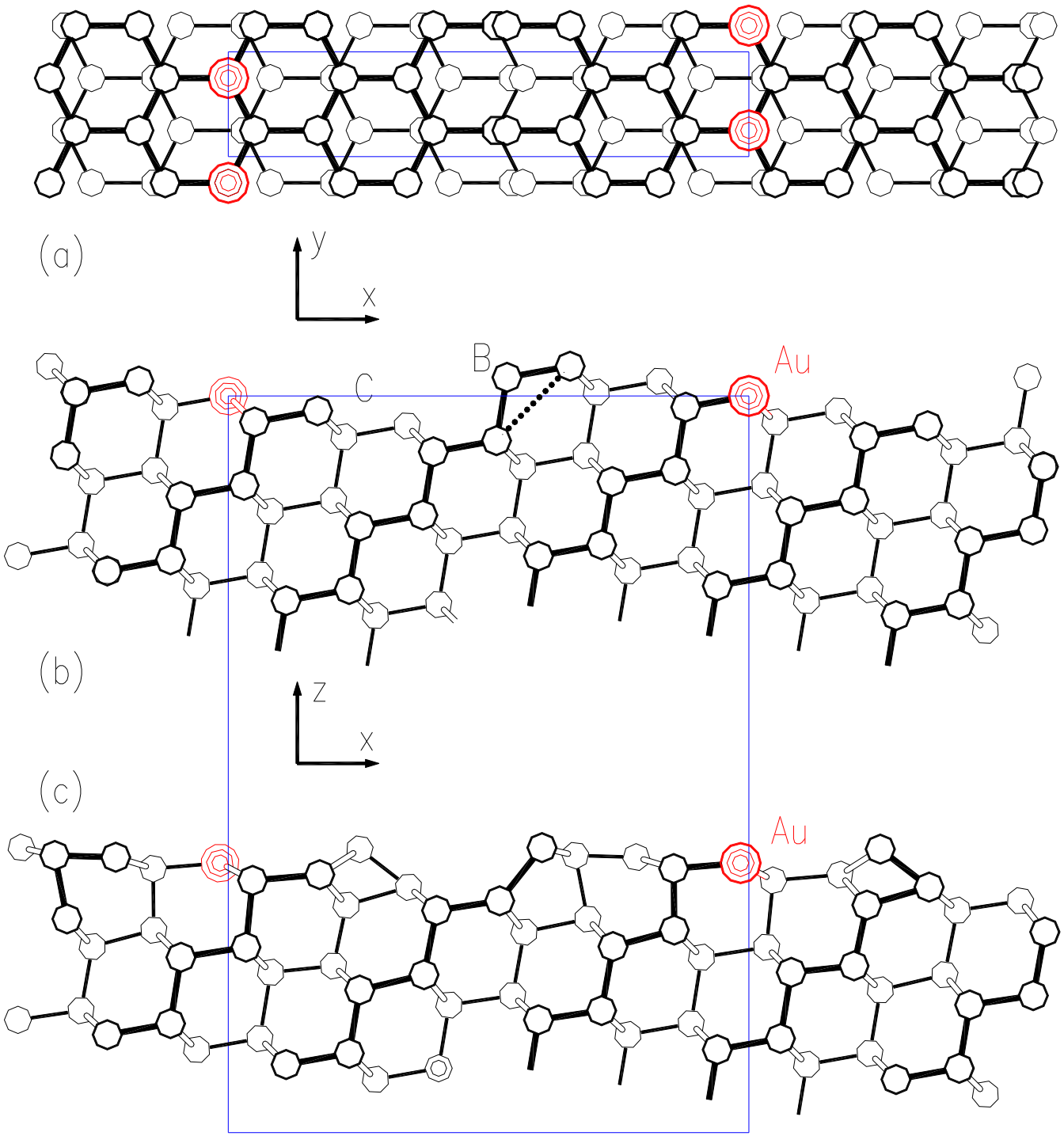
(a)
y
x
B
C
Au
(b)
z
x
(c)
Au

Comparison with STM

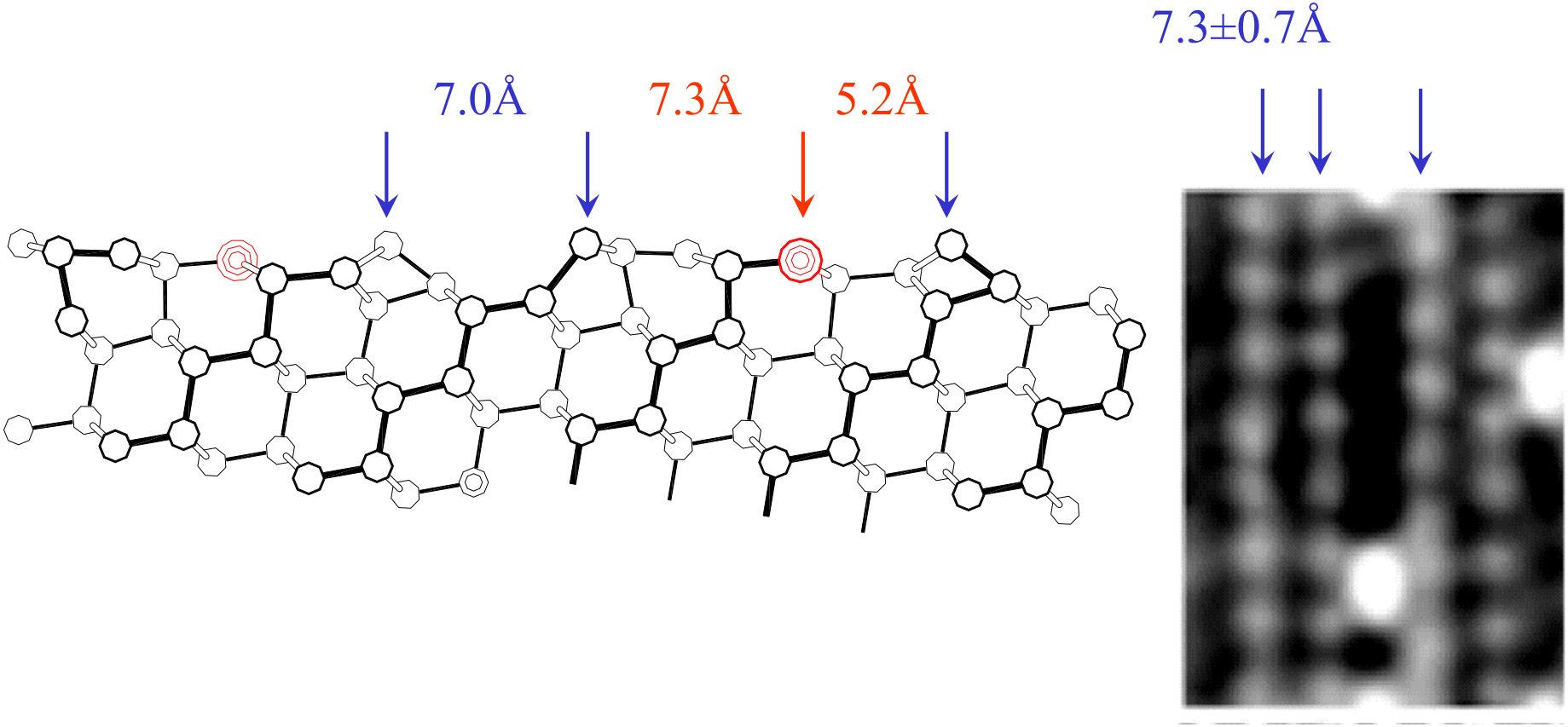

Menu of Topics

- Crystal Truncation Rods
- Au quantum nanowires on Stepped Si
- Reconstruction of Pt(110)1x5
- Facetting of Cu(115) to Cu(104)
- Au ‘physisorption’ on Si(111)7x7
- Deep subsurface strain in Pt(111)/CO
- GSAXS and C-GSAXS new methods

Surface “Reconstruction”

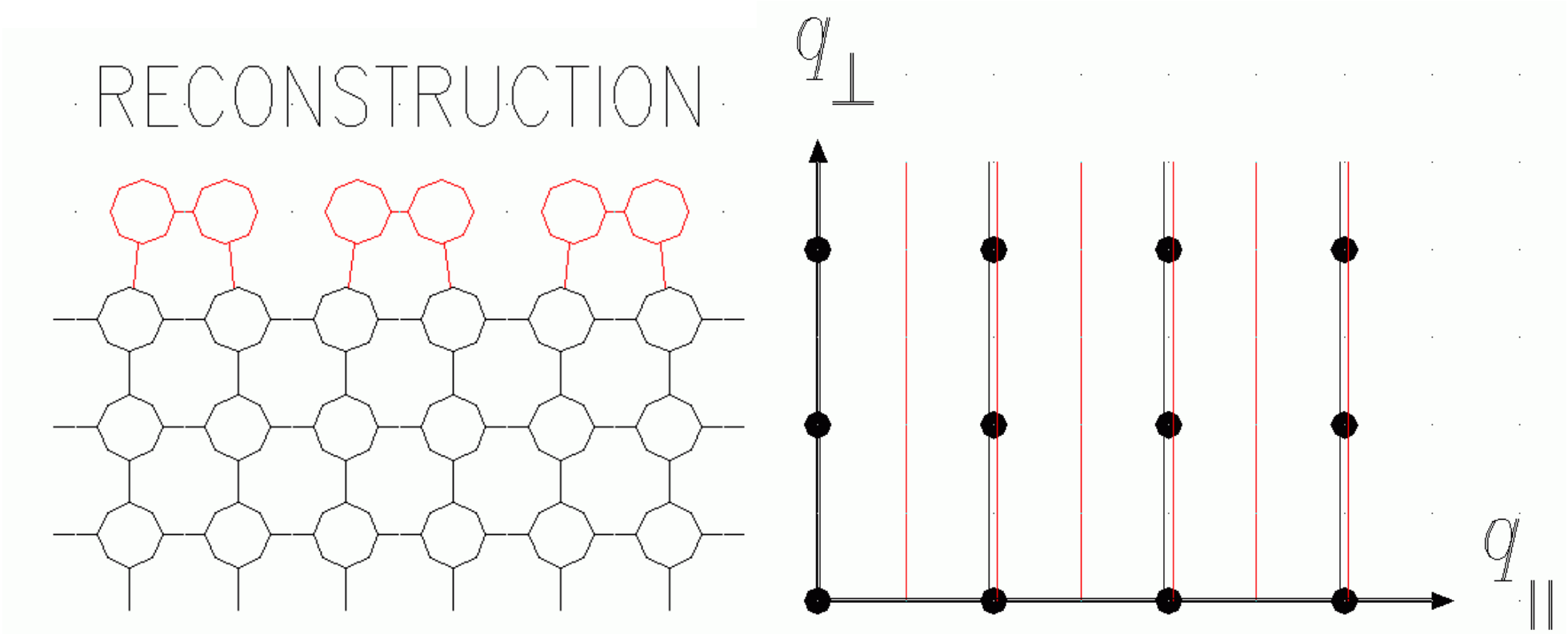

Missing Row structure of FCC(110)

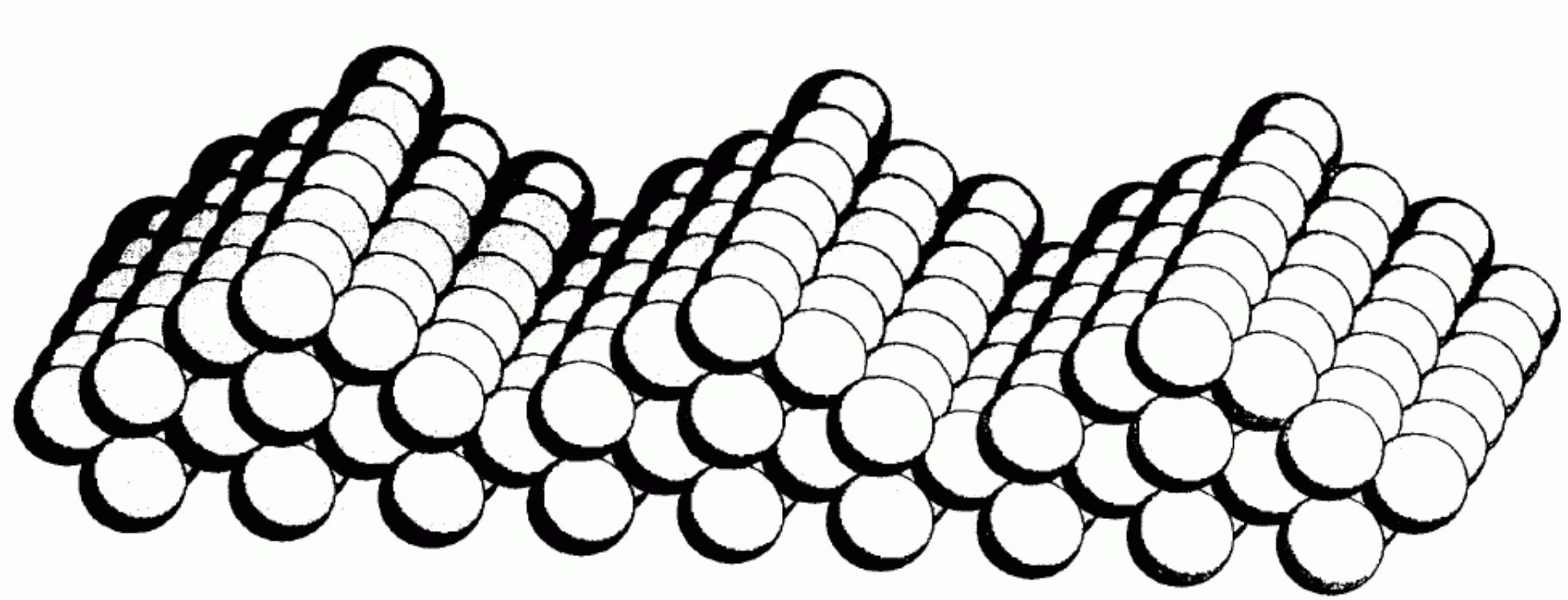

Pt(110) 1×3 Missing Row Structure

Variations of Missing Row structure

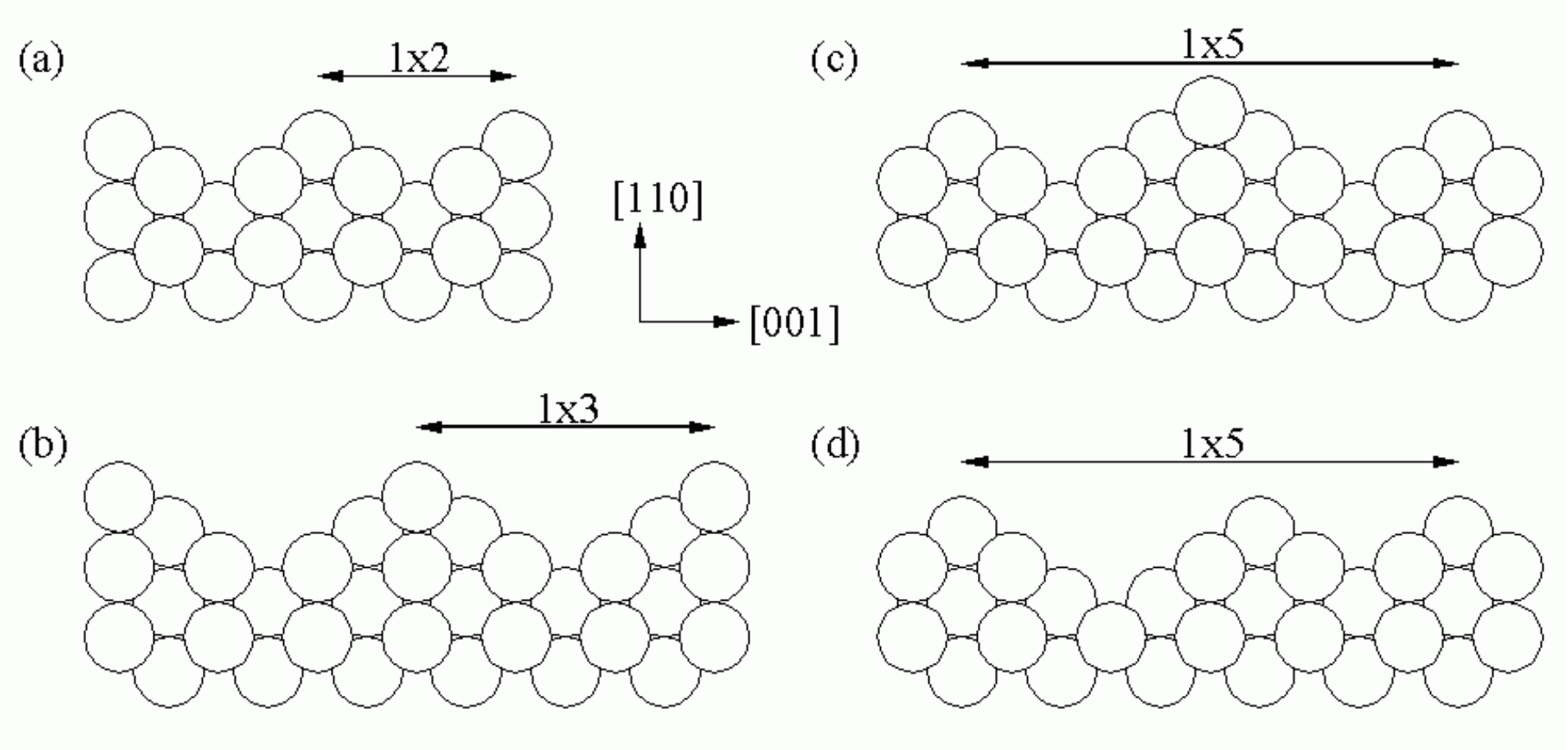

Pt(110) during heating at 600C

Accompanied by segregation of Carbon

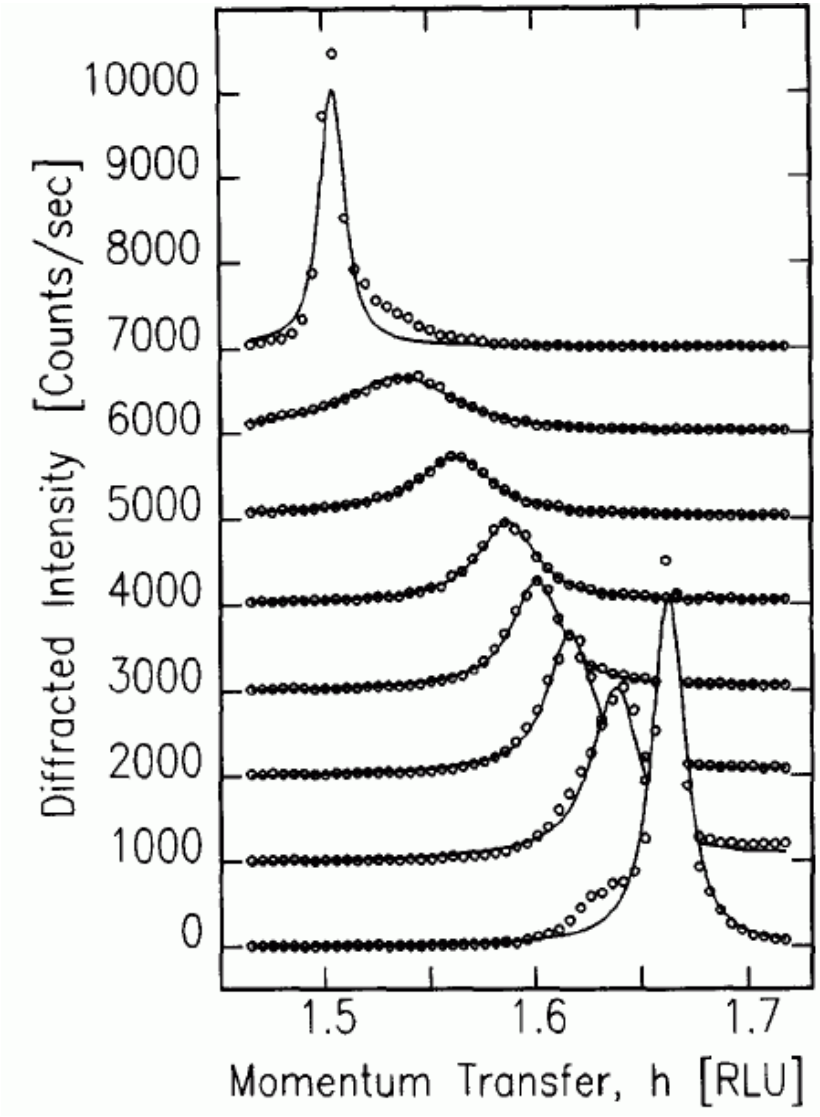

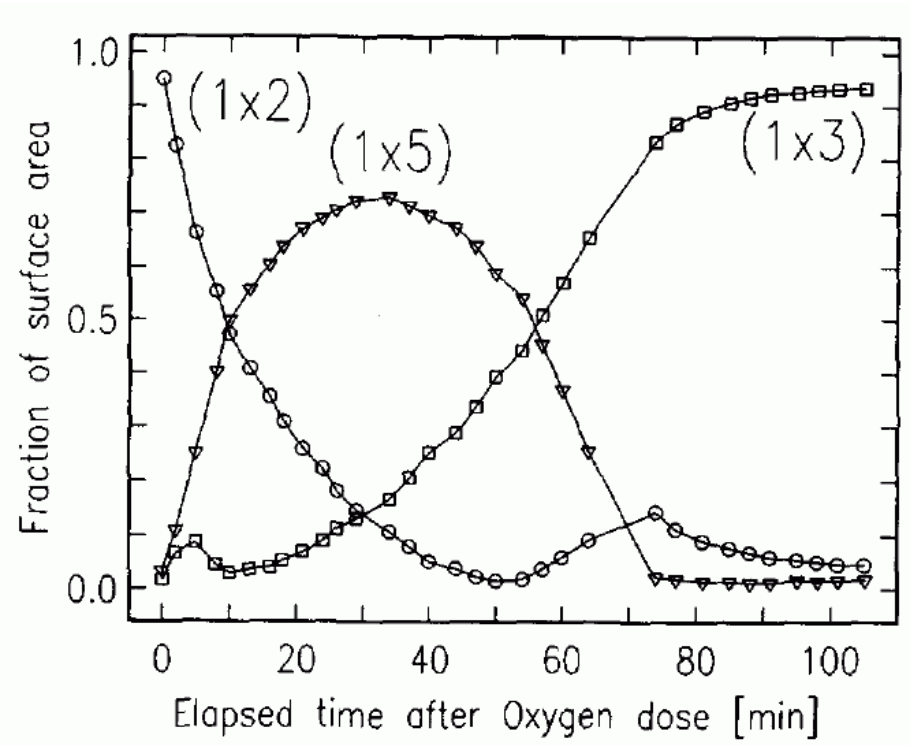

I. K. Robinson, P. J. Eng, C. Romainczyk and K. Kern, Surf. Sci. **367** 105-112 (1996)

BM32 measurements of Pt(110)1x5

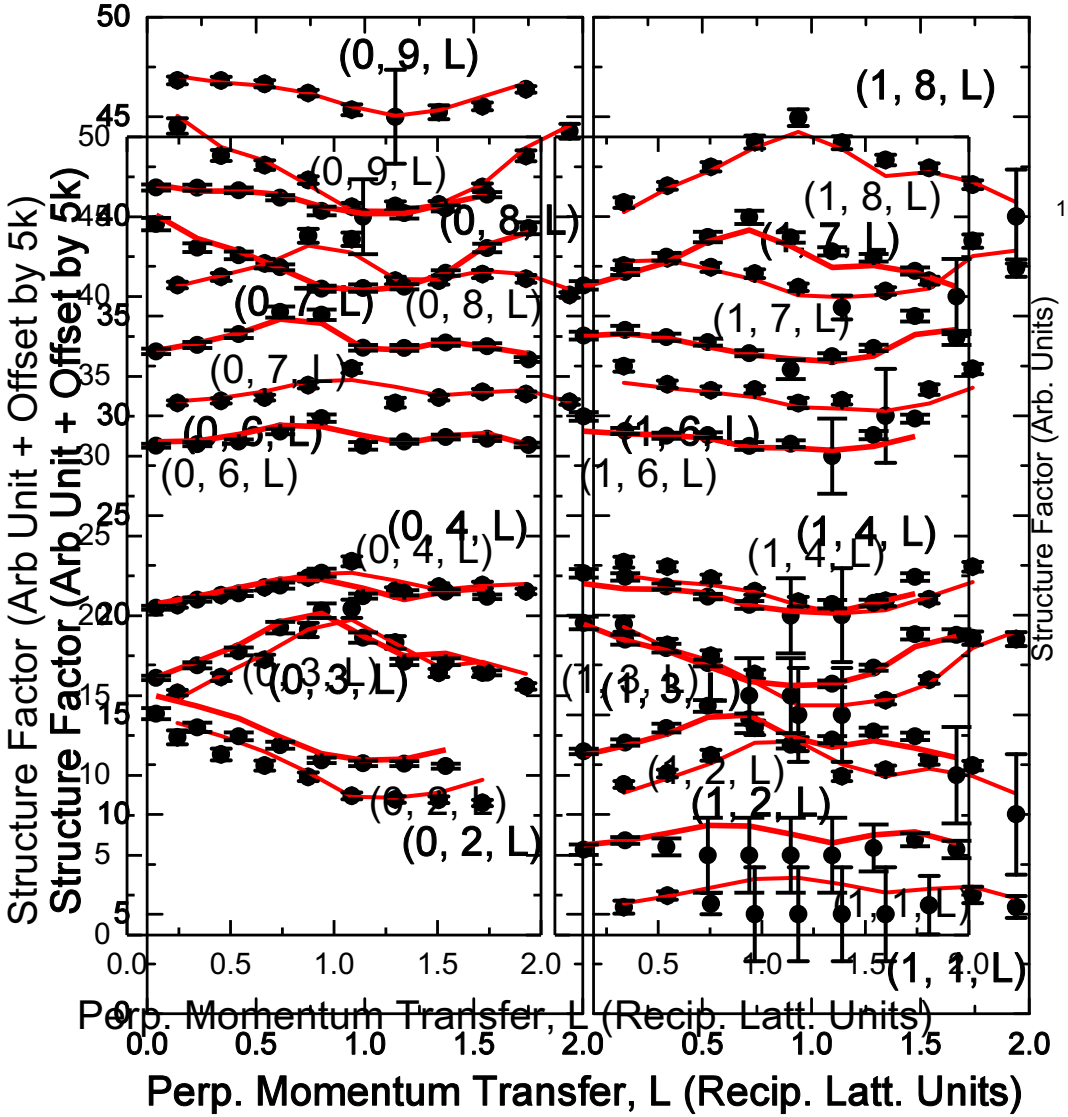

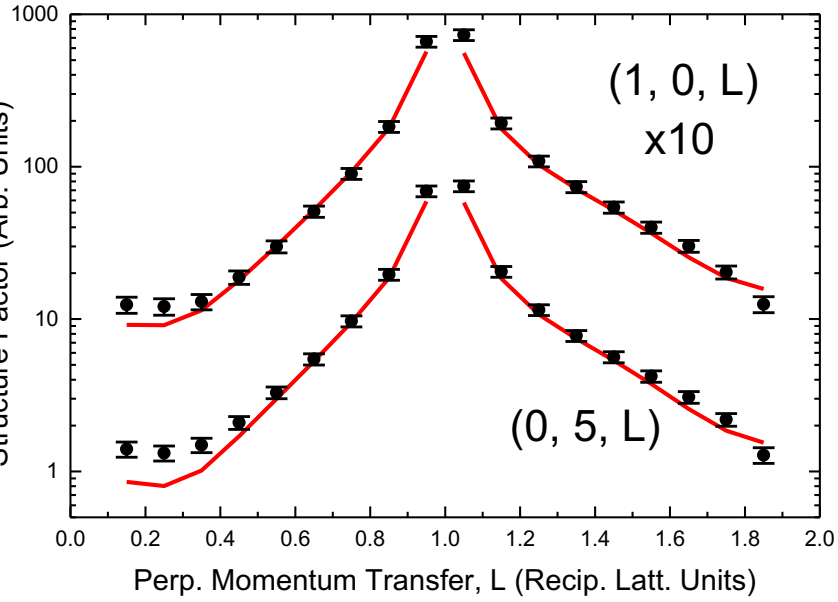

$$F(Q) = F_1(Q)F_2(Q)$$

$$I(Q) = |F_1(Q)|^2|F_2(Q)|^2$$

$$F_j(Q) = \int \rho_j(x)e^{iqx}dx$$

$$F_j^*(Q) = \int \rho_j(-x)e^{iqx}dx$$

$$I(Q) = |\int \rho_1(x) \circ \rho_2(x)e^{iqx}dx|^2$$

$$I(Q) = |\int \rho_1(-x) \circ \rho_2(x)e^{iqx}dx|^2$$

Homometric structures

Identical diffraction from two structures whenever the structure factor is factorizable

Homometric structures II

Convolution of two structures without mirror symmetry

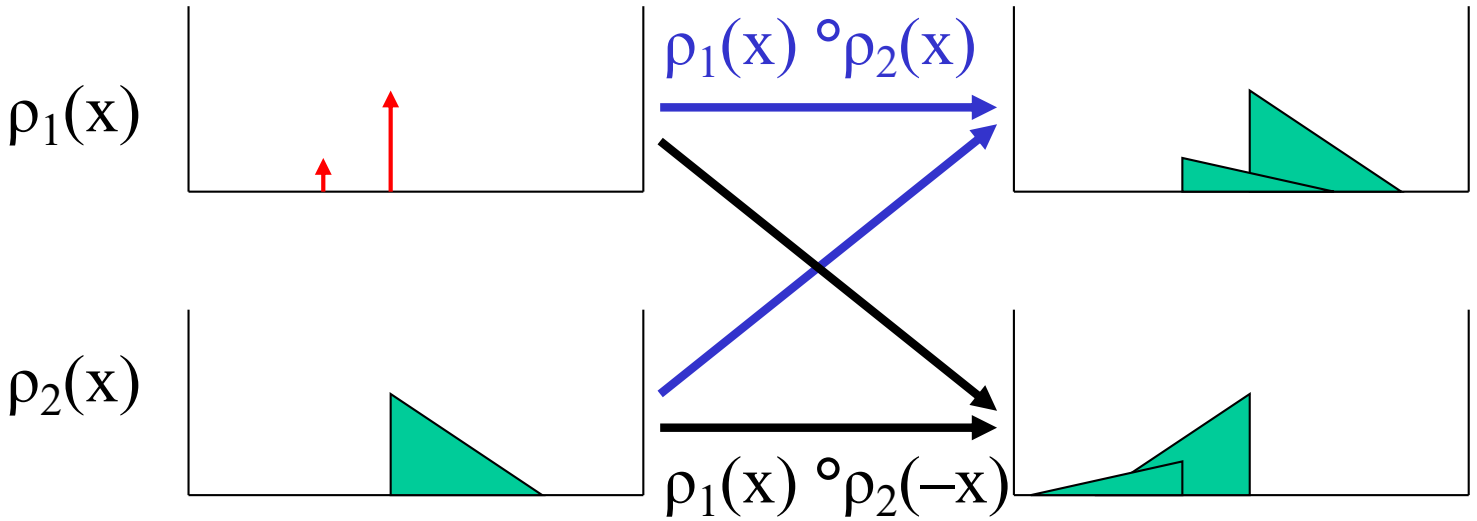

Displacements in final model

Pt(110)1x5 “hill” model

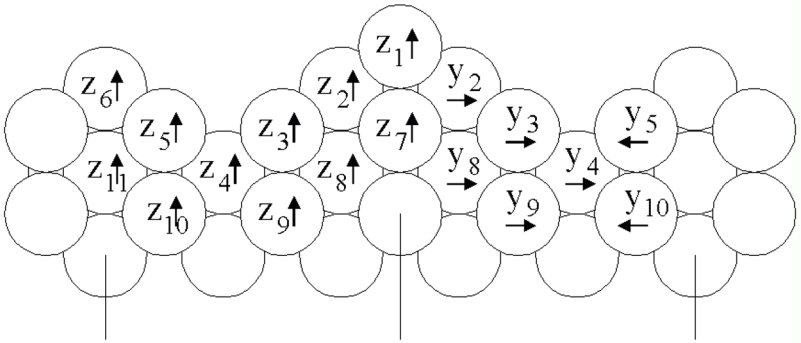

Chisq=2.7
90% hill, 10% valley
7% “1x1”

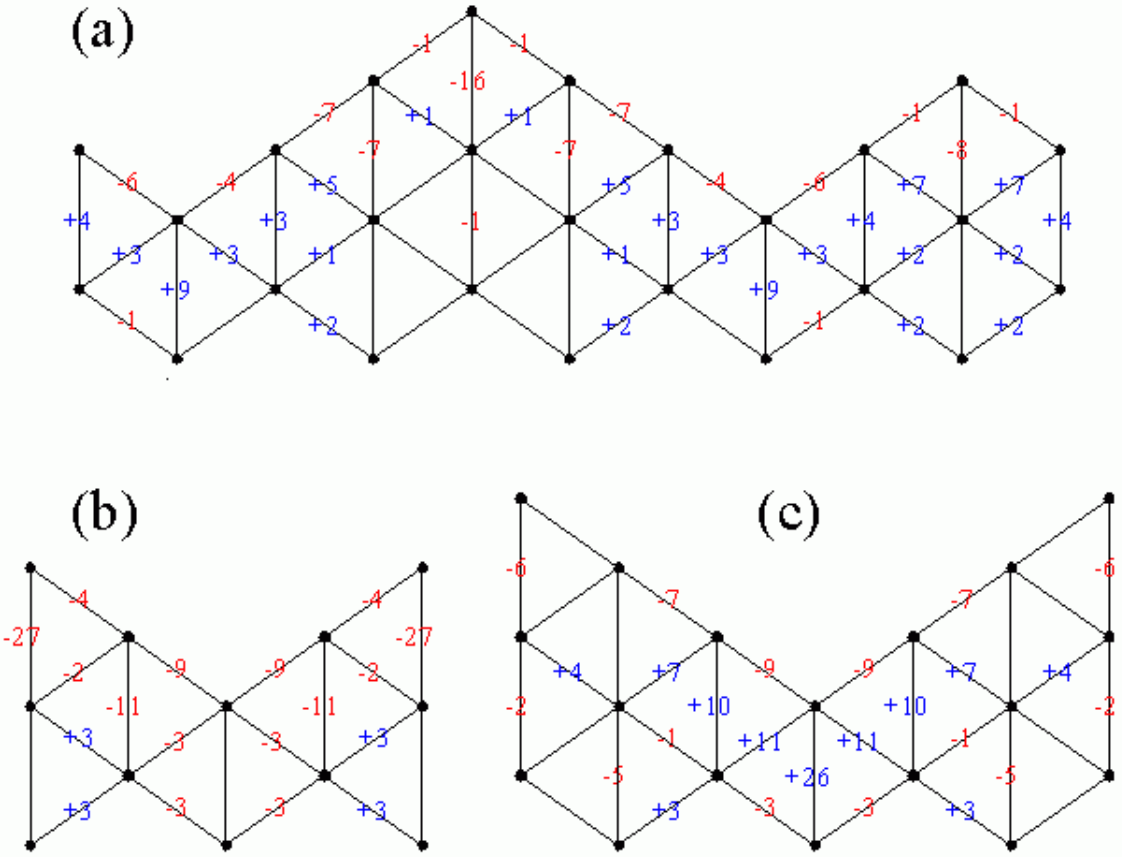

Pt(110)1x3

Menu of Topics

- Crystal Truncation Rods
- Au quantum nanowires on Stepped Si
- Reconstruction of Pt(110)1x5
- Facetting of Cu(115) to Cu(104)
- Au ‘physisorption’ on Si(111)7x7
- Deep subsurface strain in Pt(111)/CO
- GSAXS and C-GSAXS new methods

Cu(115) after Oxidation: STM

S. Reiter and E. Taglauer, Surf. Sci. **367** 33 (1996)

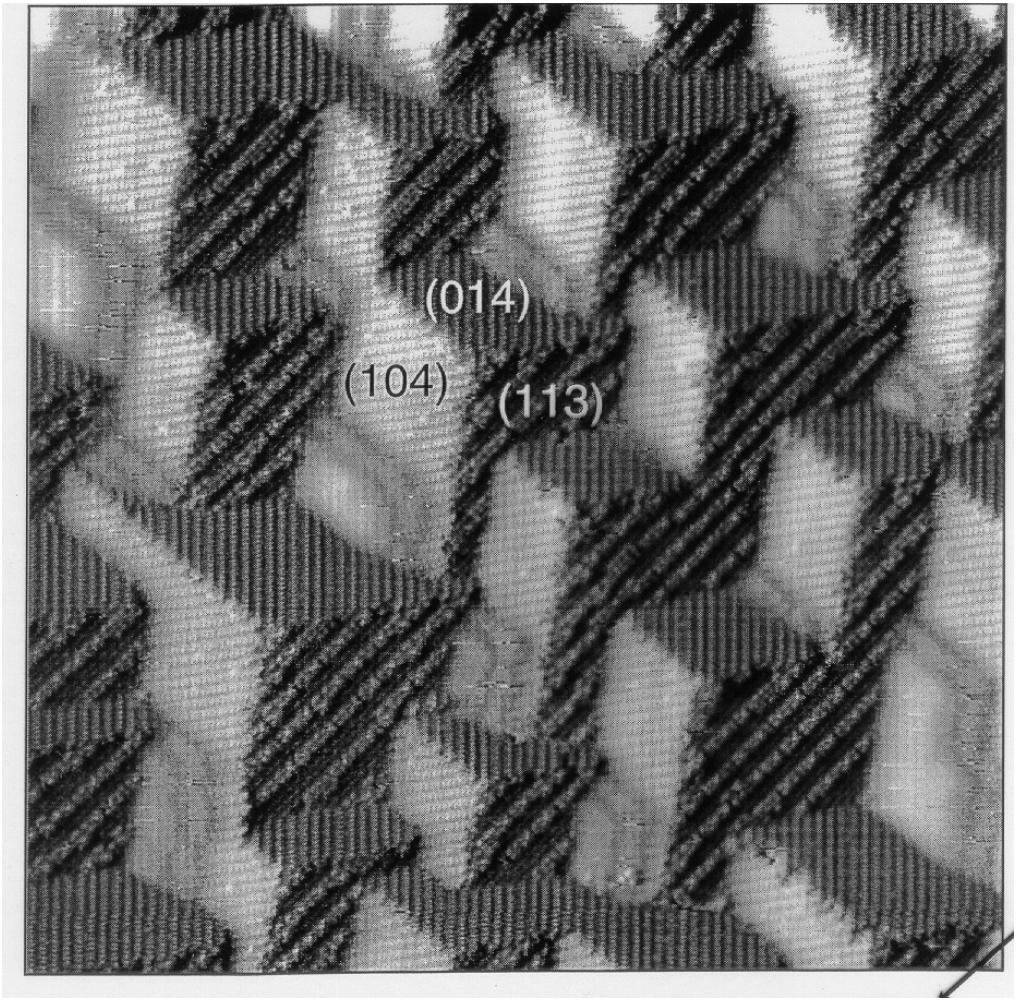

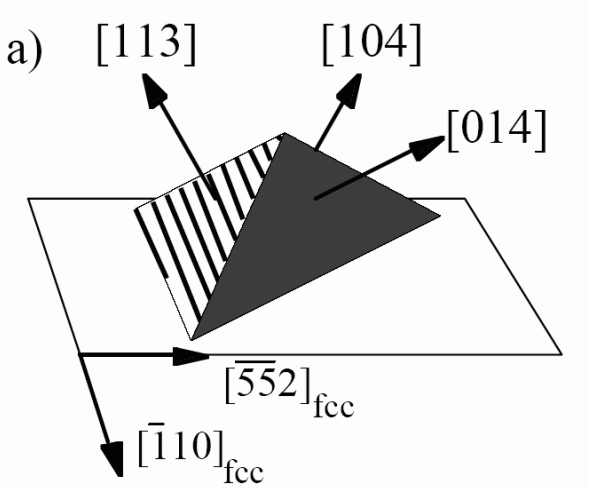

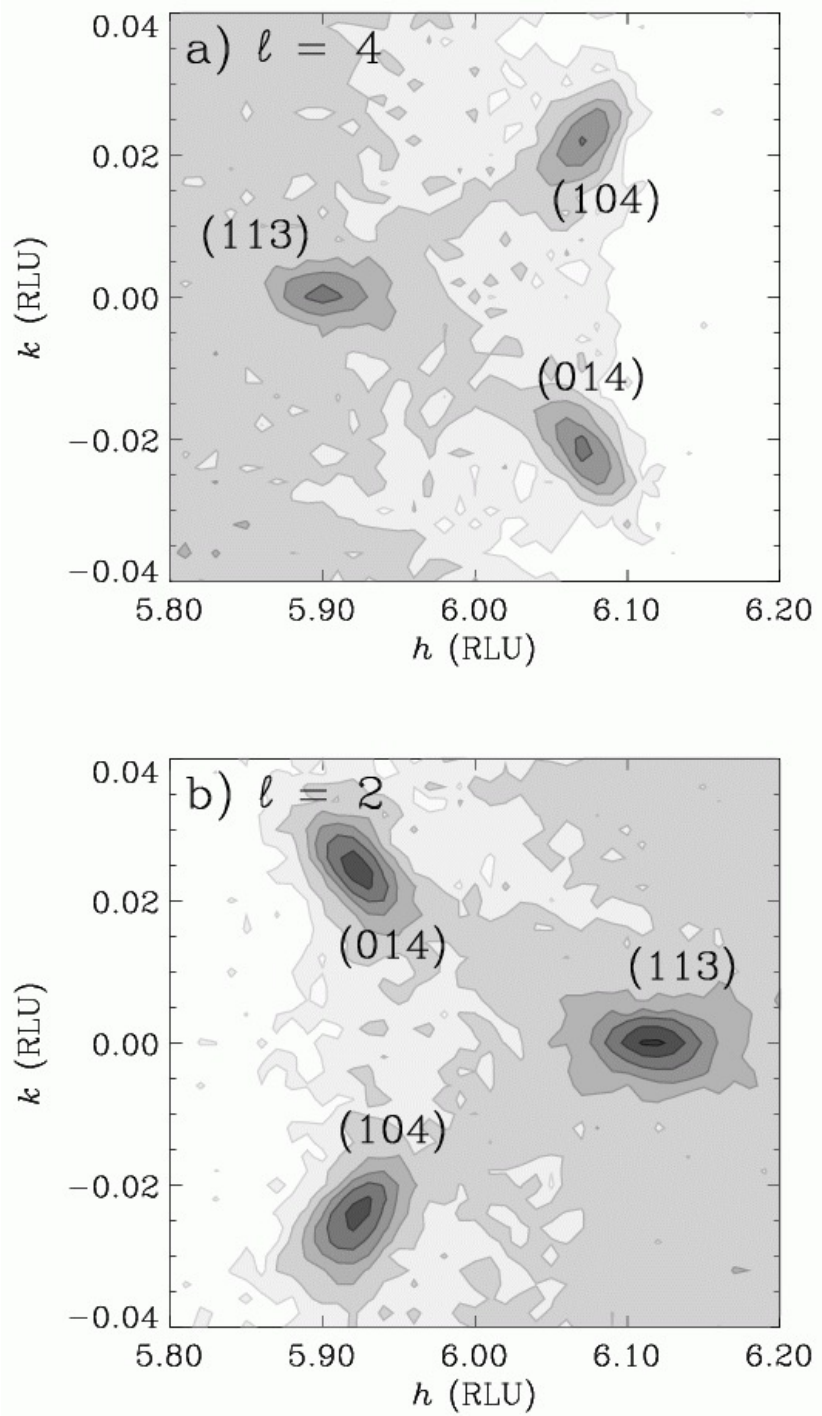

Cu(115) after Oxidation: X16A

Don Walko, UIUC PhD Dissertation (2000)

Re-index CTRs for Cu(104) facets

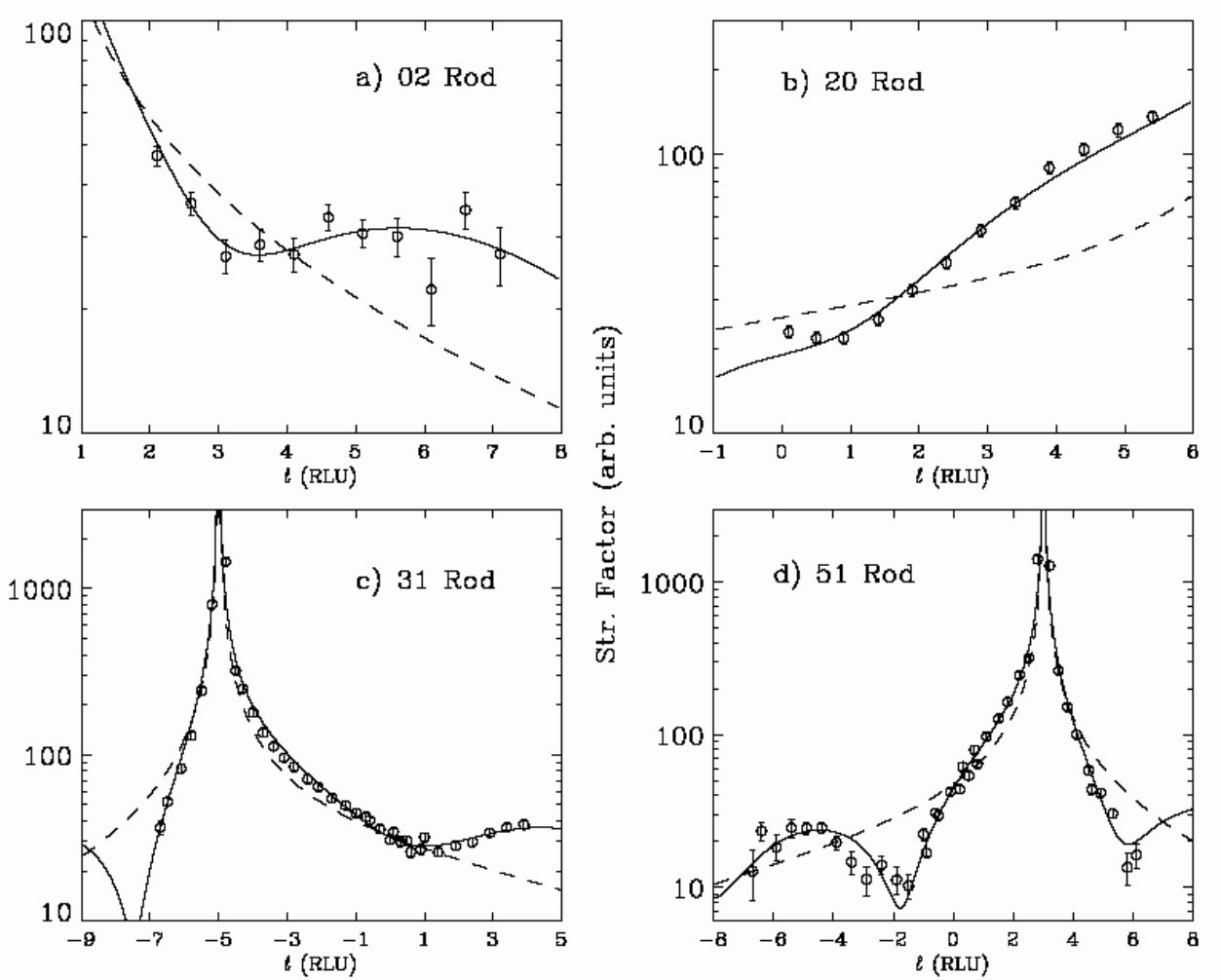

Surface Structures of Cu(104)-O

E. Vlieg, S. M. Driver, P. Goedtkindt, P. J. Knight, W. Liu, J. Luedecke, K. A. Mitchell, V. Murashov, I. K. Robinson, S. A. de Vries and D. P. Woodruff, Surface Science **516** 16-32 (2002)

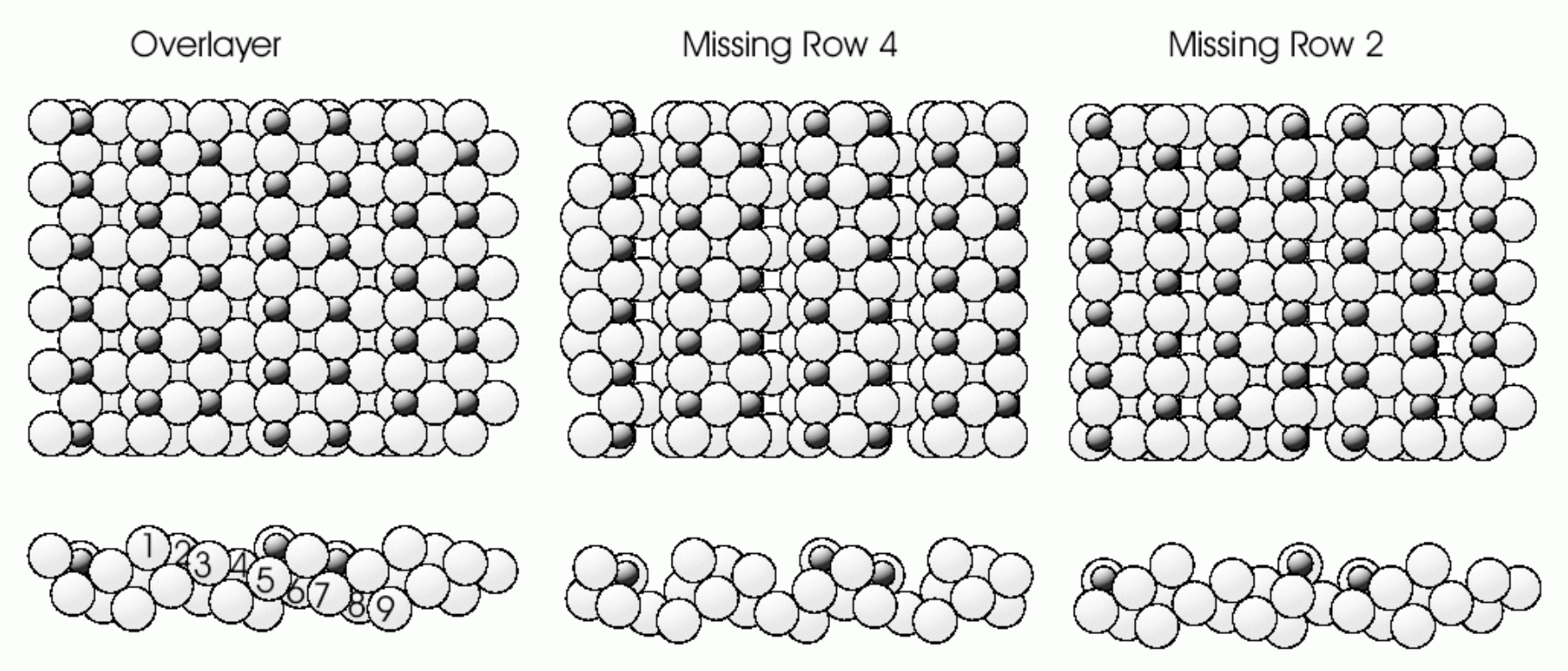

Perderau and Rhead | Robinson et al | Woodruff et al

In-plane and CTR data at Daresbury

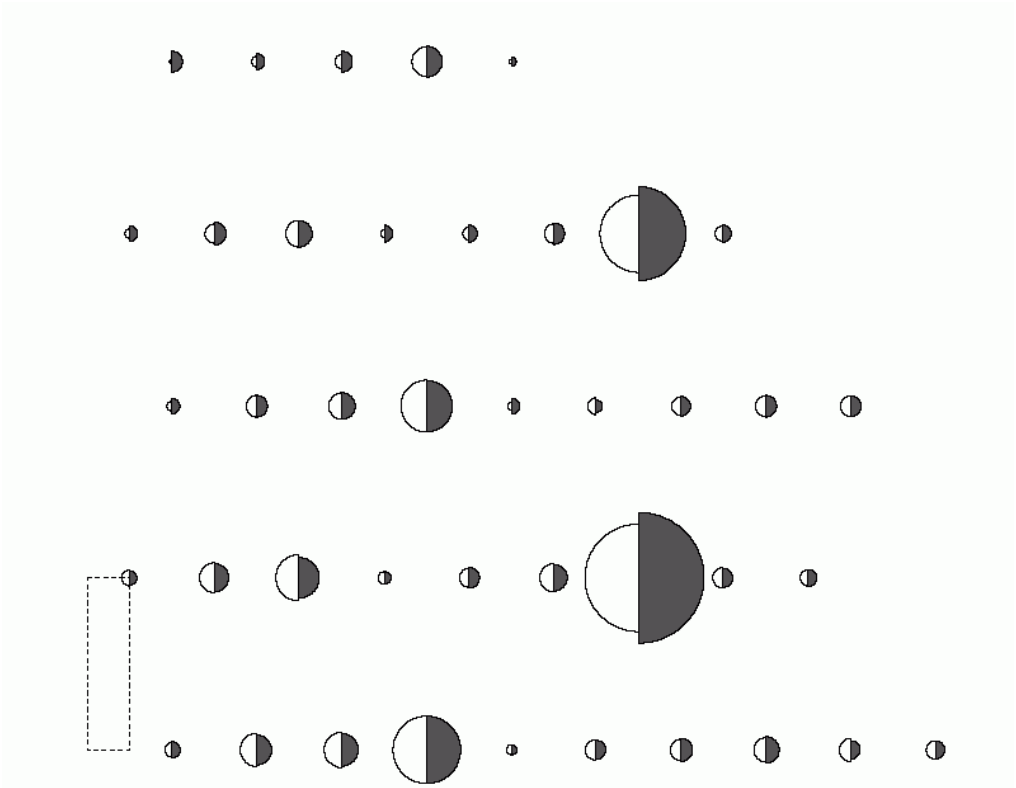

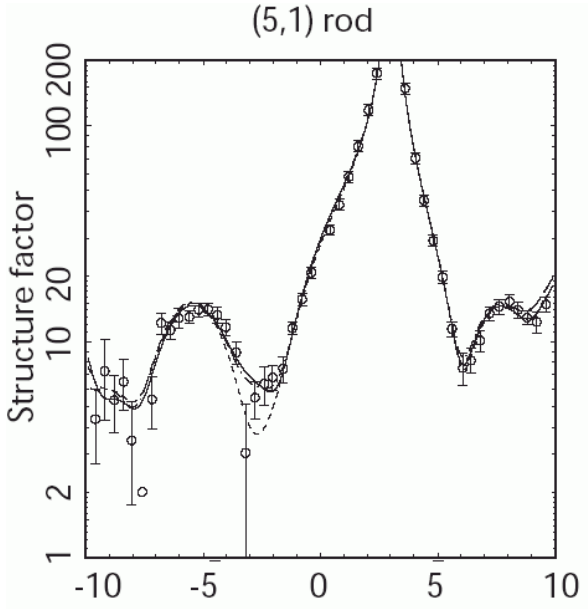

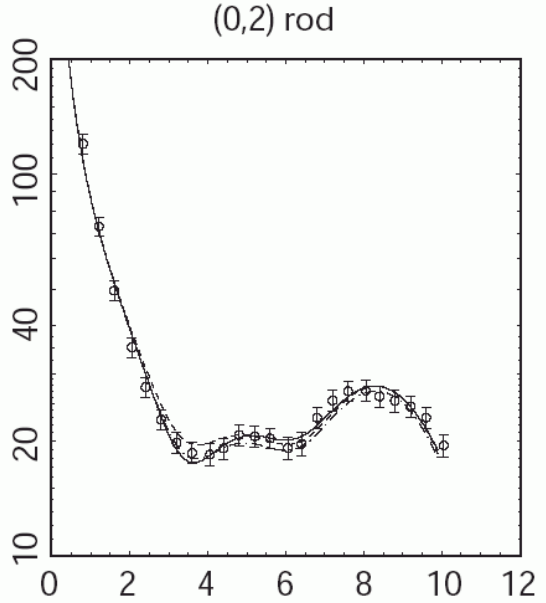

Problems with refinement of structure

O row number	Cu row number	Unconstrained fit	Constrained fit LJ1	Constrained fit LJ2	Walko & Robinson	DFT calculation
1	1	1.86	1.86	1.82	1.86	1.85
1	2	2.55	2.49	1.88	2.41	1.90
1	5	2.08	1.94	1.99	2.55	2.21
3	2	1.53	1.71	1.79	1.85	1.90
3	3	1.96	1.93	1.88	1.84	1.98
3	4	2.25	2.11	1.93	1.85	2.03
3	7	2.69	2.61	2.52	2.43	2.72

$\chi^2=2.66$ $\chi^2=2.83$

Two Structures that fit the Data

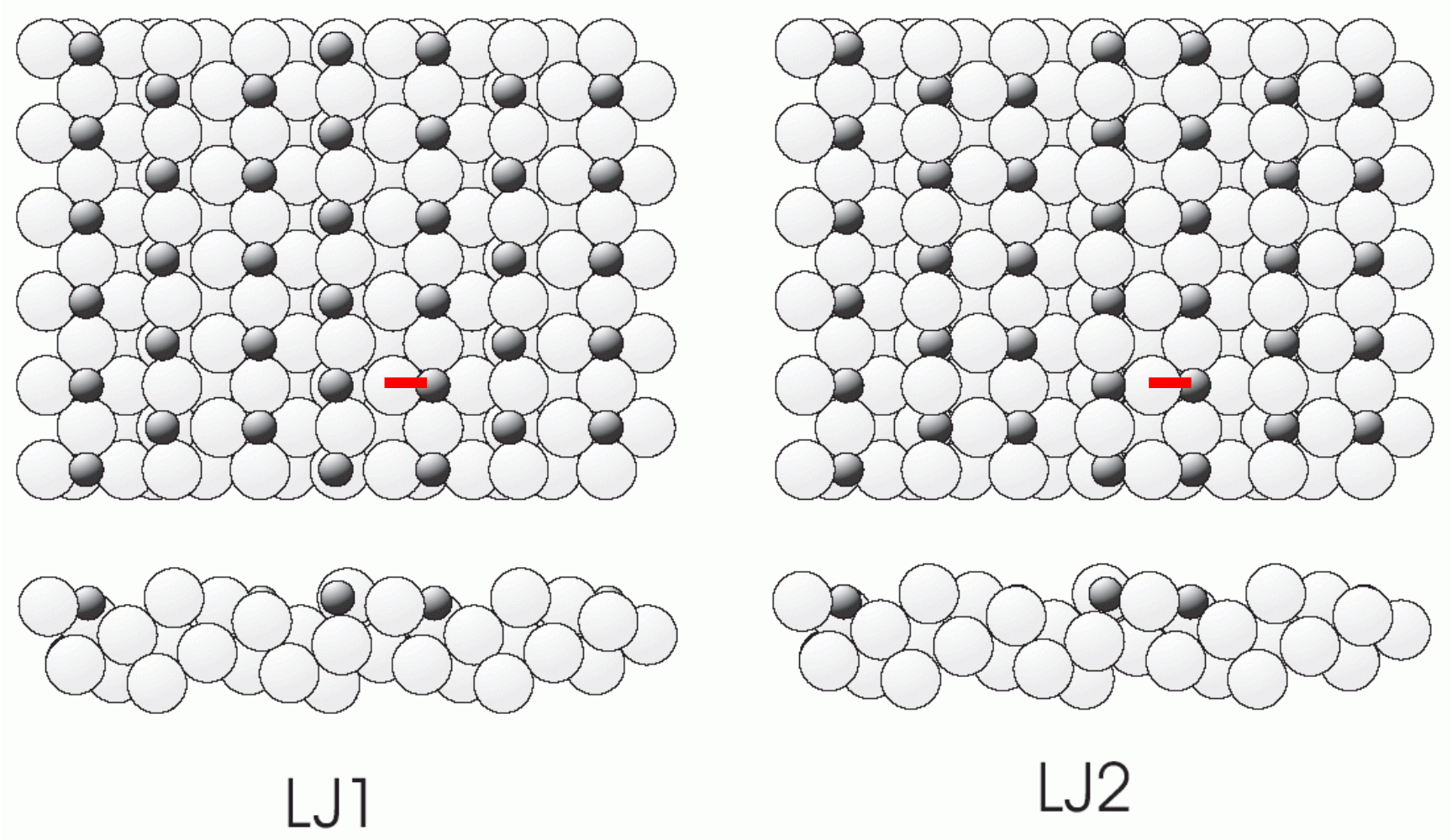

If we had measured ...

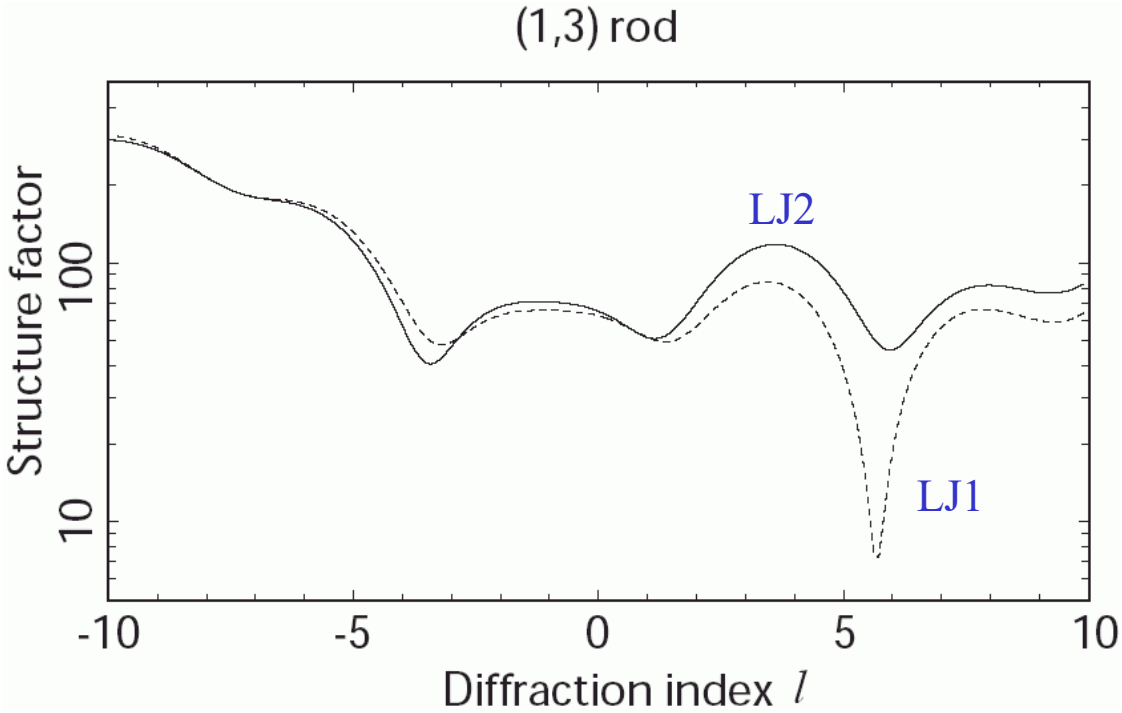

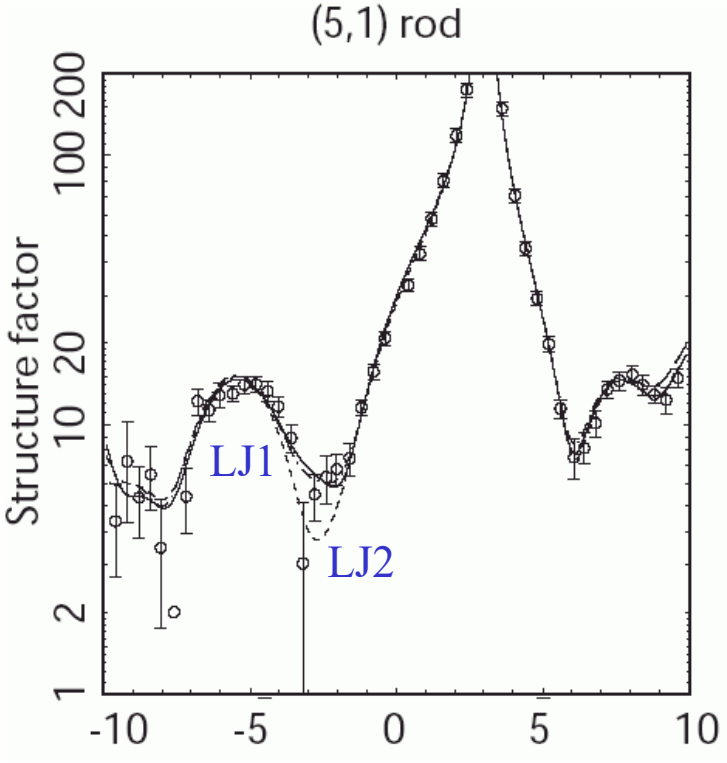

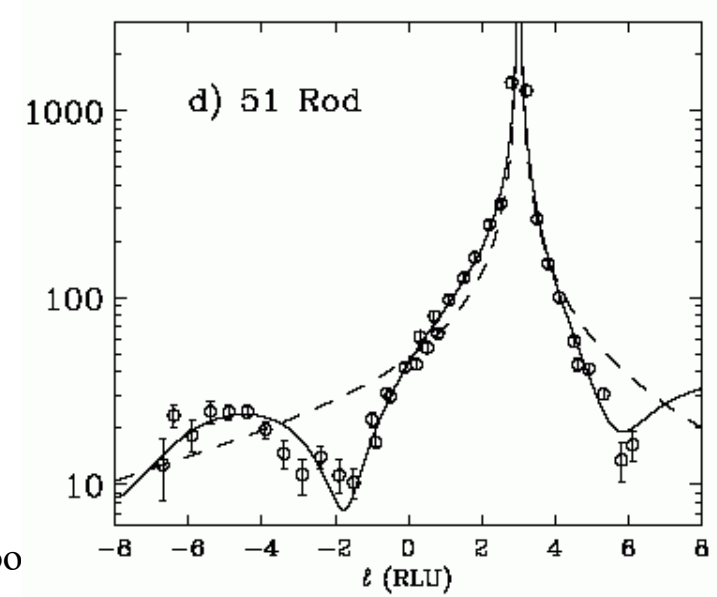

Menu of Topics

- Crystal Truncation Rods
- Au quantum nanowires on Stepped Si
- Reconstruction of Pt(110)1x5
- Facetting of Cu(115) to Cu(104)
- Au ‘physisorption’ on Si(111)7x7
- Deep subsurface strain in Pt(111)/CO
- GSAXS and C-GSAXS new methods

Si(111) 7x7 Reconstruction

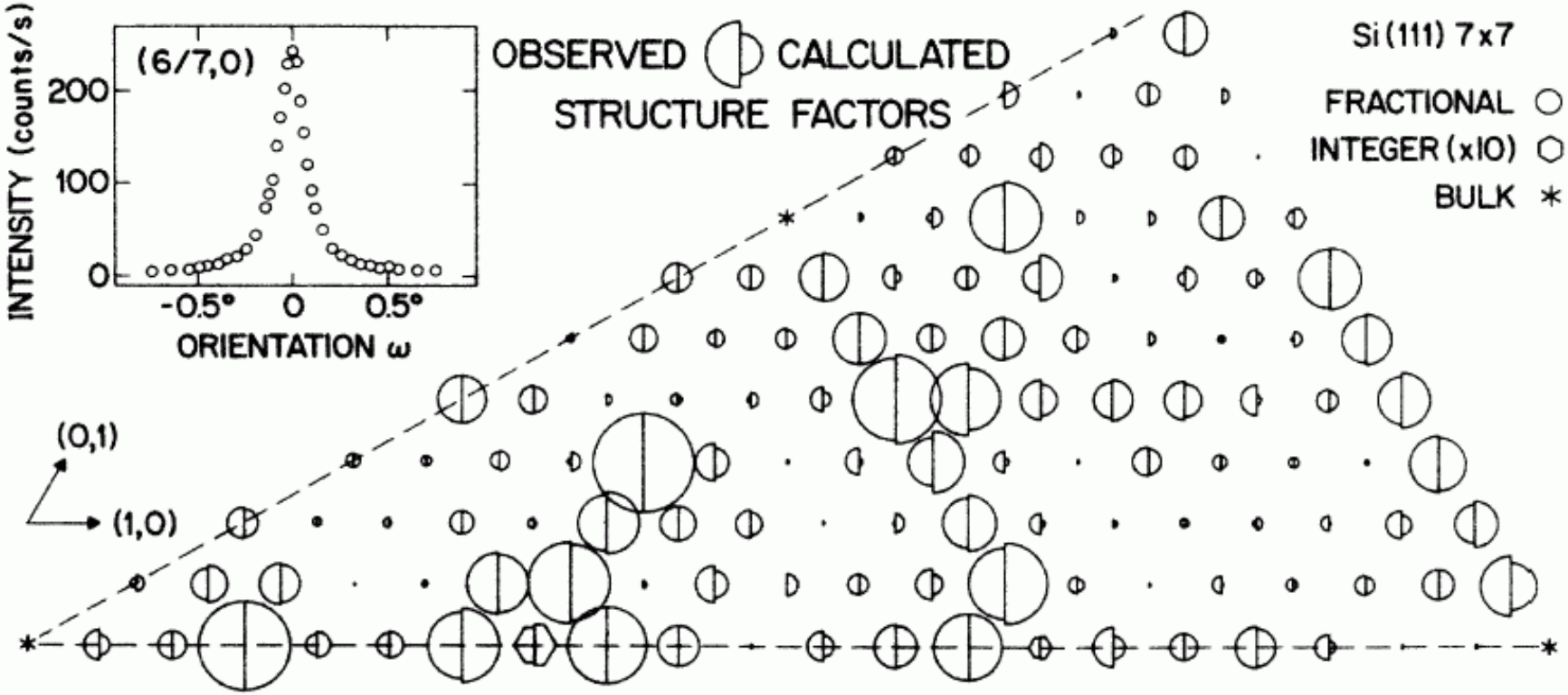

Dimer-Adatom-Stacking Fault model

K.Takayanagi by Transmission Electron Diffraction (1987)

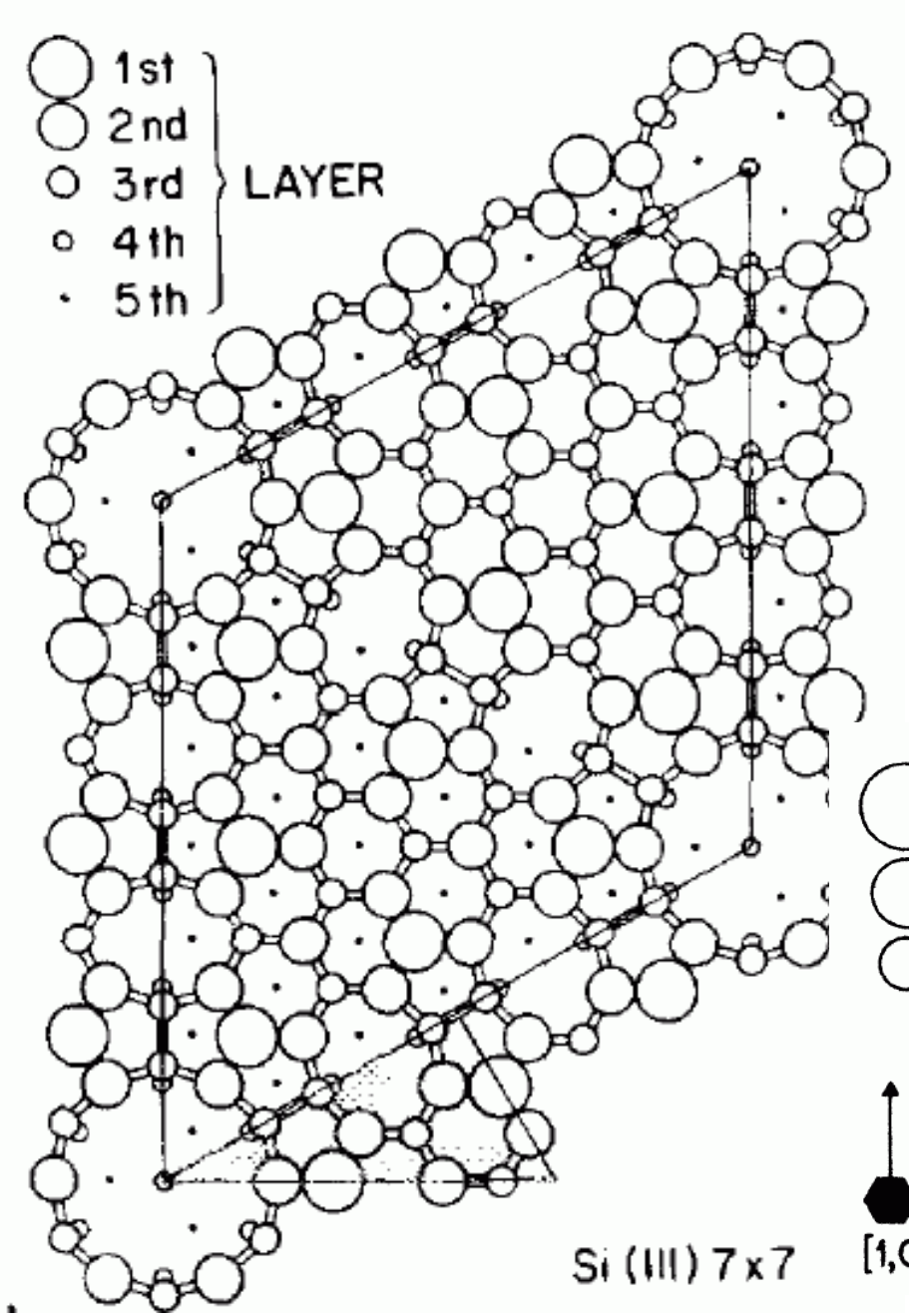

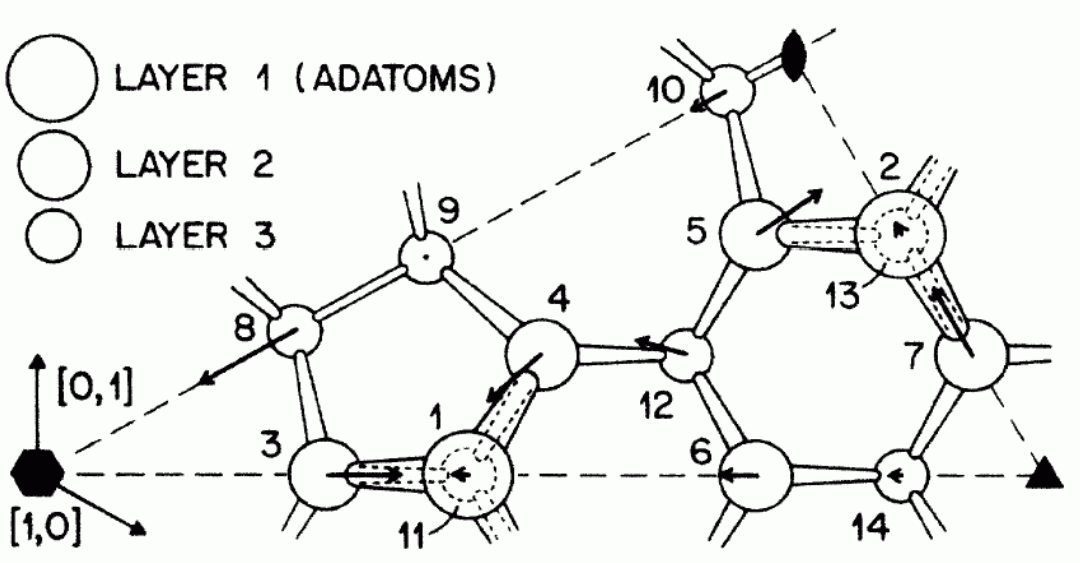

MEM inversion of X-ray data

L.D. Marks, Northwestern University

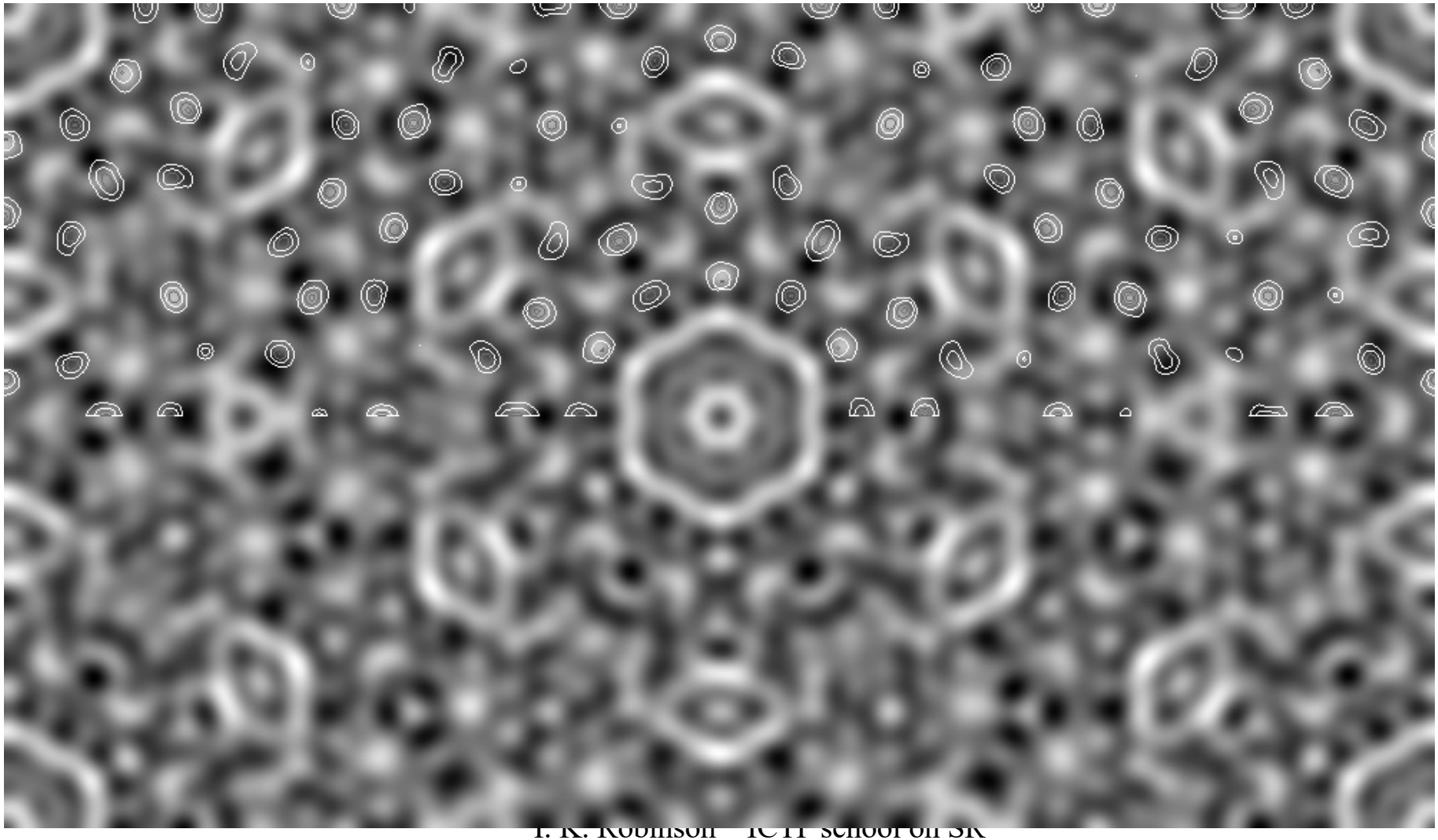

Importance of Symmetry in Si(111)7x7

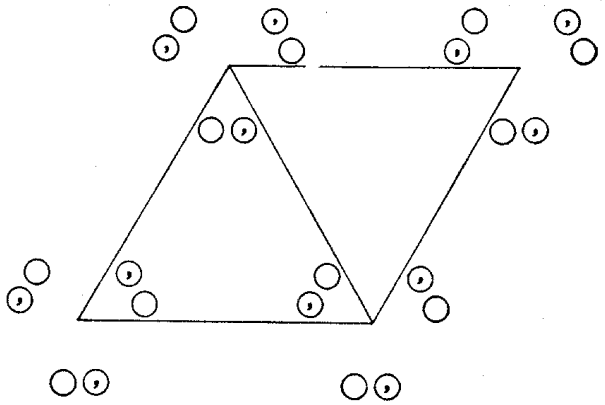

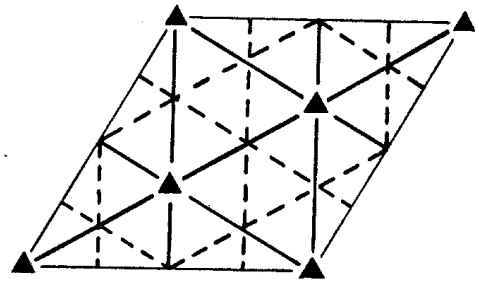

p3m1 → Bulk Symmetry

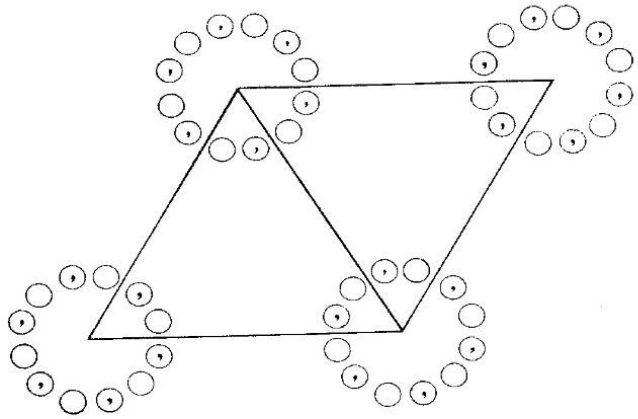

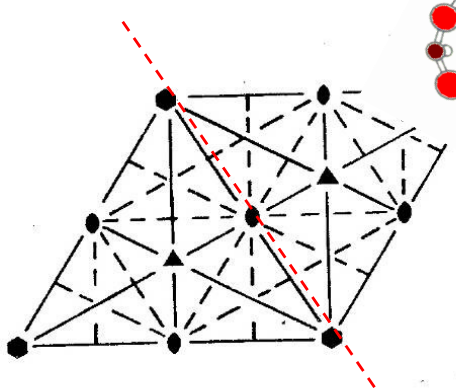

p6mm → Surface Symmetry

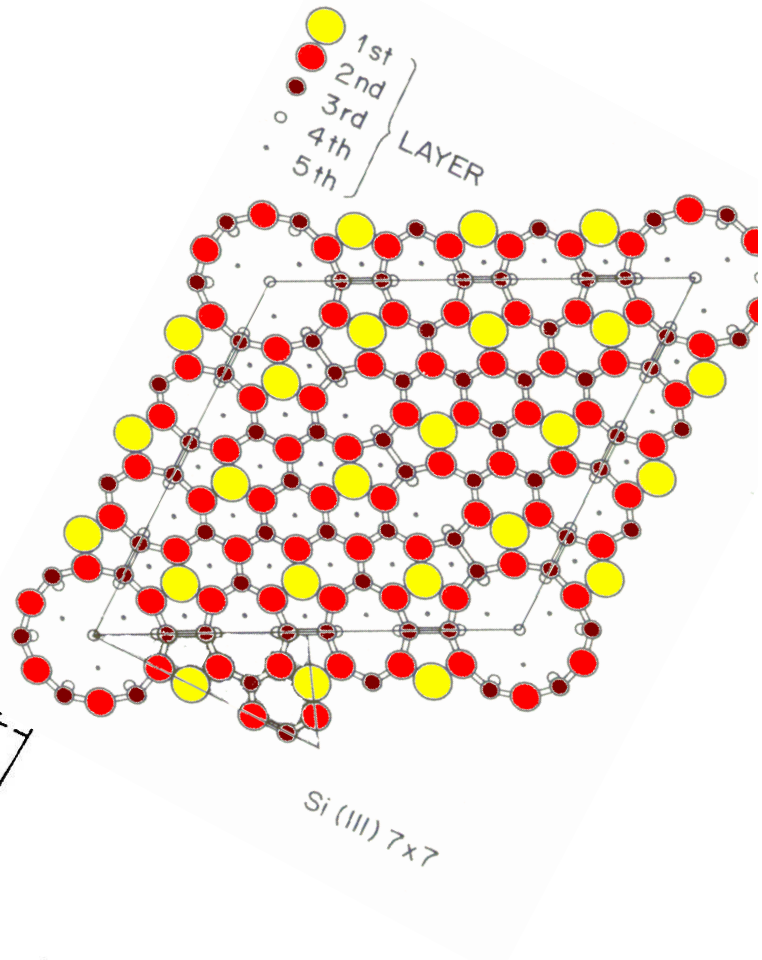

Au physisorption on Si(111)7x7?

Motivation

To study the structure of self assembled metal nanostructures on Si(111)7x7 surface

Adsorption processes of Au on Si(111)7x7 surface

Physisorption (Physical absorption)

Adsorption in which the forces involved are inter-molecular (van der Waals forces), which do not involve a significant change in electronic orbital patterns of the species involved

Chemisorption (Chemical absorption)

Adsorption in which the forces involved are electronic valence forces of the same kind as those operating in the formation of chemical compounds, i.e., ionic and covalent bonds

Au on Si(111) Phase Diagram

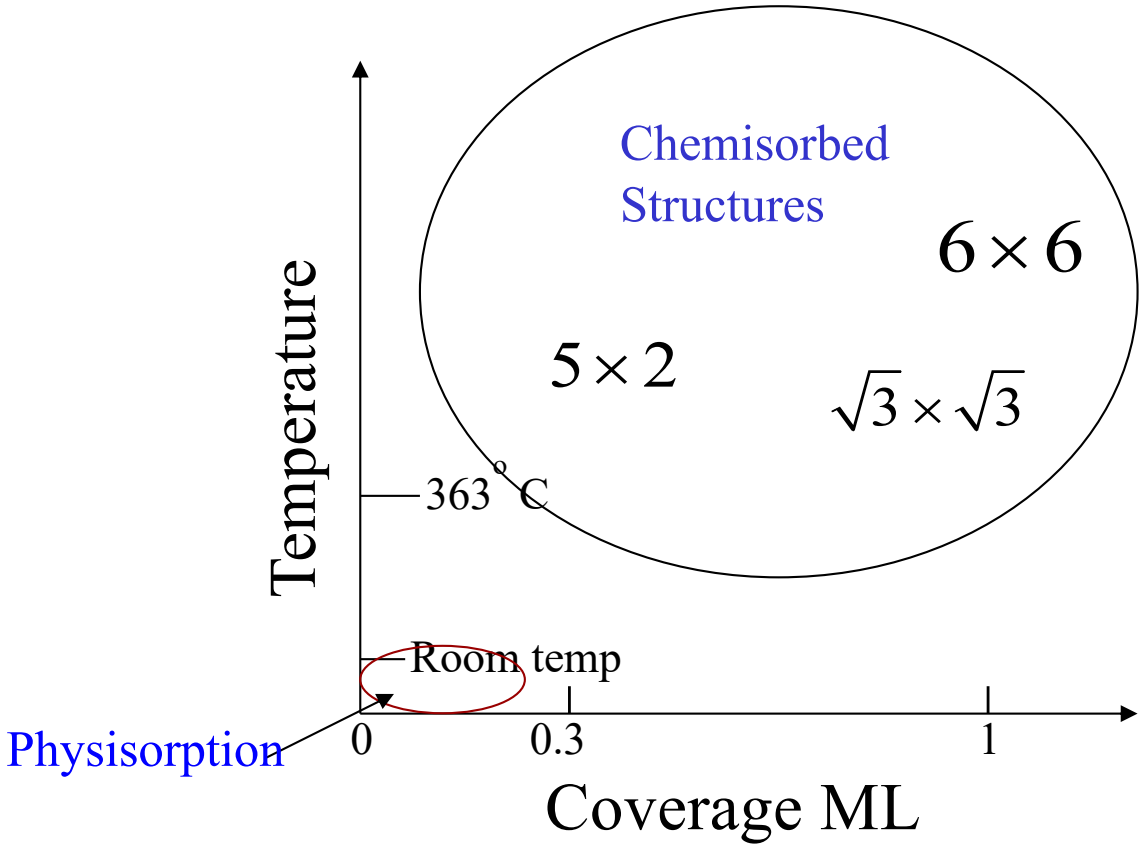

D. Grozea, E. Bengu and L. D. Marks, Surf.Sci. 461, 23(2000)

Surface Symmetry

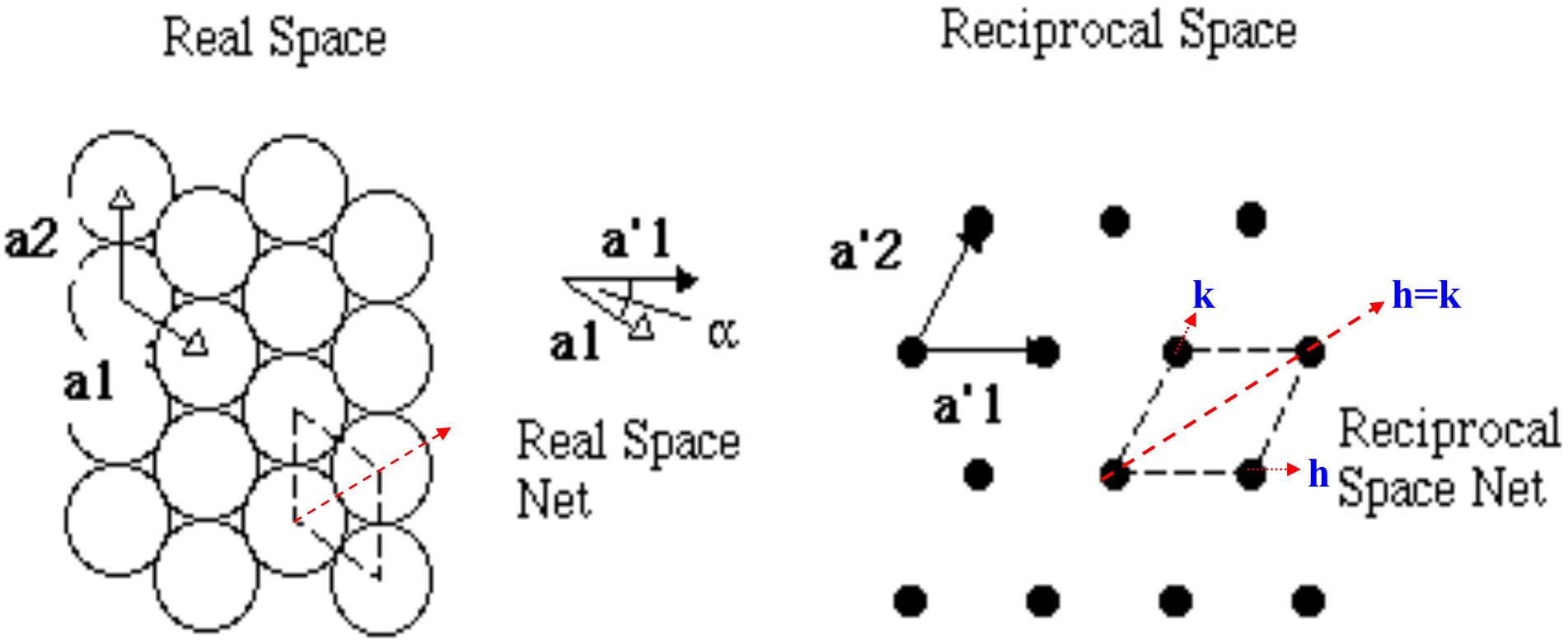

L=1.5 symmetry breaking

Clean | 0.06ML Au

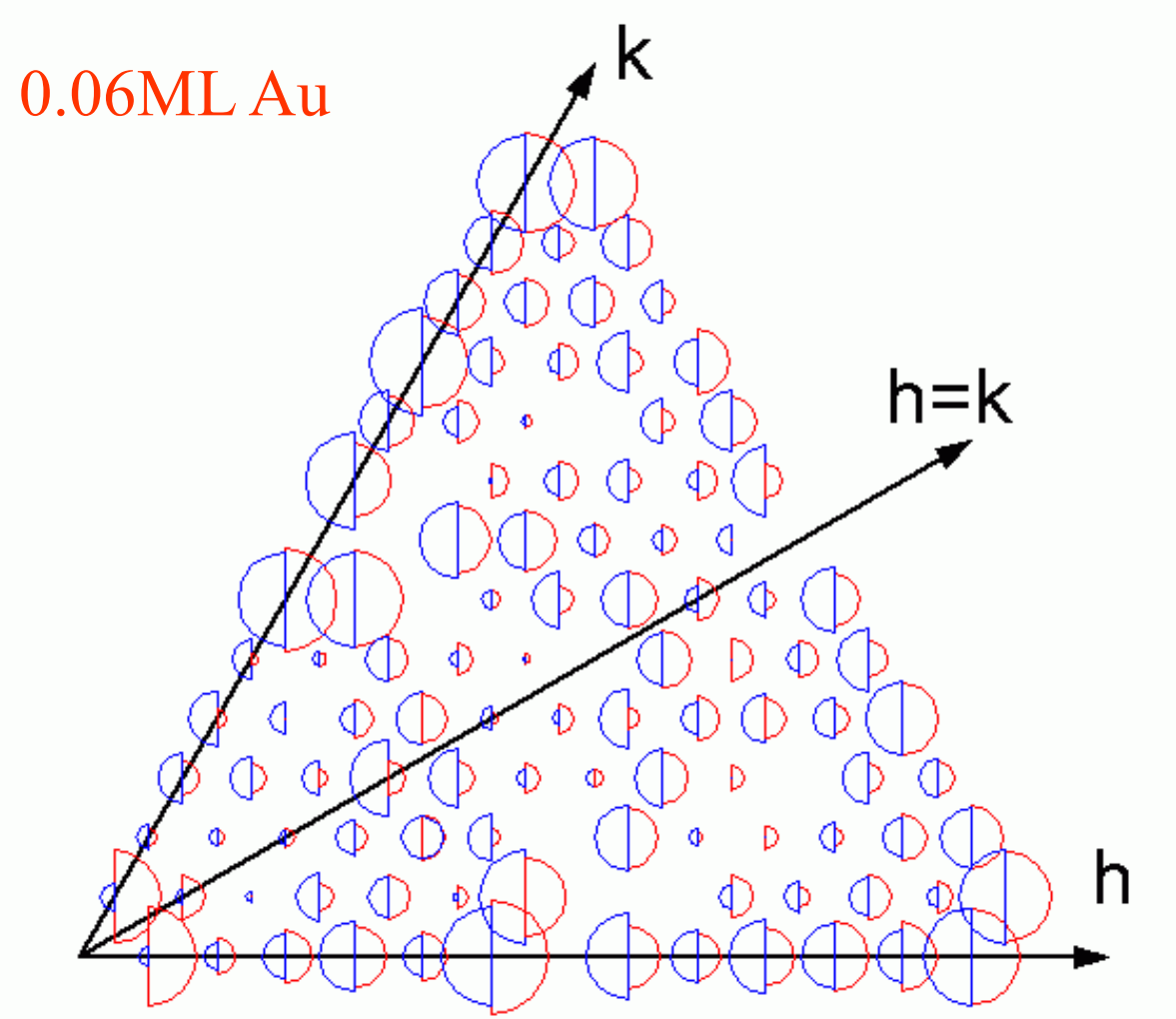

Structure factor data shows p6mm symmetry breaking

Clean Si(111)7x7

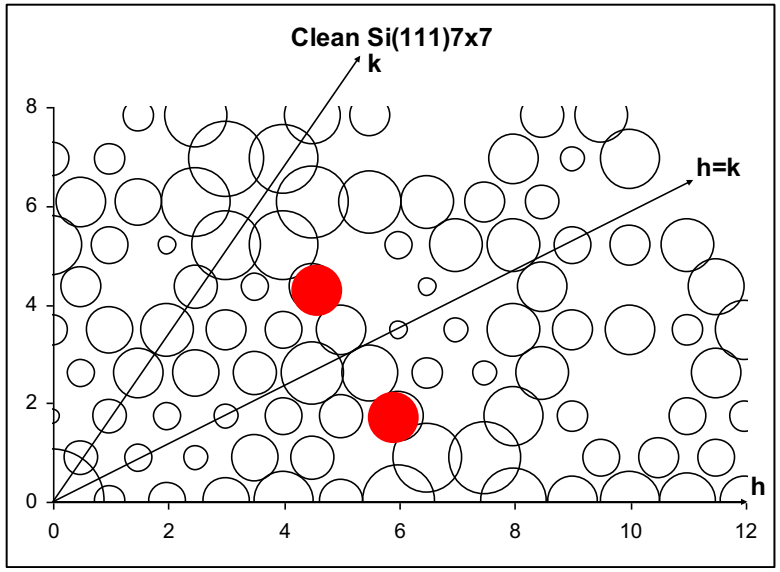

0.06 ML Au on -Si(111)7x7

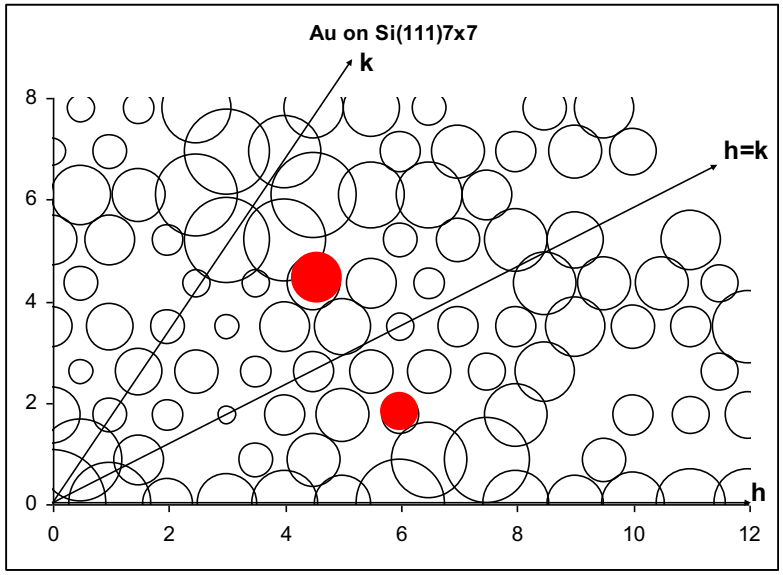

Agreement factor (□) between equivalent reflections (L = 1.5) averaged assuming P3m1 and P6mm symmetry

Sample Type	Agreement factor (□) P3m1	P6mm
clean	0.061	0.076
Au-0.06 ML	0.079	0.156
Au-0.12 ML	0.059	0.110
Au-0.18 ML	0.056	0.079

Real Space 3D-Density Difference Map

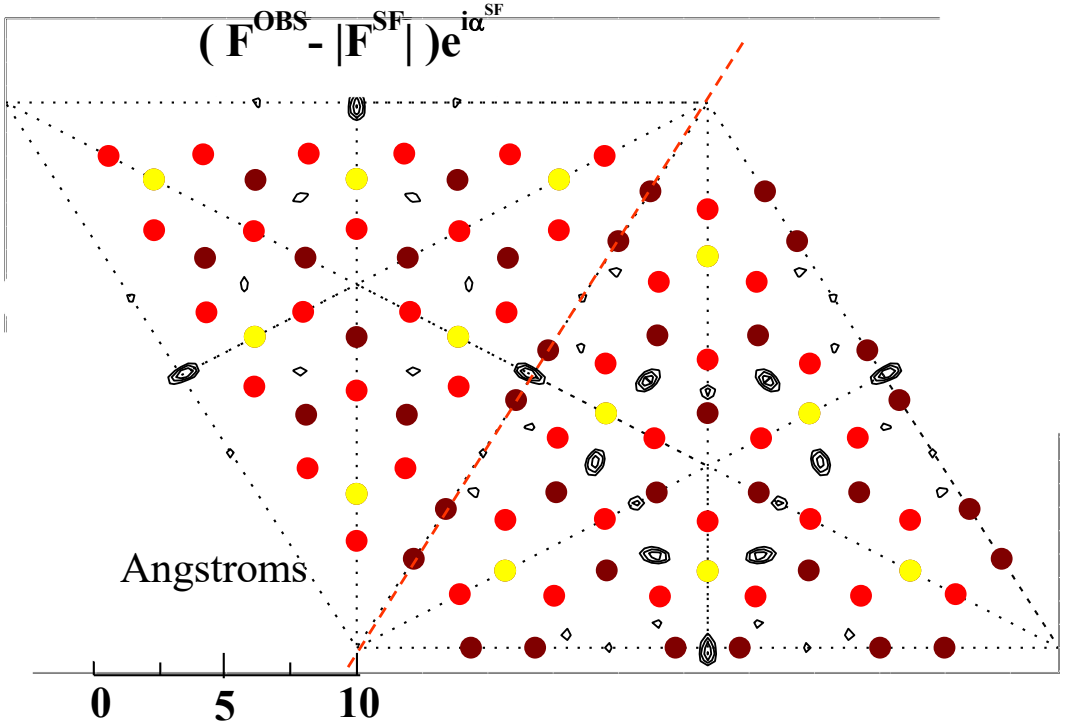

$$\rho_{xyz}^{obs} = \sum_{hkl} (|F_{hkl}^{obs}| - |F_{hkl}^{c}|) e^{i\alpha_{hkl}^{c}} \exp(-2\pi(hx + ky + lz))$$

z~ adatom height

Cho & Kaxiras Surf. Sci. 396 L261 (1988)

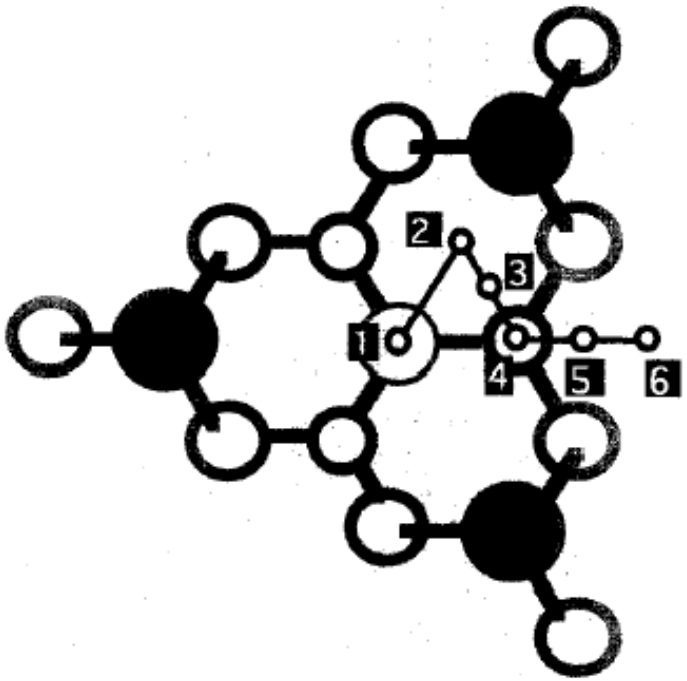

Fig. 1. Schematic top-view representation of a portion of the Si(111) reconstruction containing three Si adatoms (large black circles) and one rest-atom (grey circle) as well as the substrate atoms directly bonded to those (smaller open circles). The sites where the adsorbate atoms are placed are indicated by the numbers 1–6. These sites are used for the energy plots in Fig. 2.

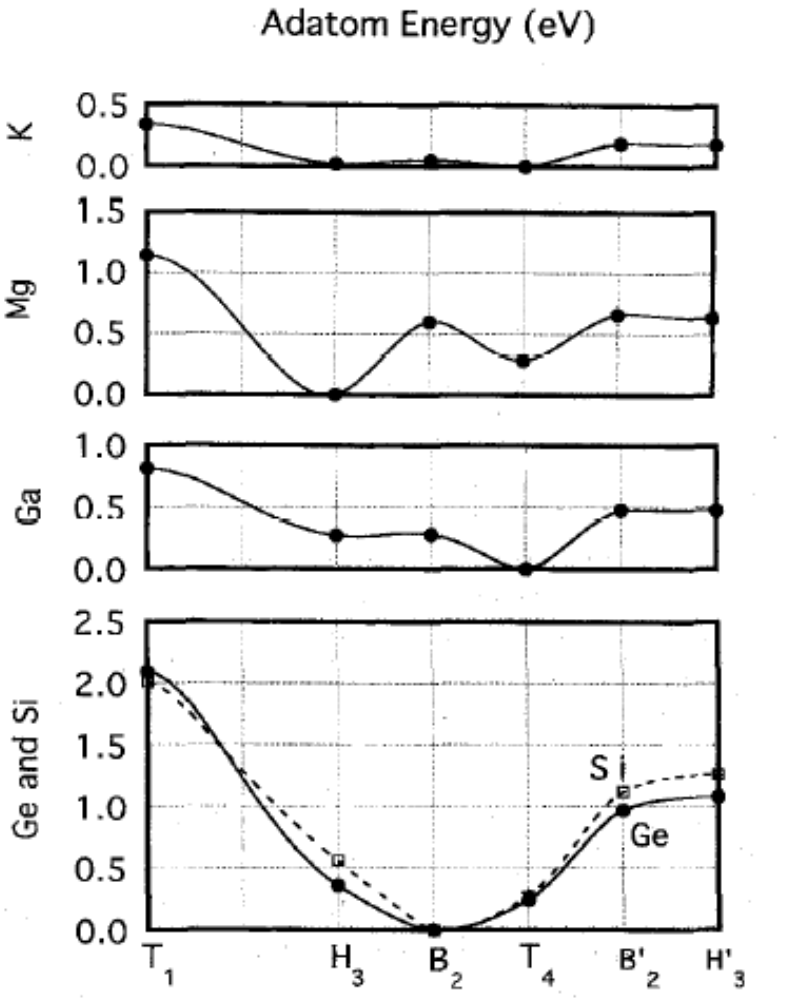

Fig. 2. Plots of the adsorbate atom energies along the six sites defined in Fig. 1 (from left to right the six sites are T_1, H_3-type, B_2-type, T_4-type, B_2'-type and H_3'-type). The energies are relative to the lowest energy sites for each adsorbate atom (see Table 1).

Potential from Anistropic DWF

One Particle Potential $V(x,y) = - k_B T [\text{Log} \{ \text{FT (DWF)} \}]$
$= -25.84 [\text{Log} \{ \text{FT (DWF)} \}]$ meV at 300 K

Potential Energy within Basin of Attraction

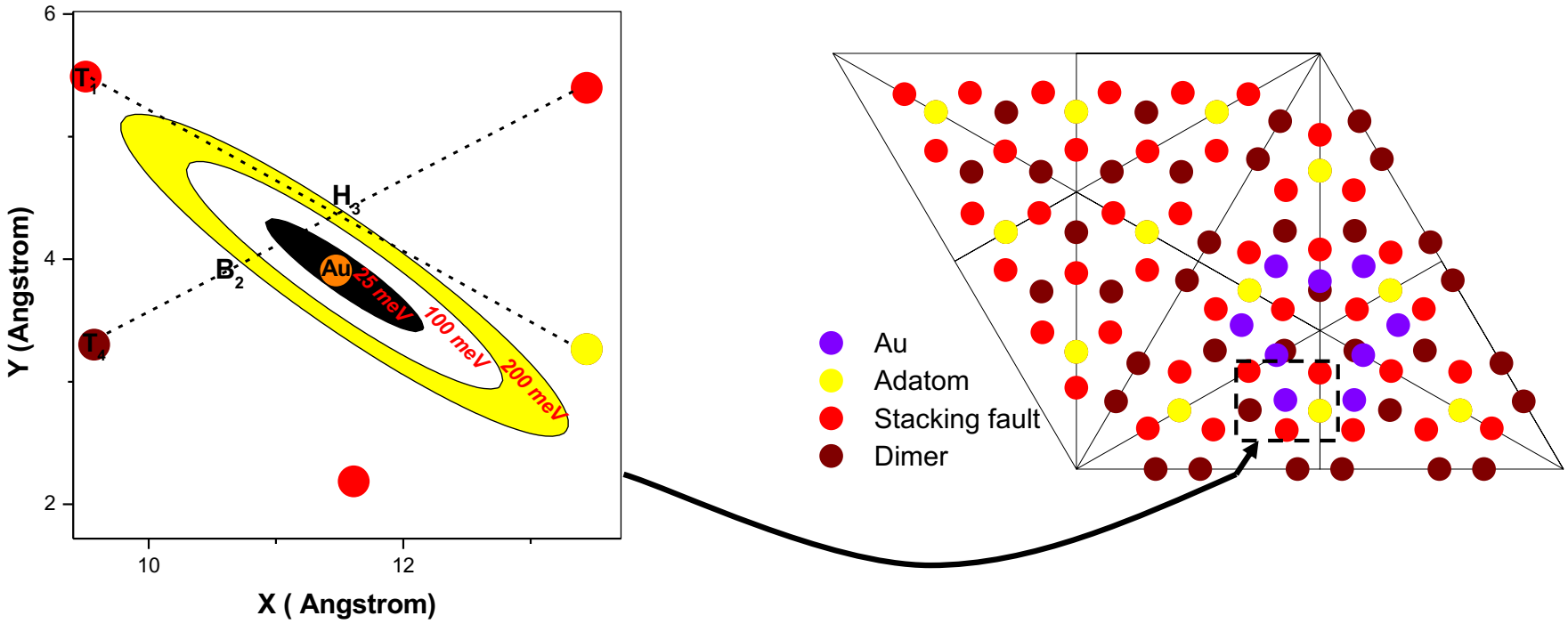

H. L. Meyerheim, I. K. Robinson and R. Schuster, Surf. Sci., 370,268(1997)

Comparison with Theory

Basin of Attraction

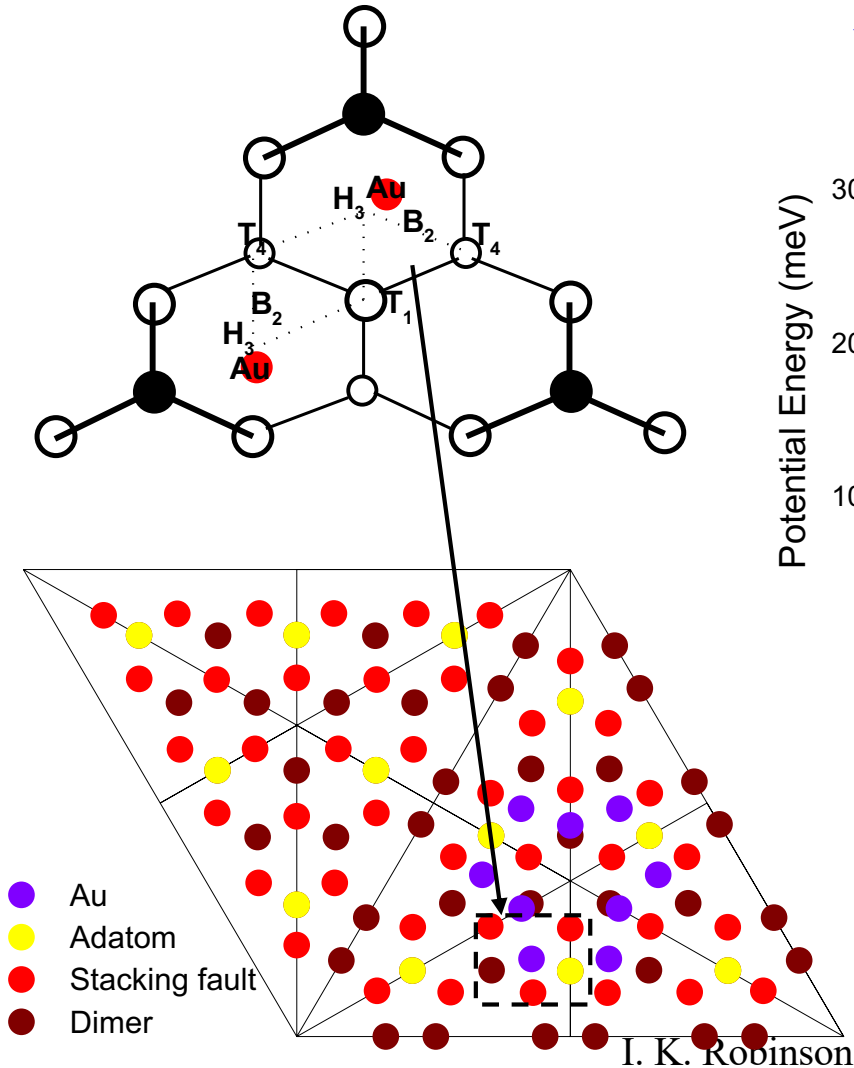

Potential Energy within Basin of Attraction

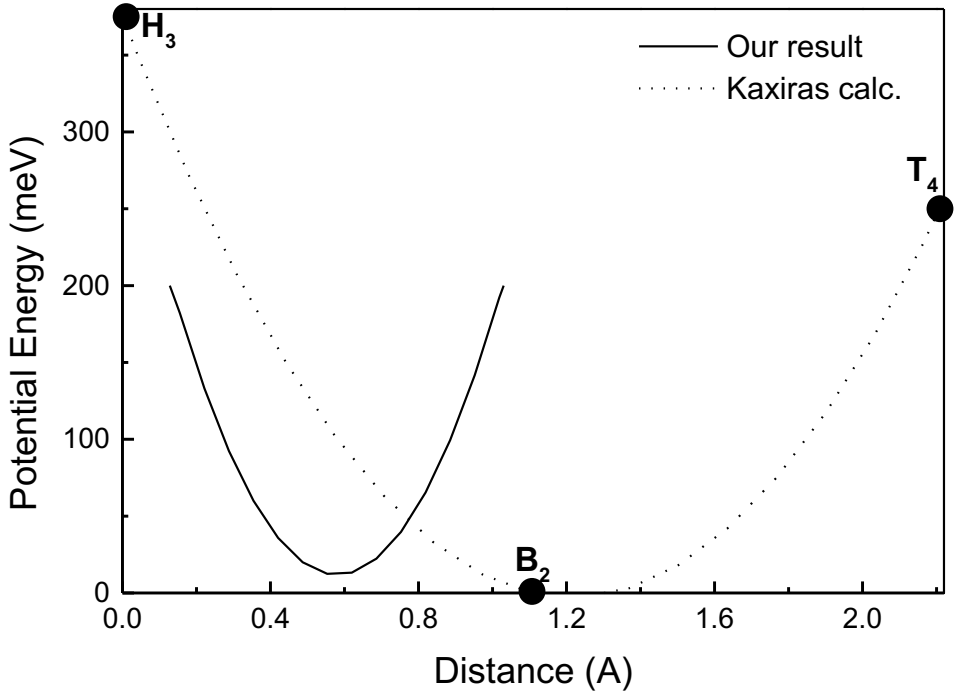

Kyeongjae Cho and Efthimios Kaxirax, Surf. Sci, 396, L261(1998)

Menu of Topics

- Crystal Truncation Rods
- Au quantum nanowires on Stepped Si
- Reconstruction of Pt(110)1x5
- Facetting of Cu(115) to Cu(104)
- Au 'physisorption' on Si(111)7x7
- Deep subsurface strain in Pt(111)/CO
- GSAXS and C-GSAXS new methods

CO dissolved in $HClO_4$ on Pt(111)

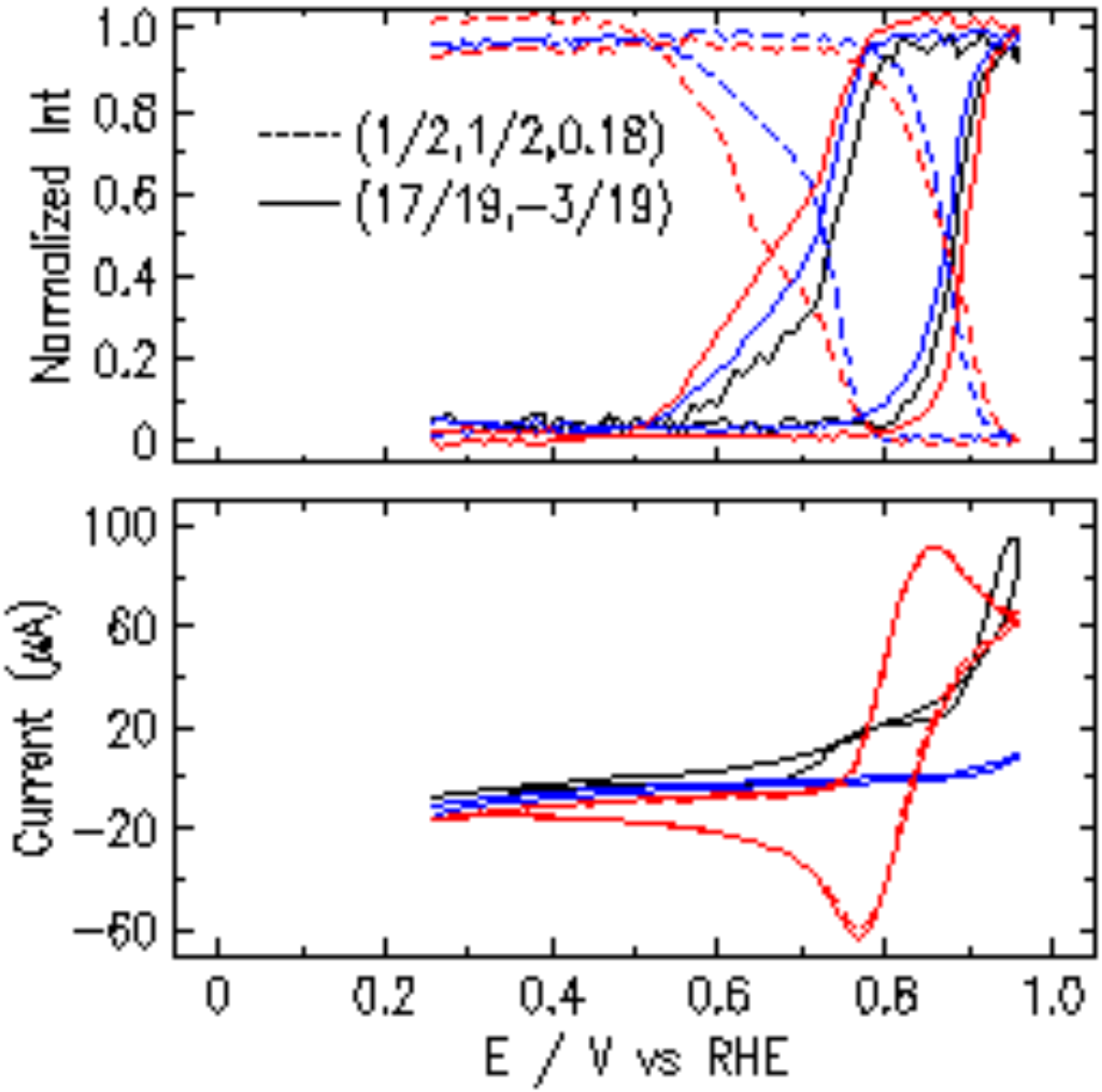

CO reciprocal lattice, rt19

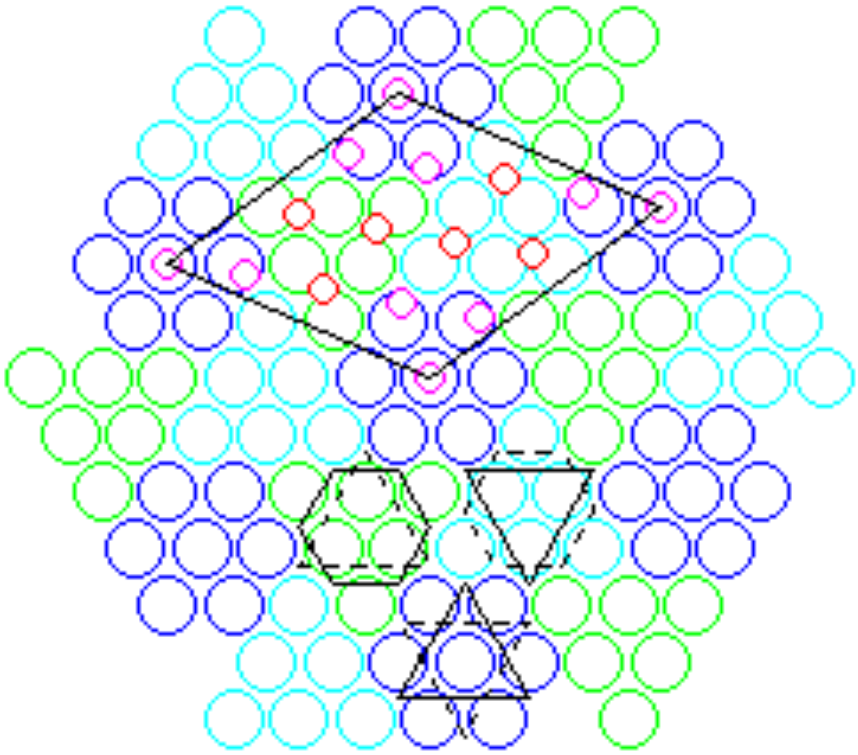

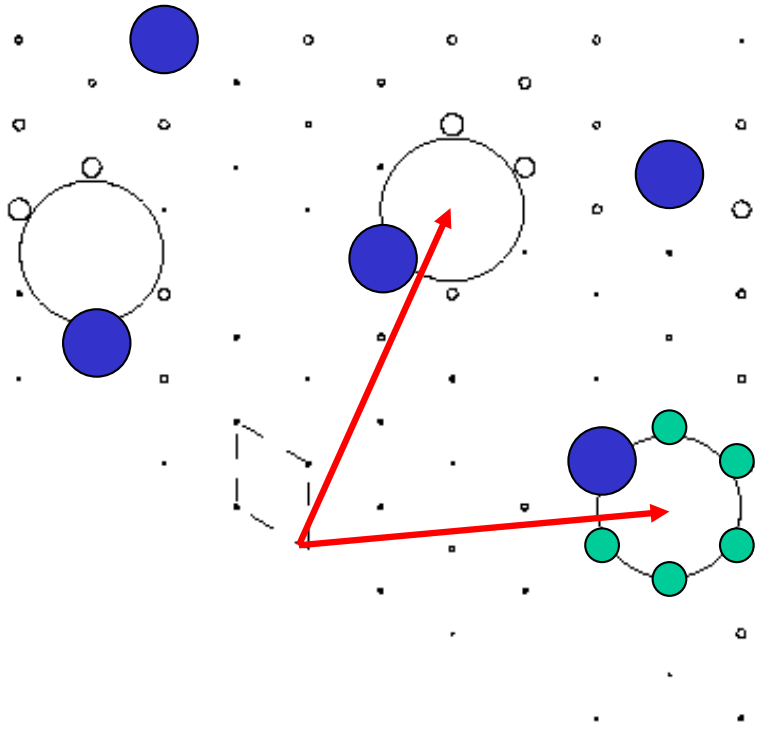

Two inequivalent packings of 13 CO's into rt(19) Pt(111) cell

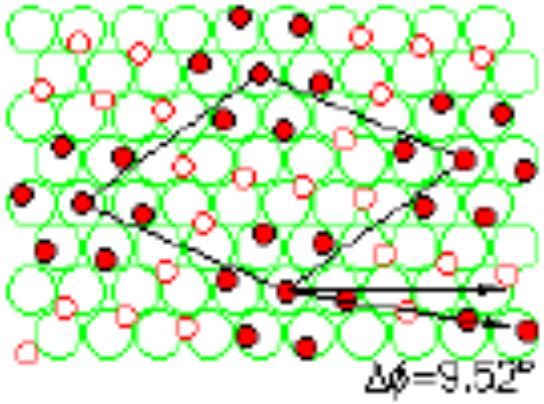

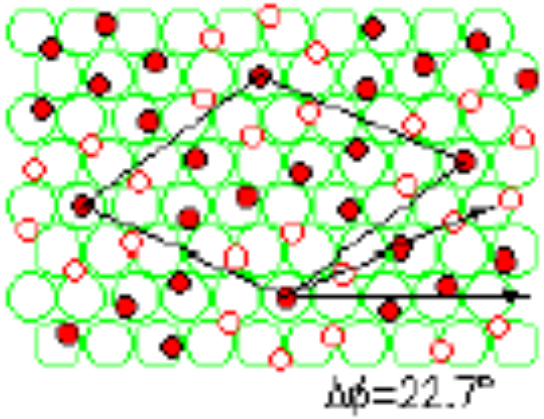

This 'patch' model is the only one observed, by the CO peak positions

This 'ring' model is not seen.

rt19×rt19 CO/Pt(111)

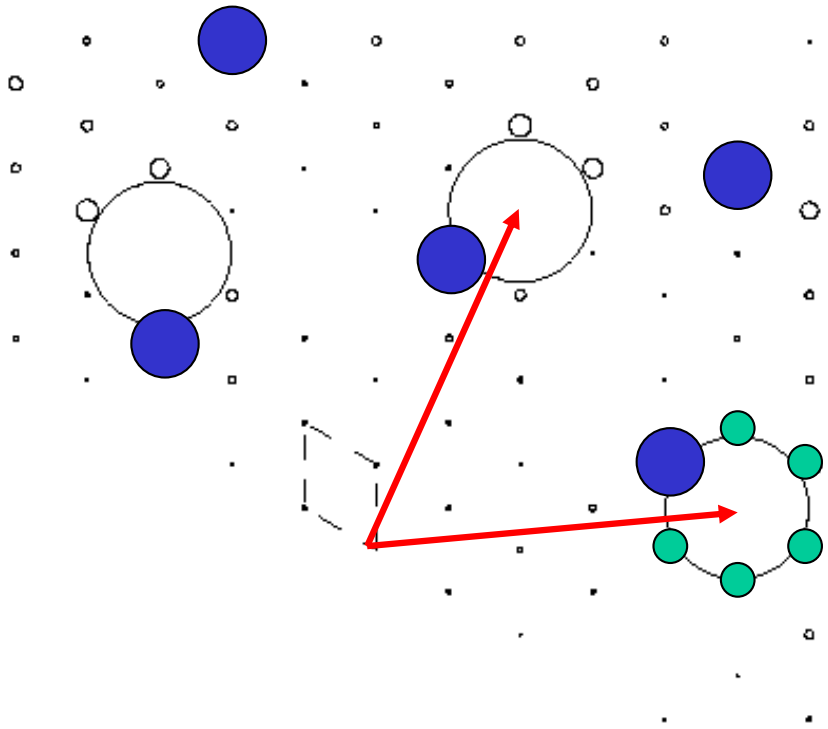

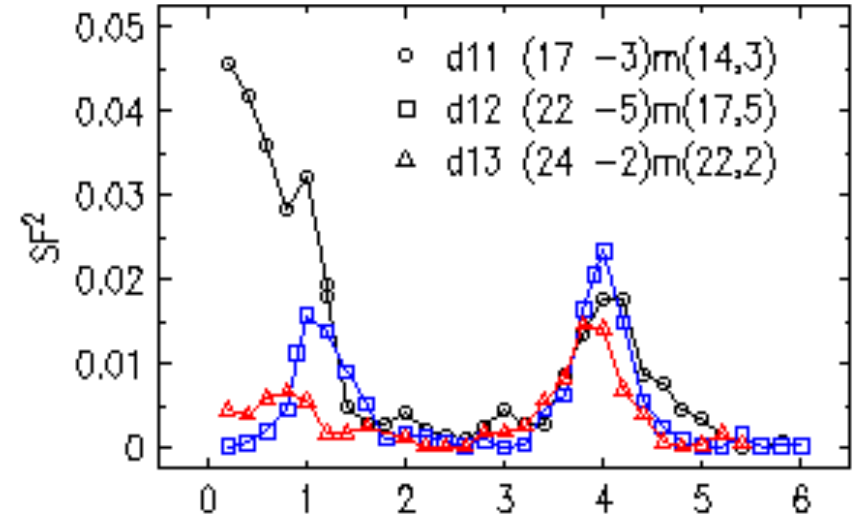

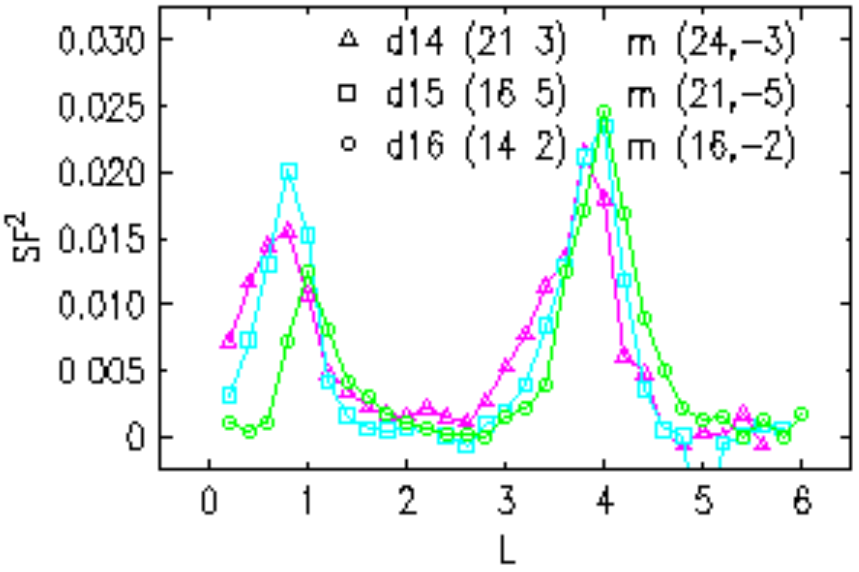

I. K. Robinson

Top and Side Views of Model

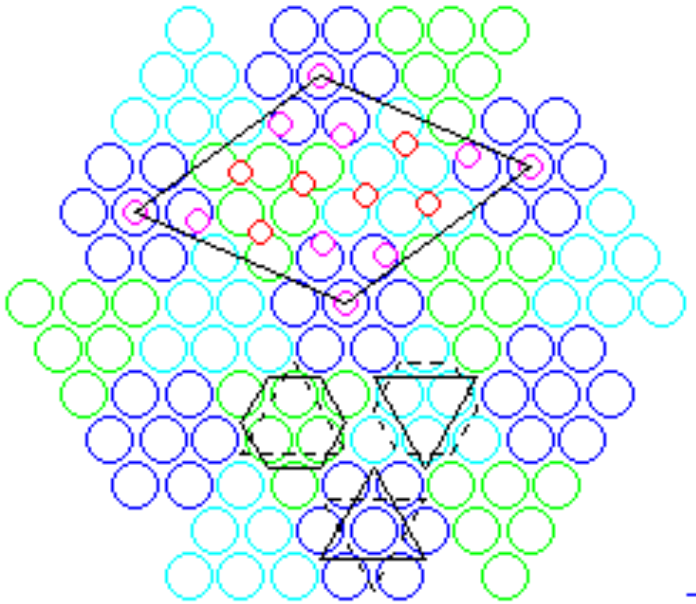

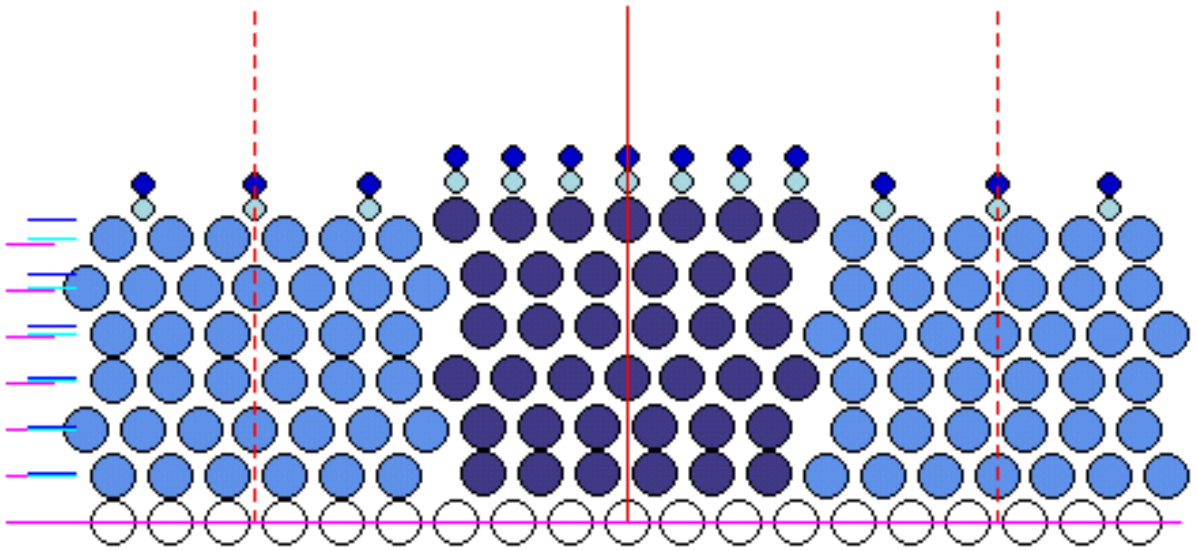

Depth=1.8 layers

D_7=0.28 A

D_{6+6}=0.04 A

σ_{CO}=0.3 A

Fit of Model to CTR Data

Dashed curve is clean Pt(111)

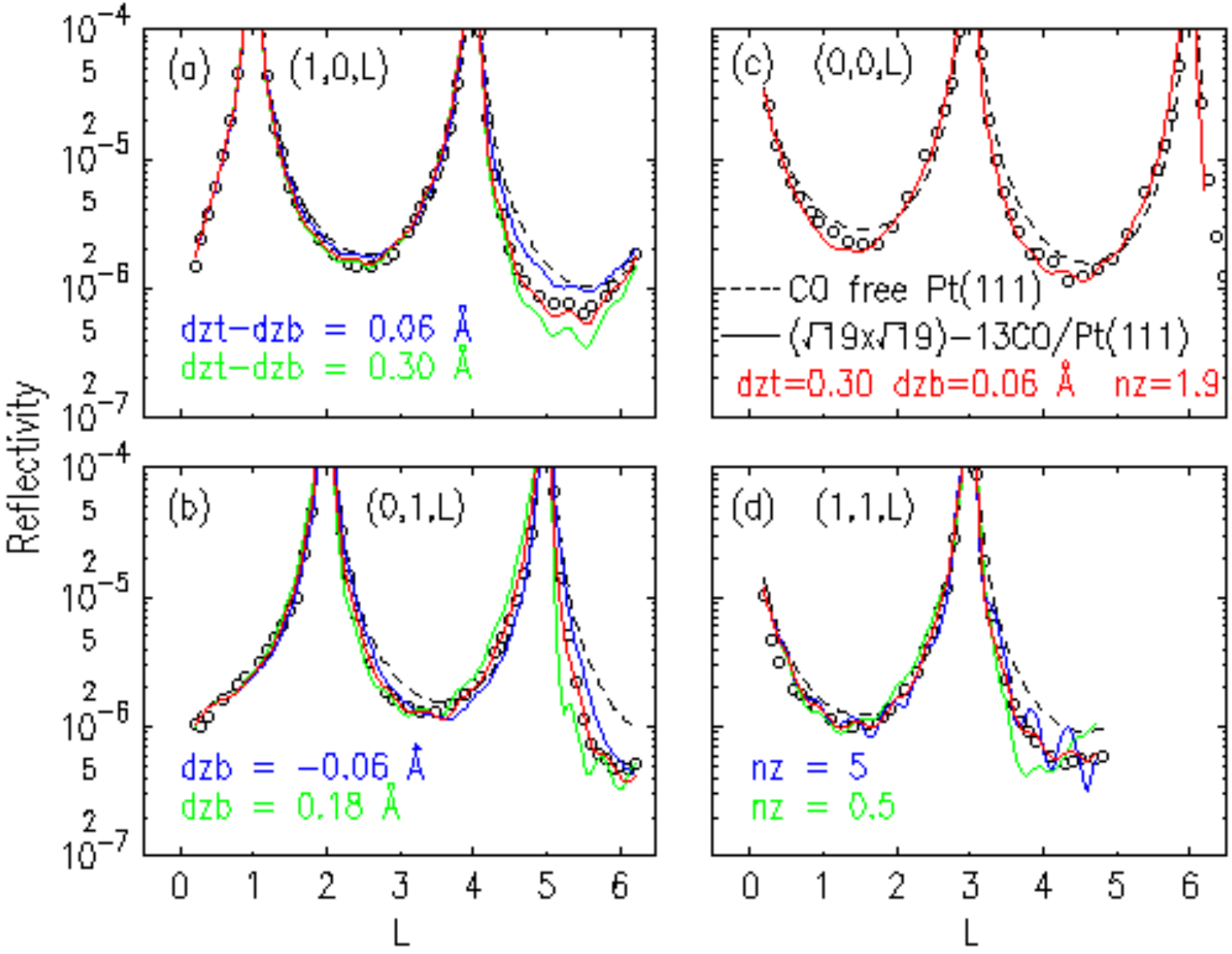

Fit of Model to Rt19 Data

Blue line has vertical relaxations turned off

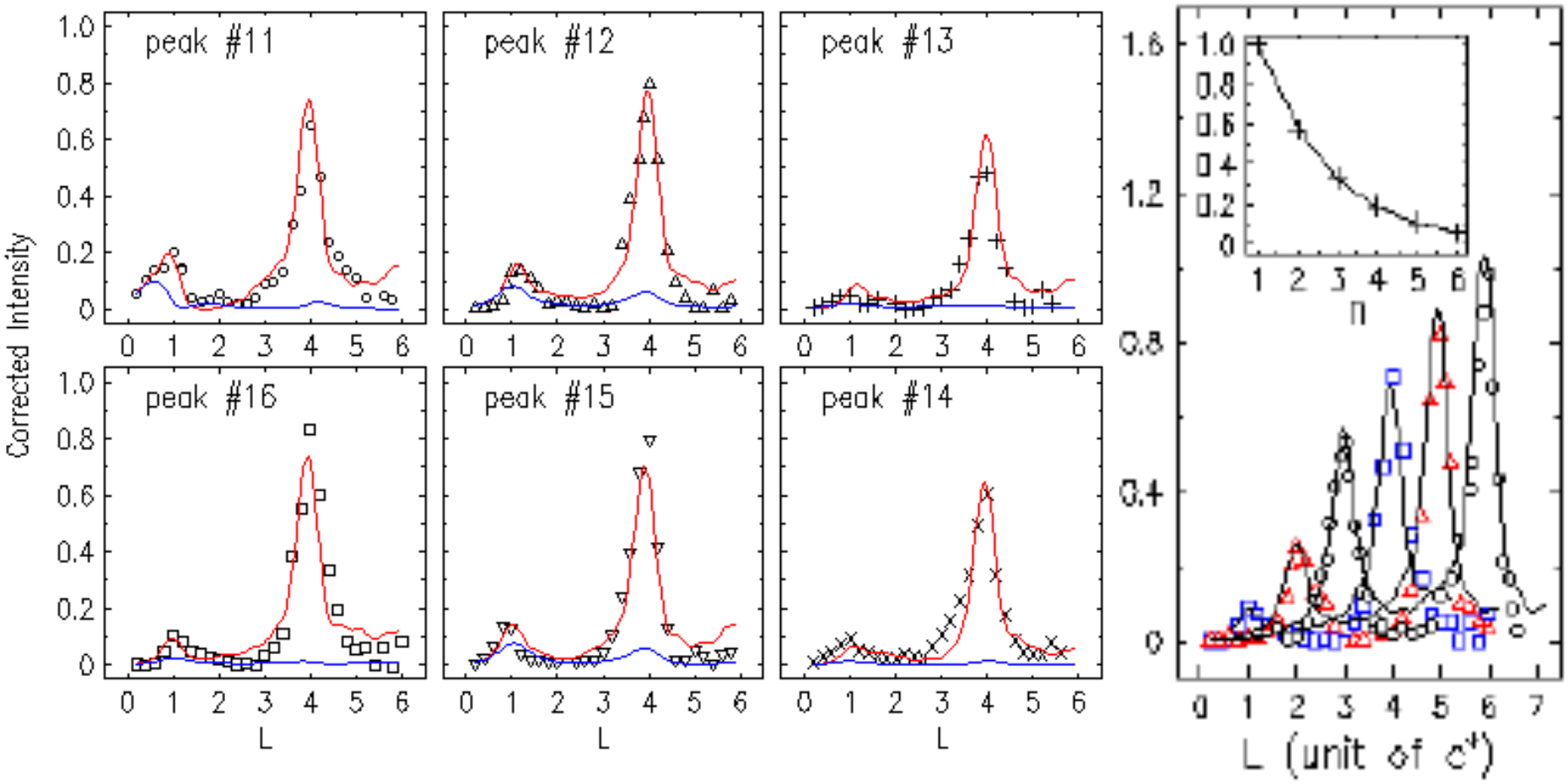

Menu of Topics

- Crystal Truncation Rods
- Au quantum nanowires on Stepped Si
- Reconstruction of Pt(110)1x5
- Facetting of Cu(115) to Cu(104)
- Au ‘physisorption’ on Si(111)7x7
- Deep subsurface strain in Pt(111)/CO
- GSAXS and C-GSAXS new methods

Use of Grazing Incidence

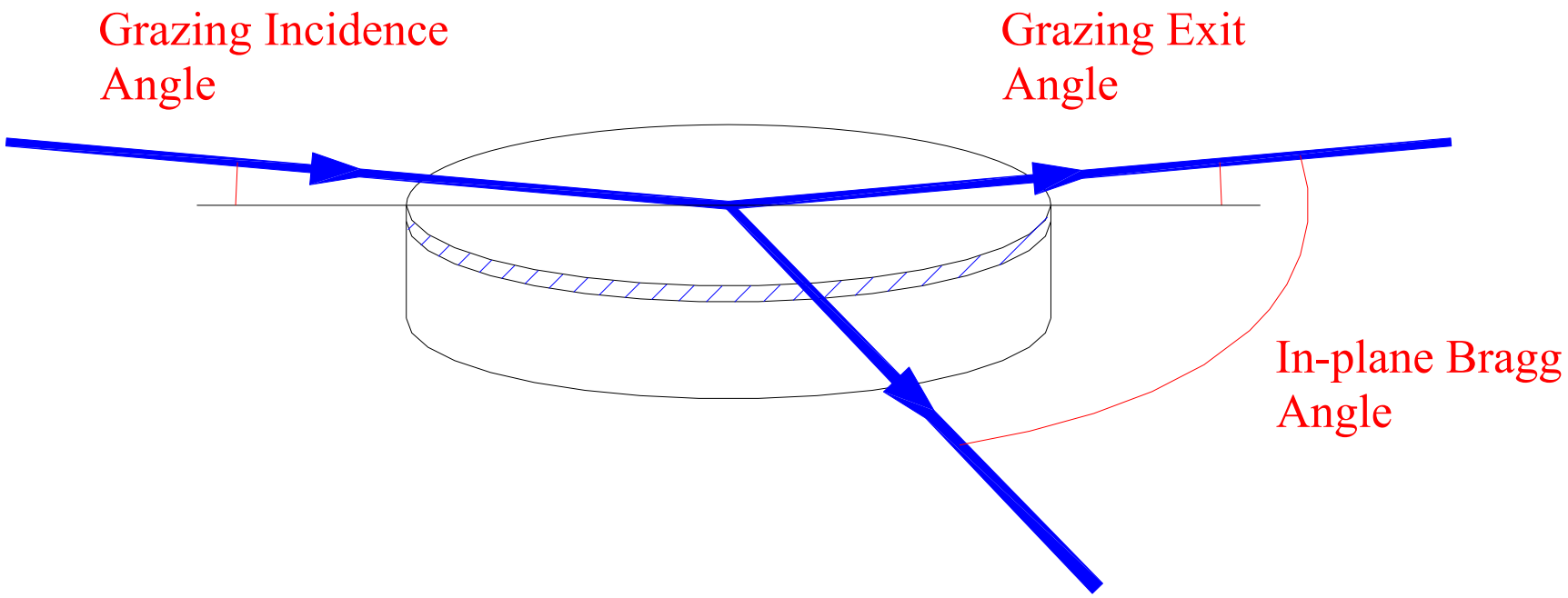

Longitudinal Coherence

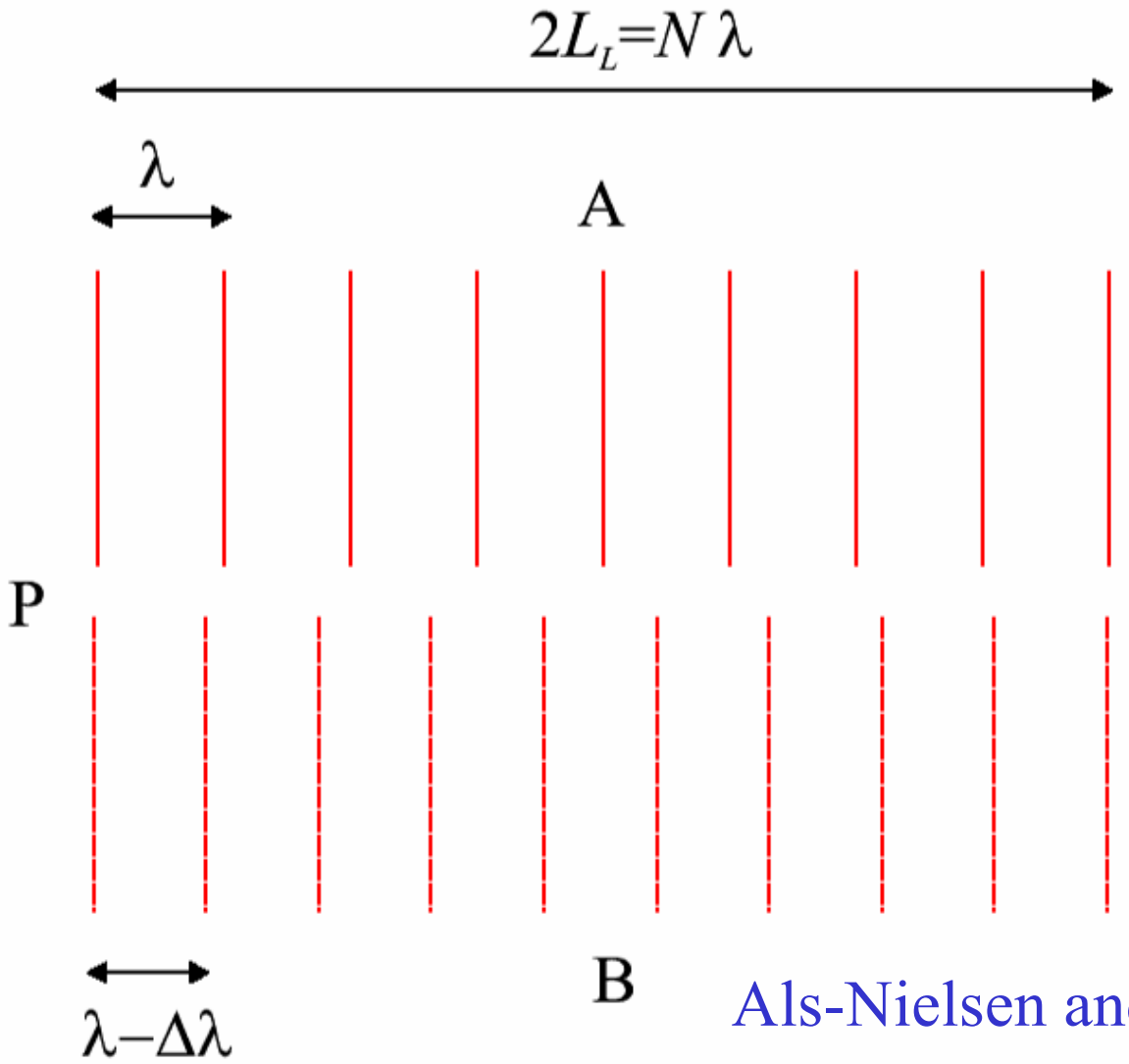

$$L_L = \frac{1}{2}\frac{\lambda^2}{\Delta\lambda}$$

Als-Nielsen and McMorrow (2001)

Lateral (Transverse) Coherence

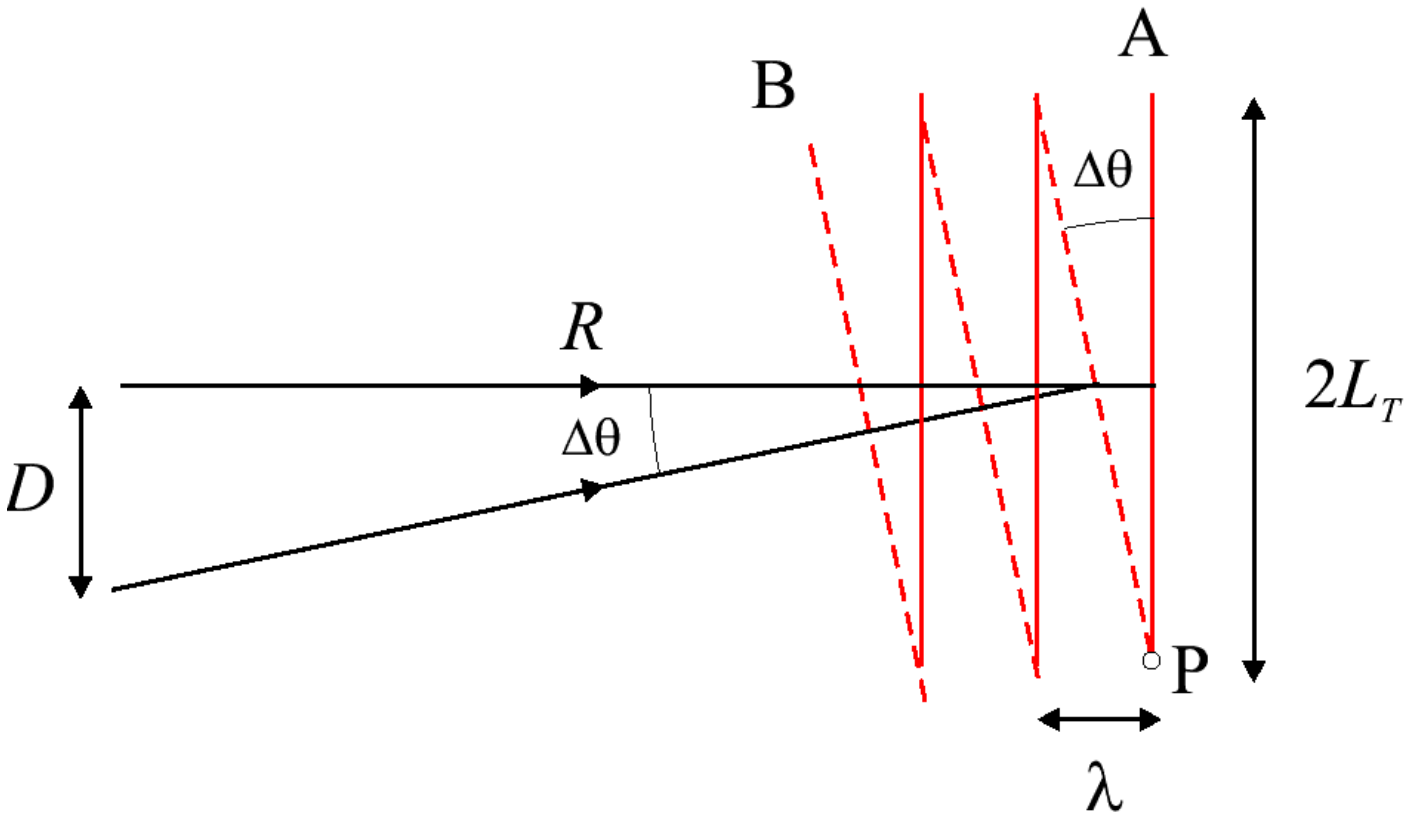

$$L_T = \frac{\lambda}{2}\frac{R}{D}$$

Als-Nielsen and McMorrow (2001)

Coherence at the APS or ESRF

Typical of 3rd Generation (undulator) Synchrotron Source

Coherence of	ξ_{VER}	ξ_{HORIZ}	ξ_{LONG}	Flux
Raw Undulator	35μm	9μm	0.004μm	2×10^{12}
Si(111) Monochromator	35μm	9μm	1μm	1×10^{10}
C(111) Monochromator	35μm	9μm	3μm	3×10^{9}

Coherent region defined by slits

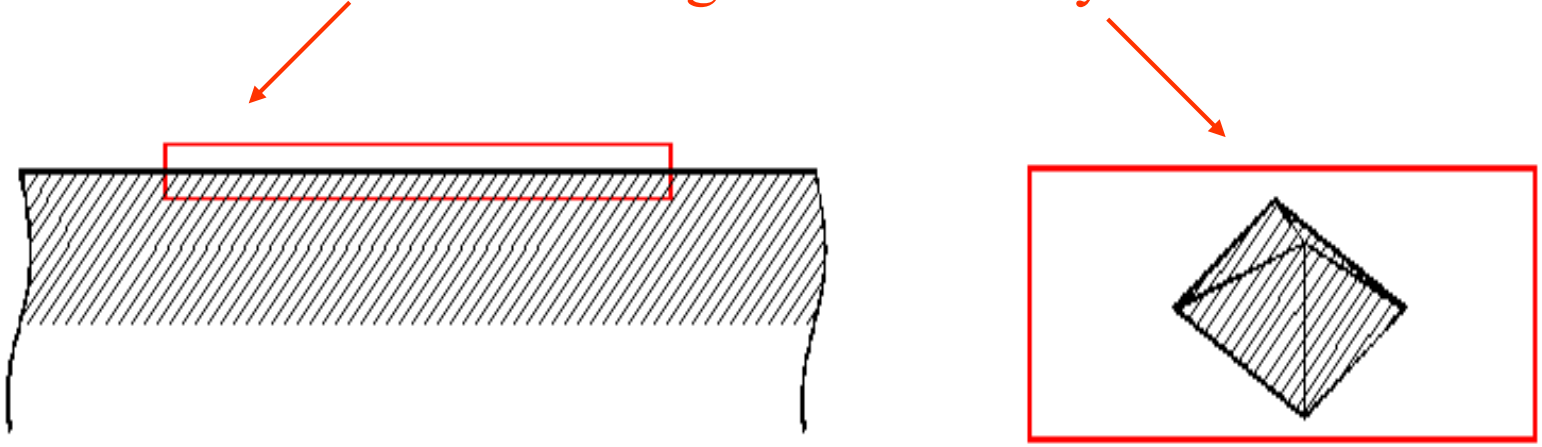

Diffuse Scattering acquires Structure using CXD

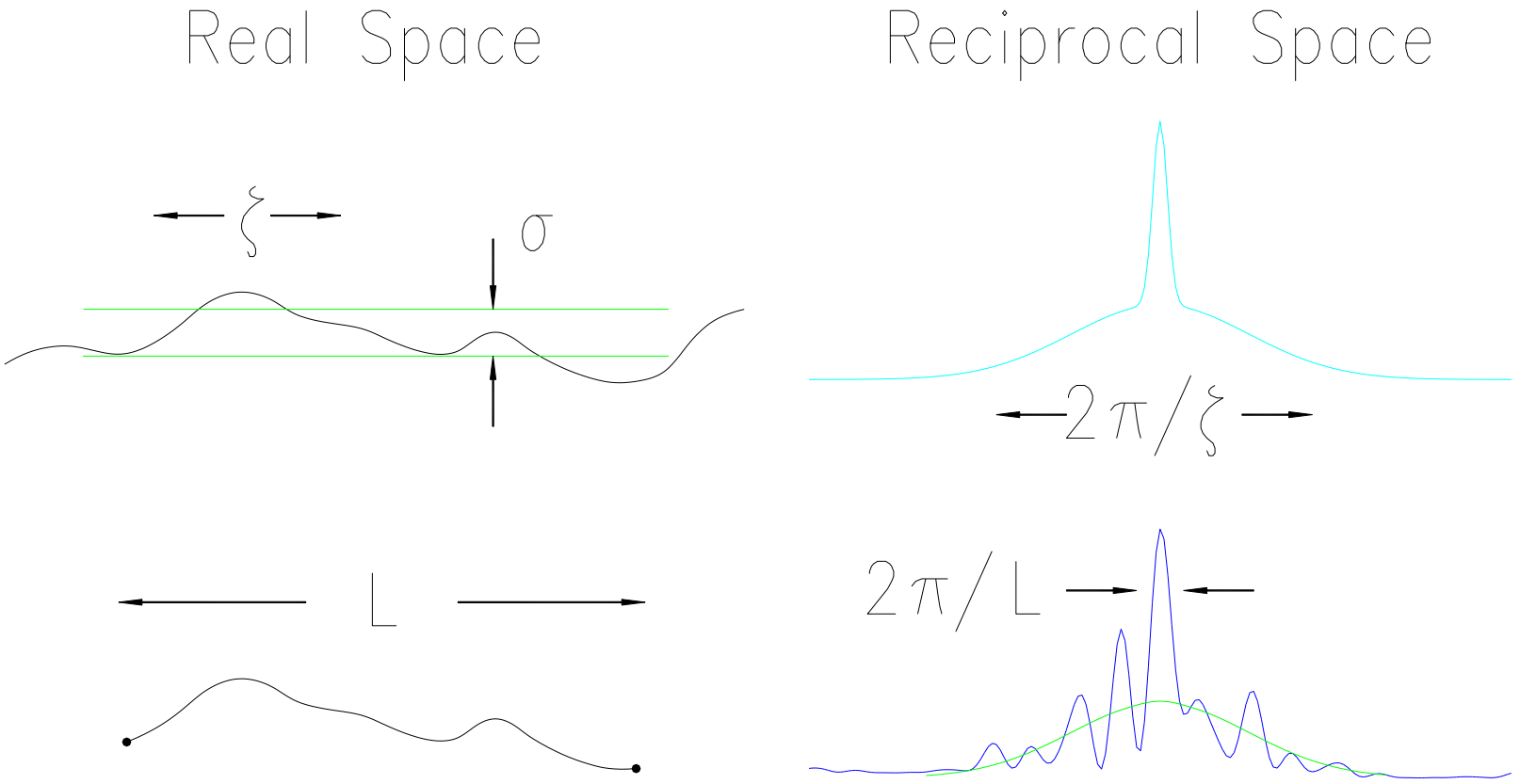

34-ID-C Capabilities

- Beam-splitting mirror
  - cuts out half of central cone
- Double Crystal Monochromator
  - Diamond, Si(111) and Si(220)
- Coarse and Fine coherence slits
  - UHV Roller-blade design
- Long-arm Microcontrole Diffractometer

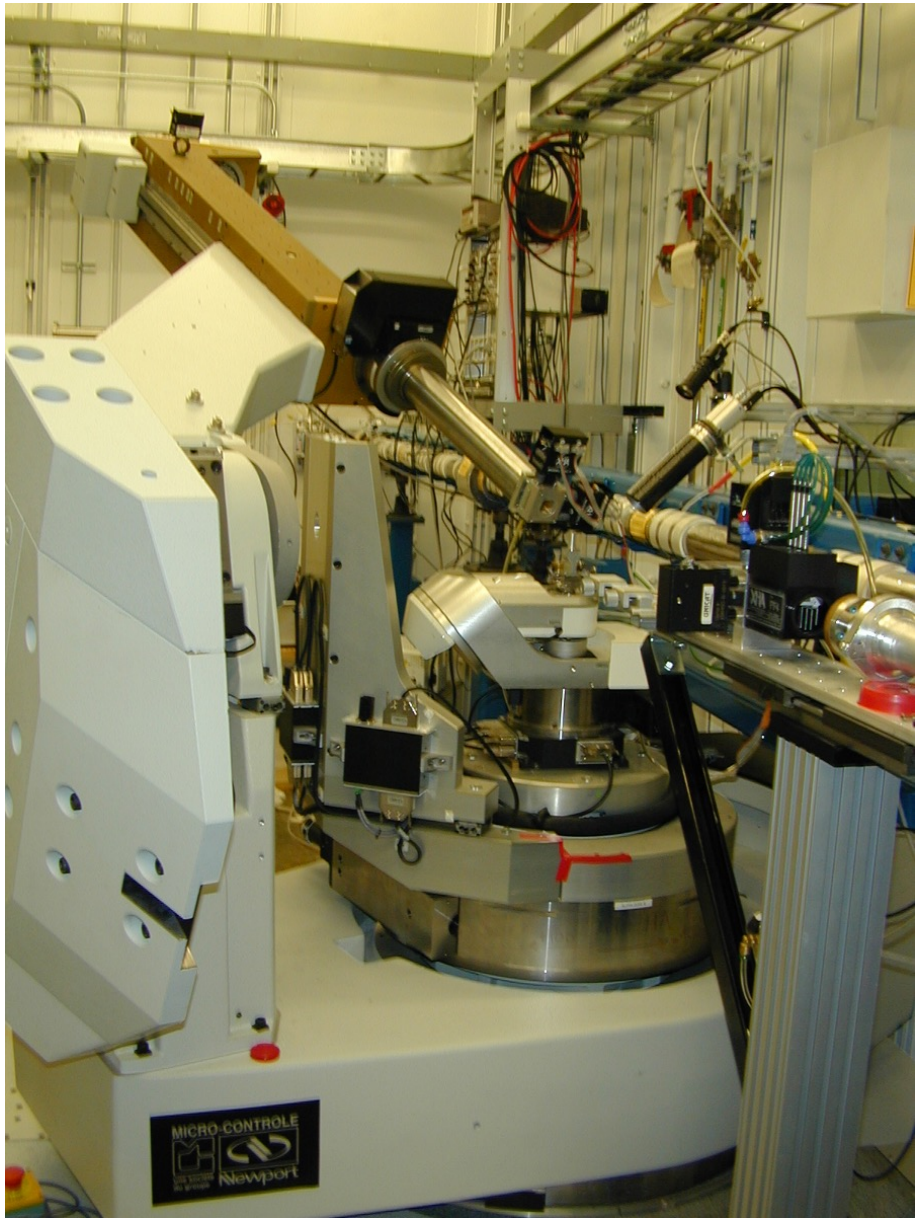
MICRO-CONTROLE
Newport

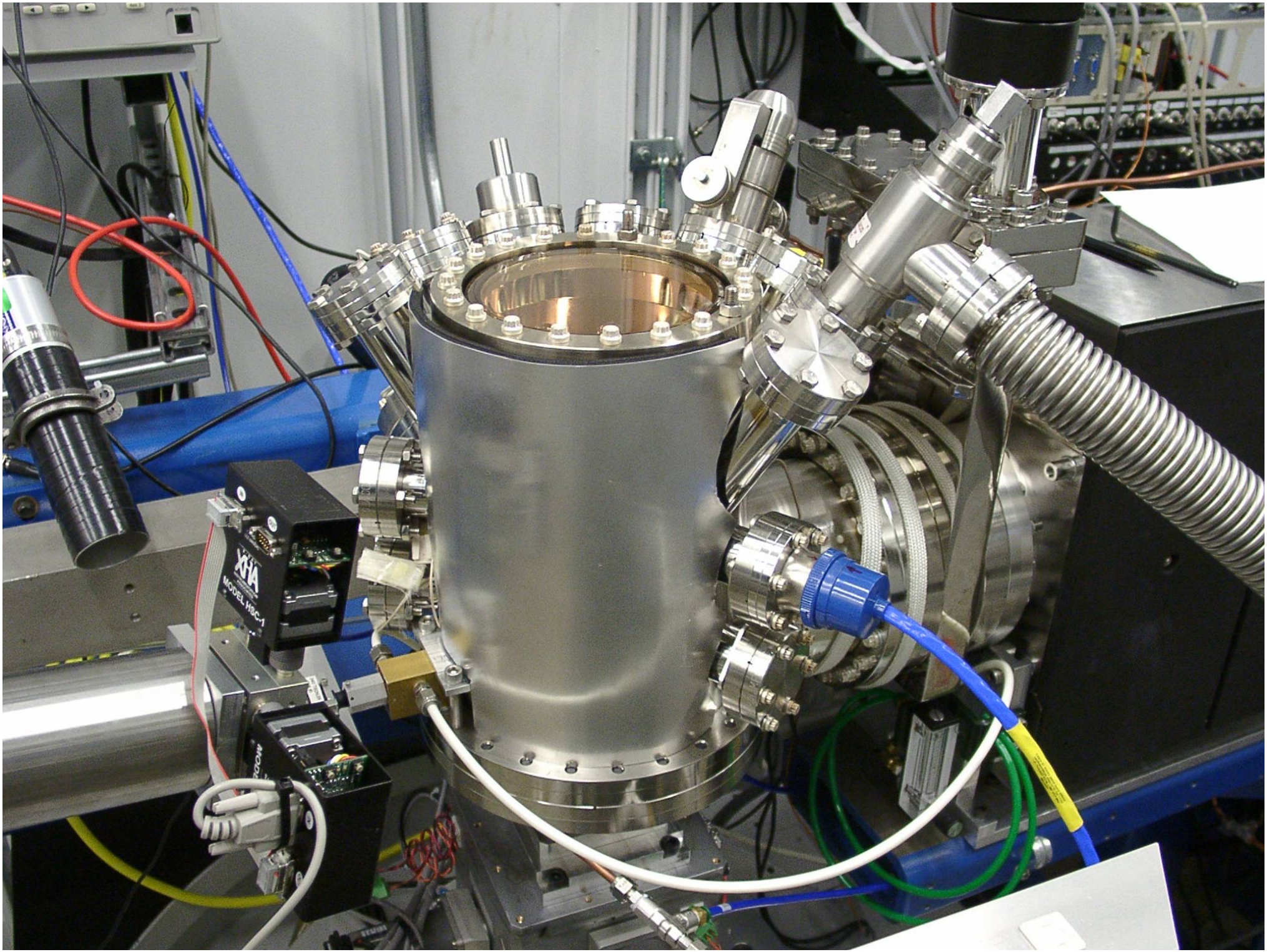
MODEL HSC-1

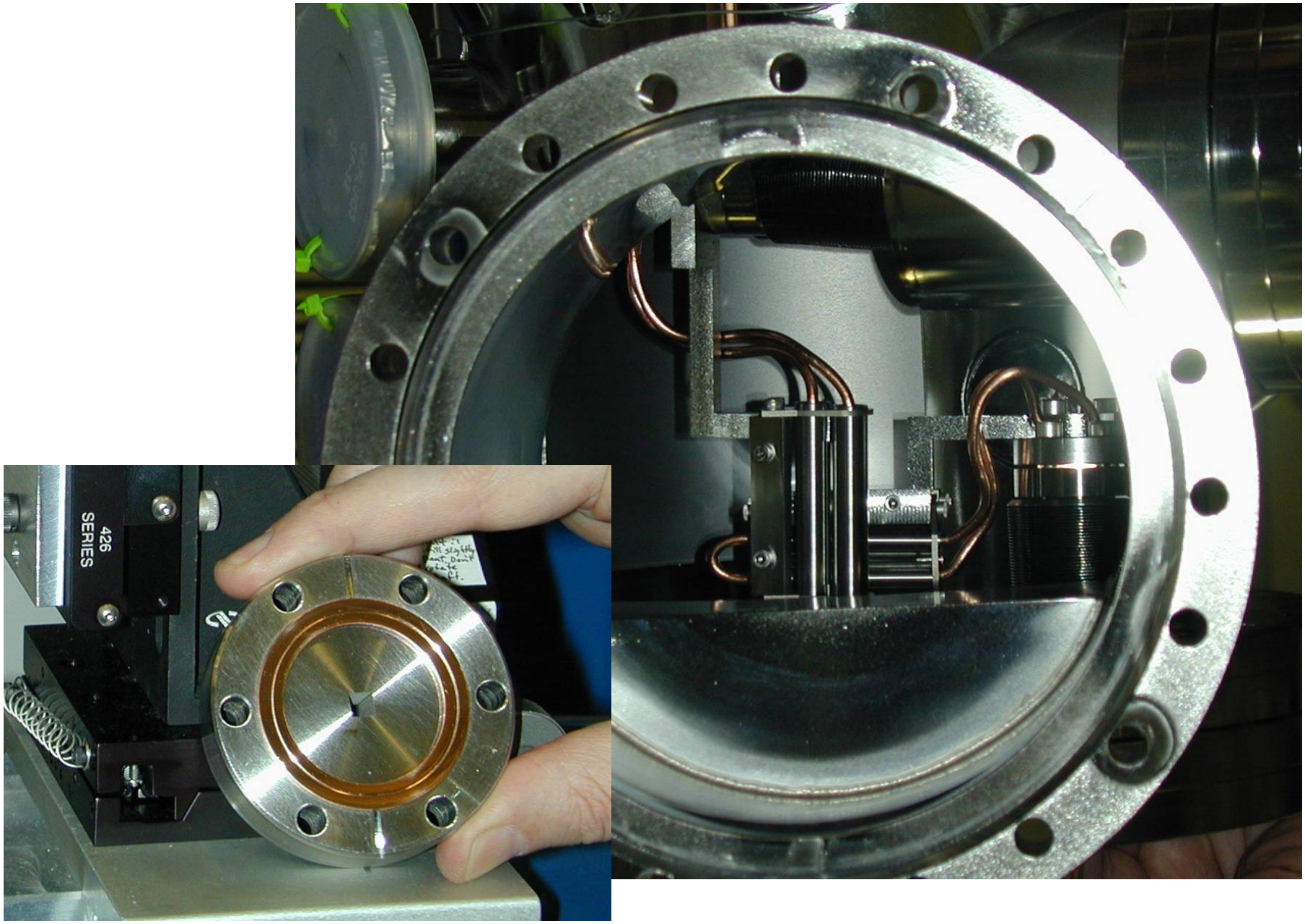
426
SERIES

Structure in "Yoneda" Peak

Grazing-exit diffraction from a 1000A Au polycrystalline film

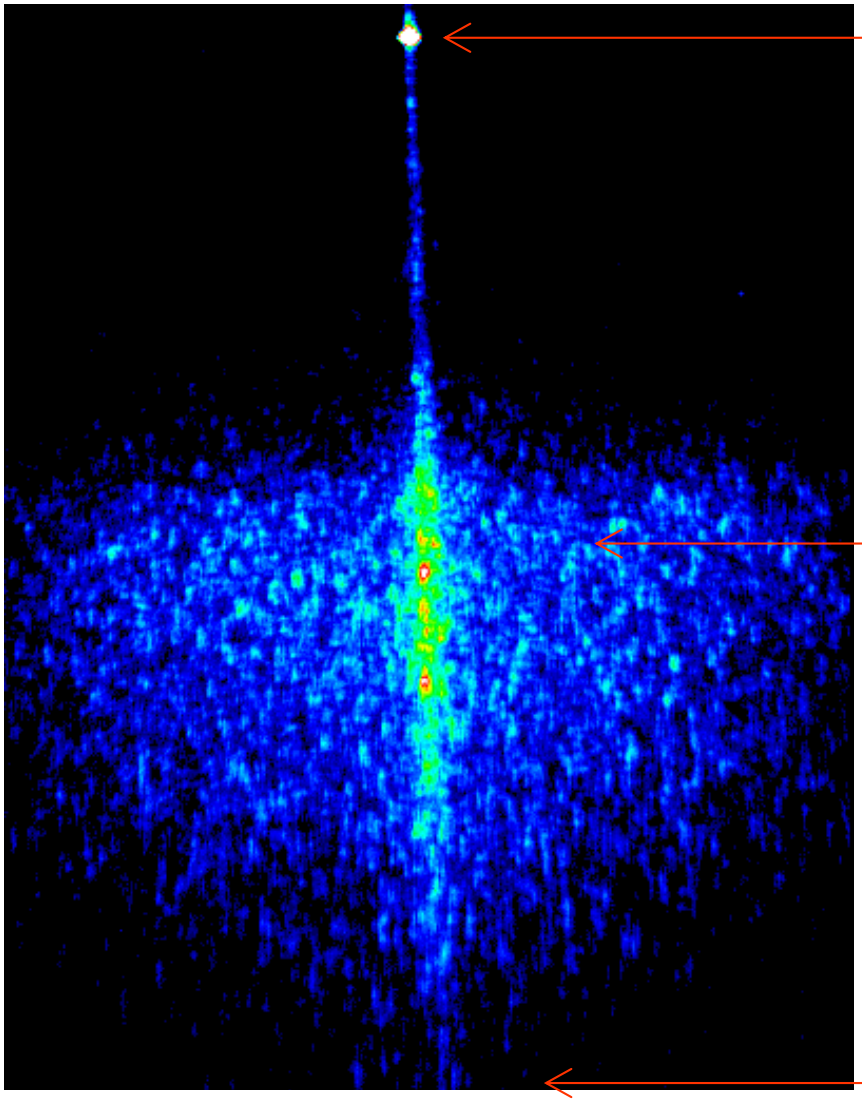

Specular ($\alpha_f \sim \alpha_i$)

$\alpha_f \sim \alpha_c$

$\alpha_f \sim 0$

Coherent "Yoneda" sample geometry

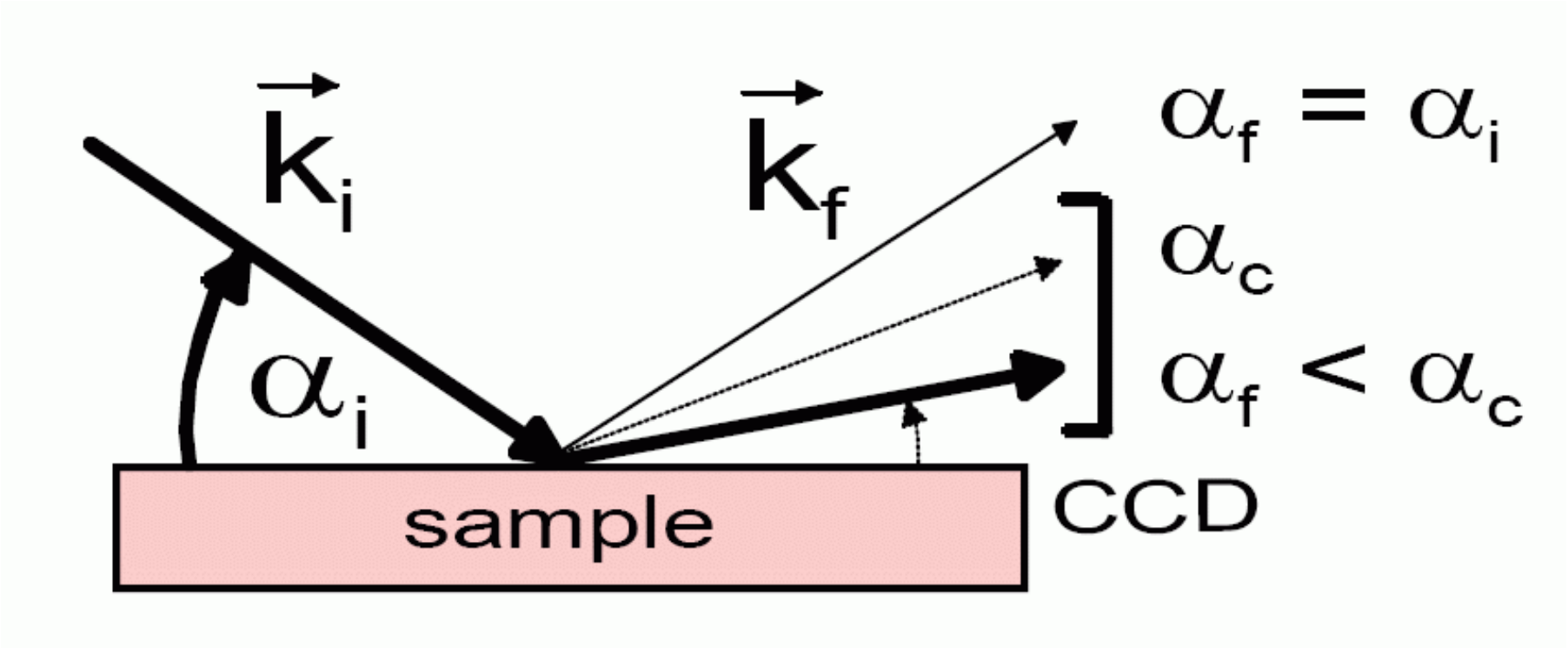

F. Pfeiffer, W. Zhang and I. K. Robinson,
Applied Physics Letters 84 1847 (2004)

Anisotropy of speckles

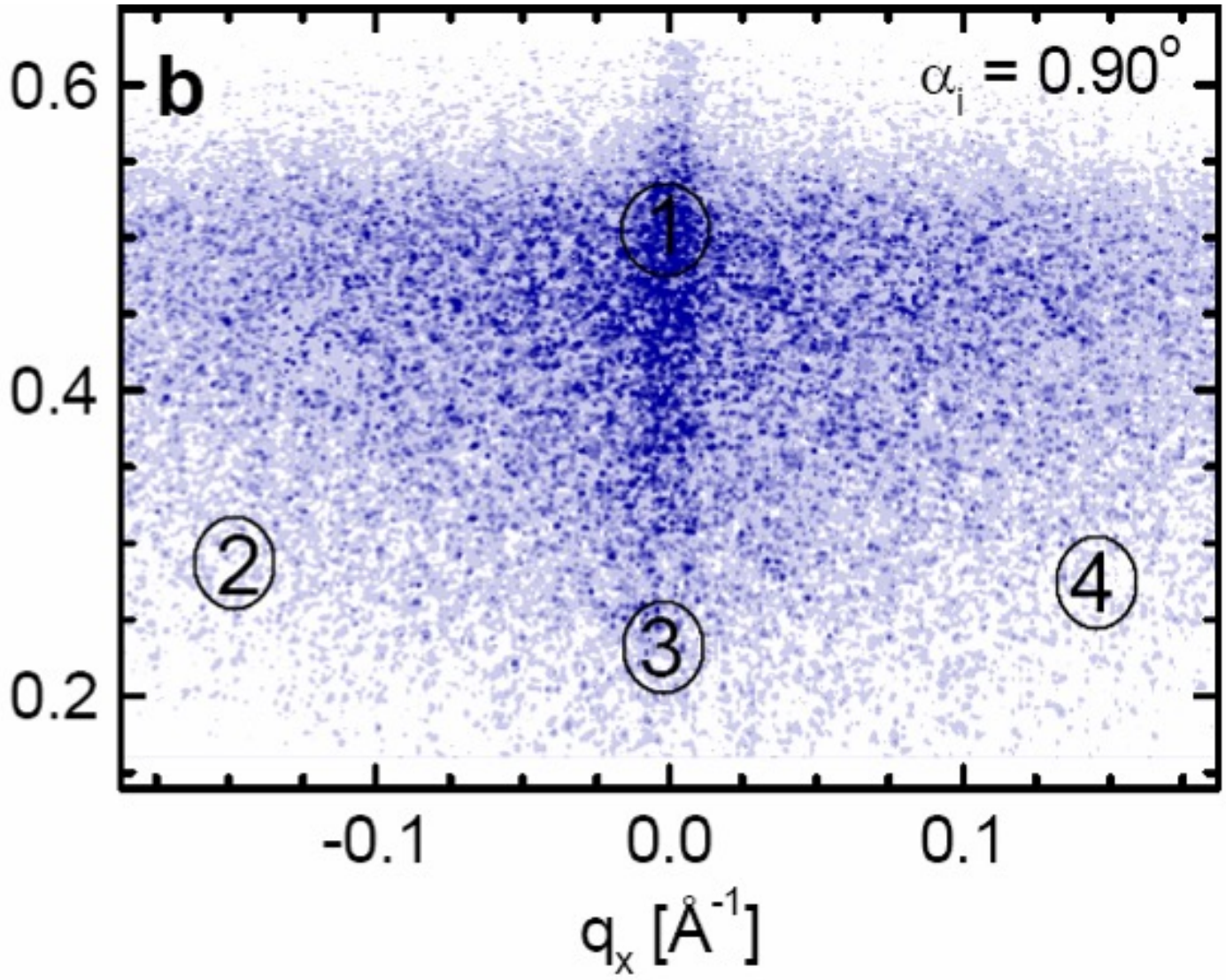

Variation with entrance slit (microns)

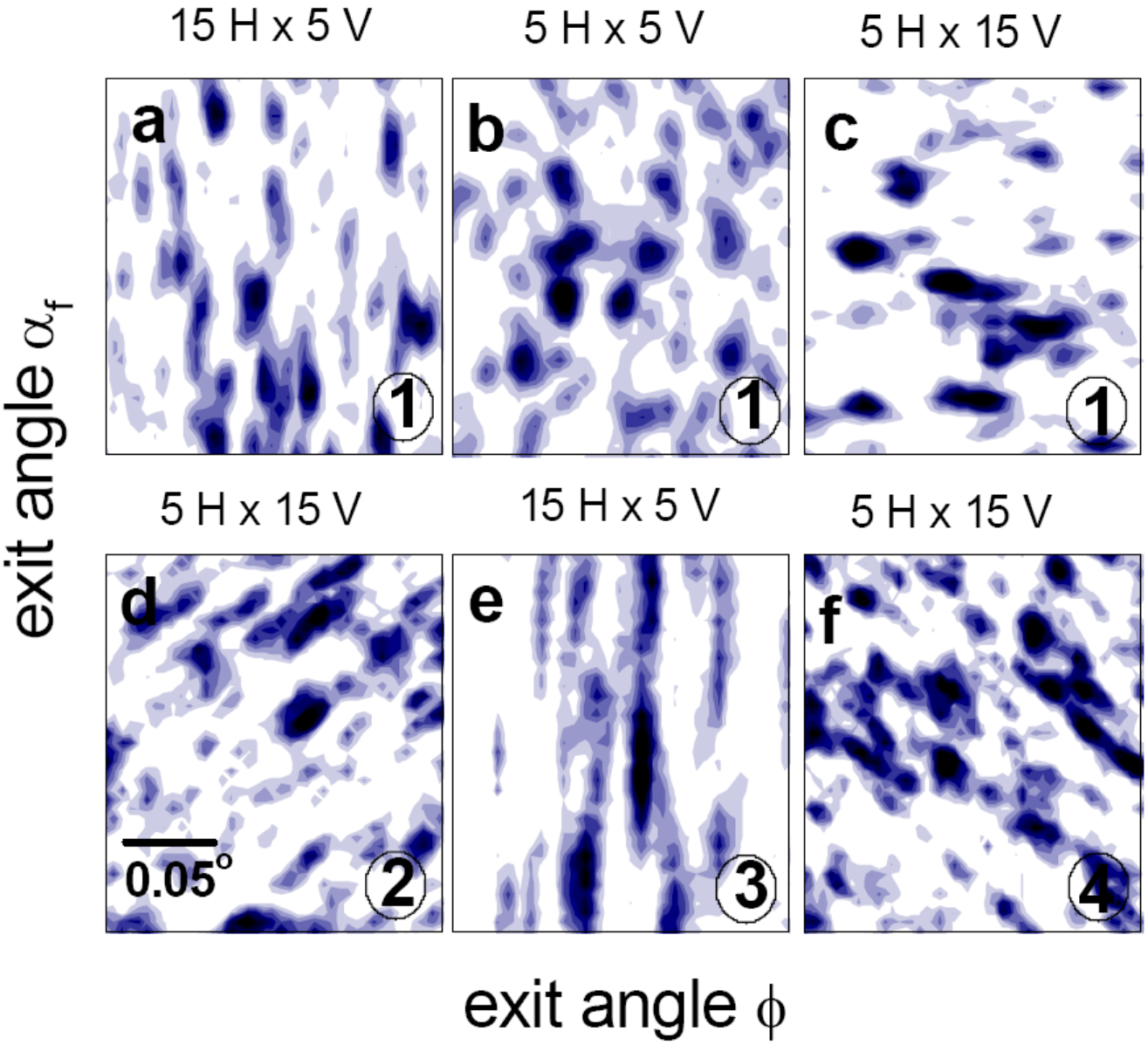

Angle series, 0.01° steps

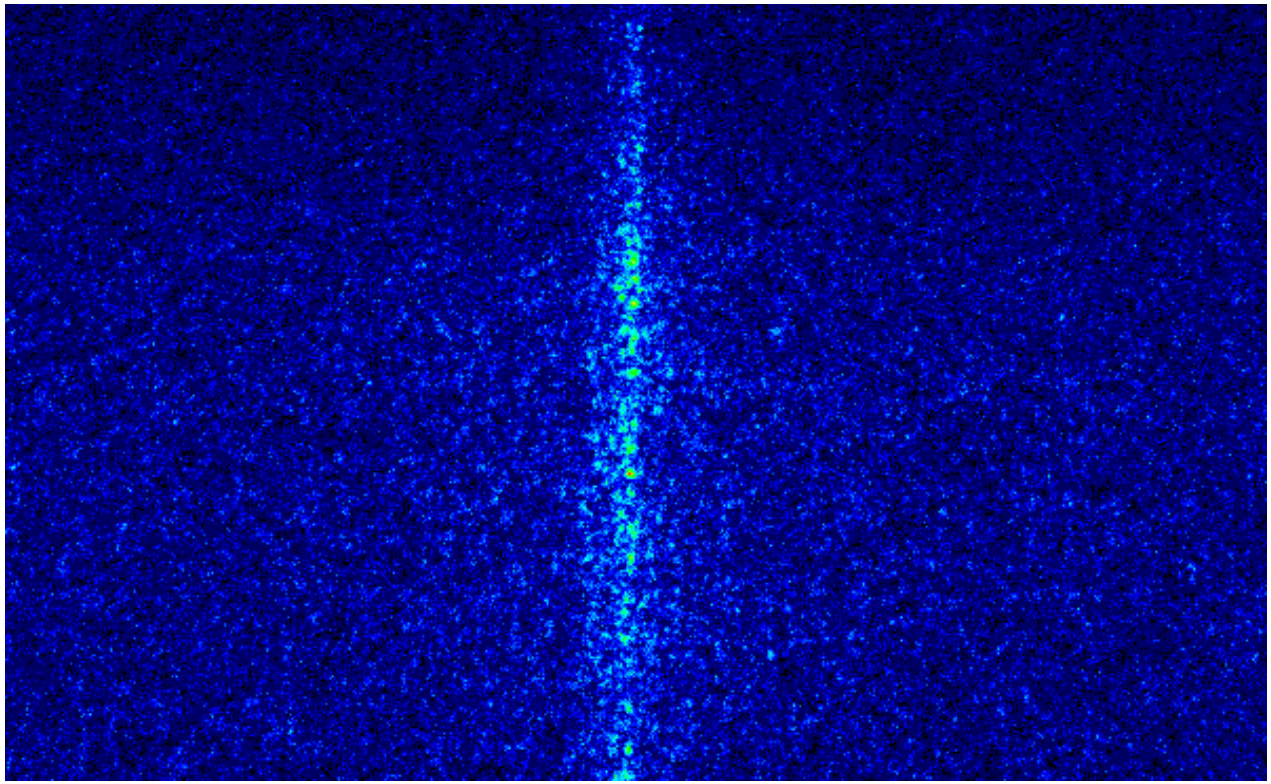

Structure in "Yoneda" Peak

Grazing-exit diffraction from a 1000A Au polycrystalline film

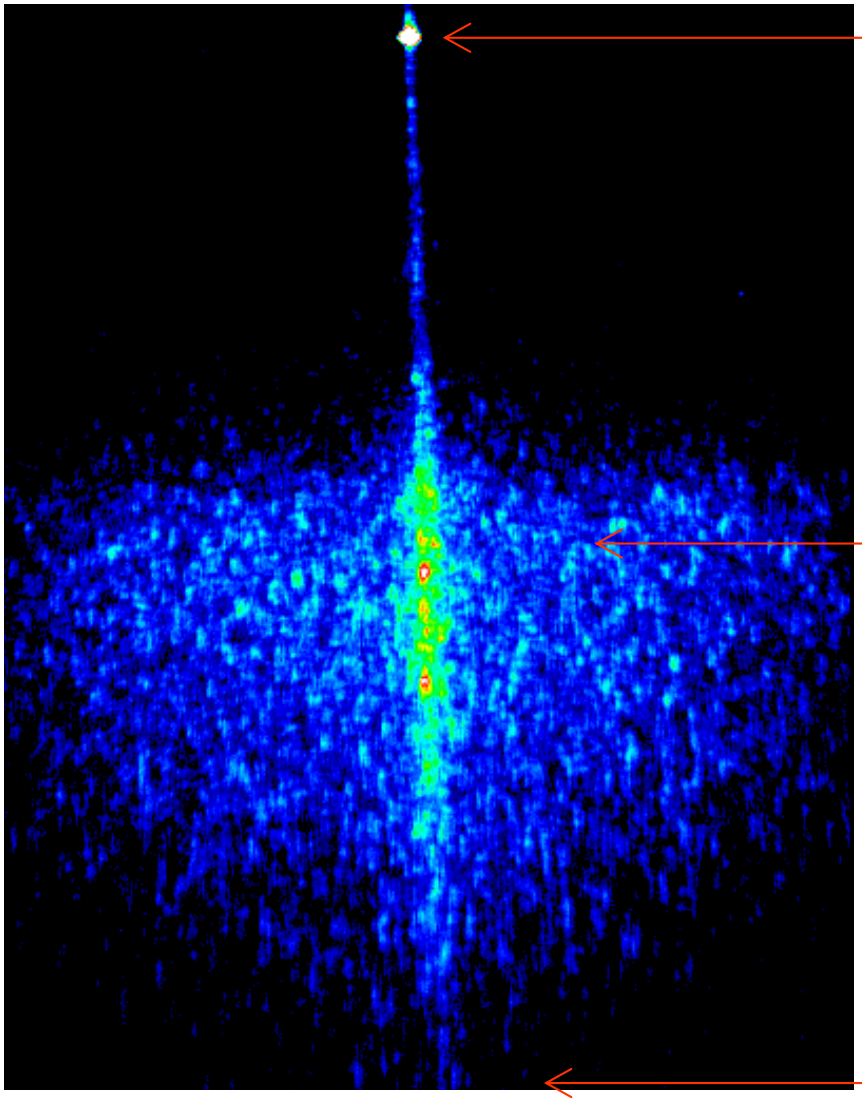

Specular ($\alpha_f \sim \alpha_i$)

$\alpha_f \sim \alpha_c$

$\alpha_f \sim 0$

Refraction by Gold Interface

$$\alpha_i' = \sqrt{\alpha_i^2 - 2\delta + 2i\beta}$$

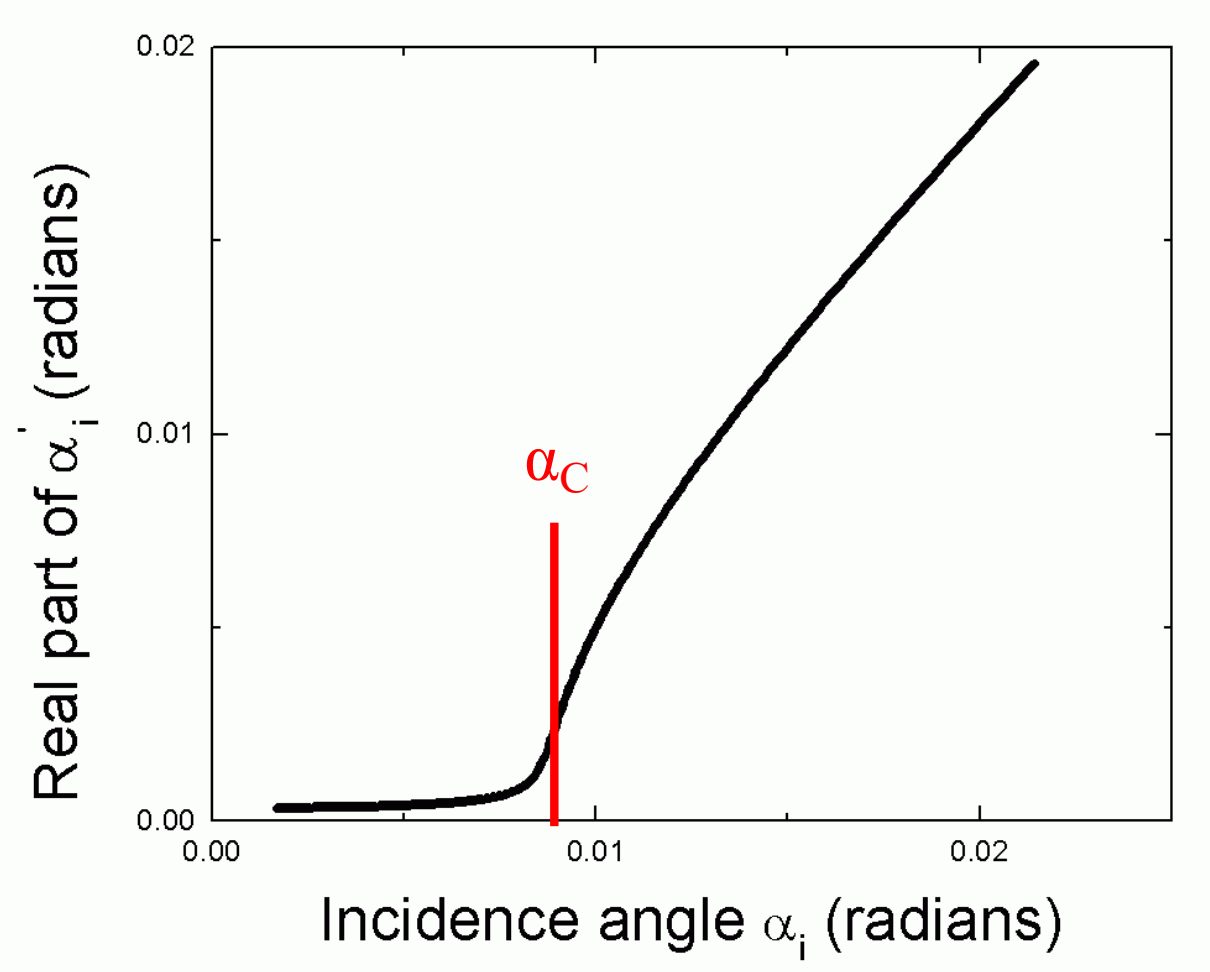

E=8.92keV
$\delta = 3.76 \times 10^{-5}$
$\beta = 2.9 \times 10^{-6}$

Competitive Grain Growth

C. V. Thompson, Ann. Rev. Mat. Sci. **30** 159 (2000)

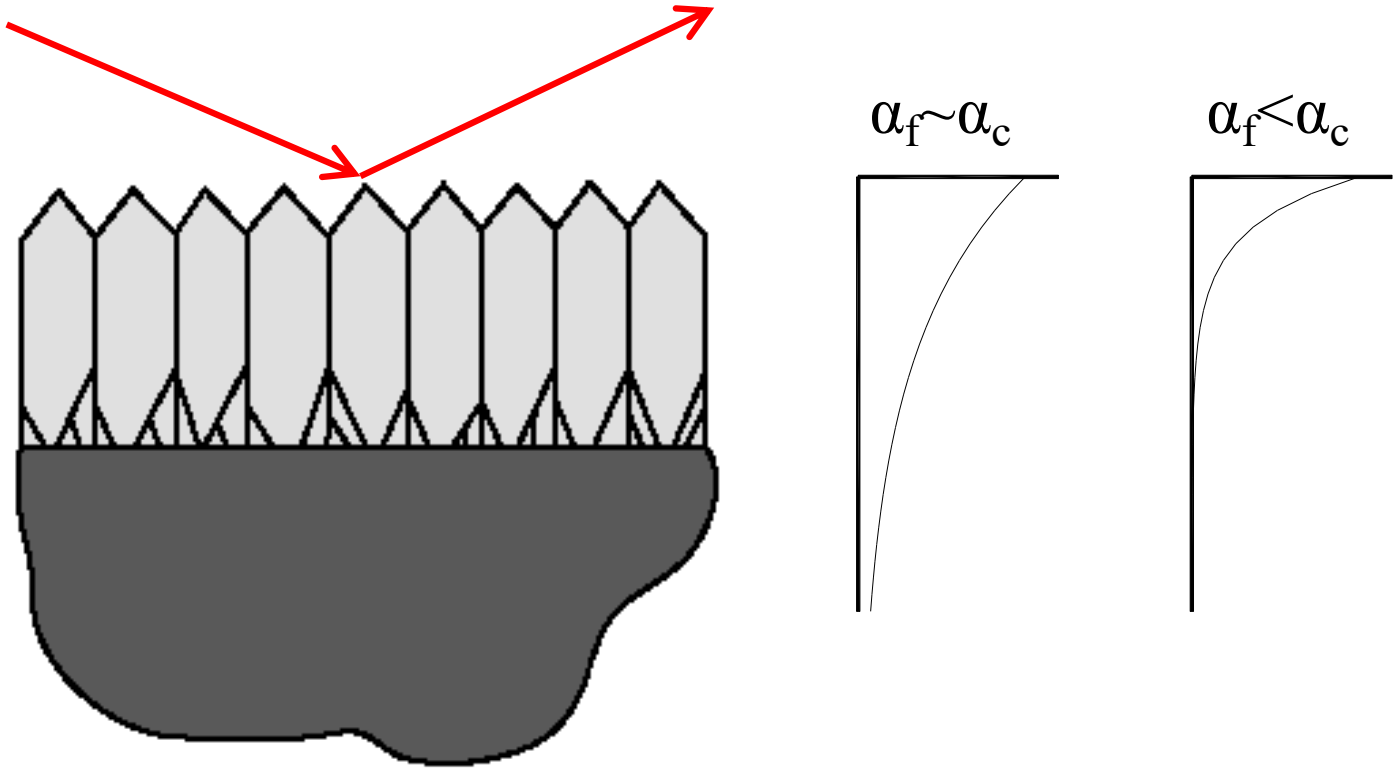

Model of grain correlations

- Density of film assumed uniform, except at location of grain boundaries
- Assume exponential size distribution in 3D
- Expect (Lorentzian)^2 lineshape

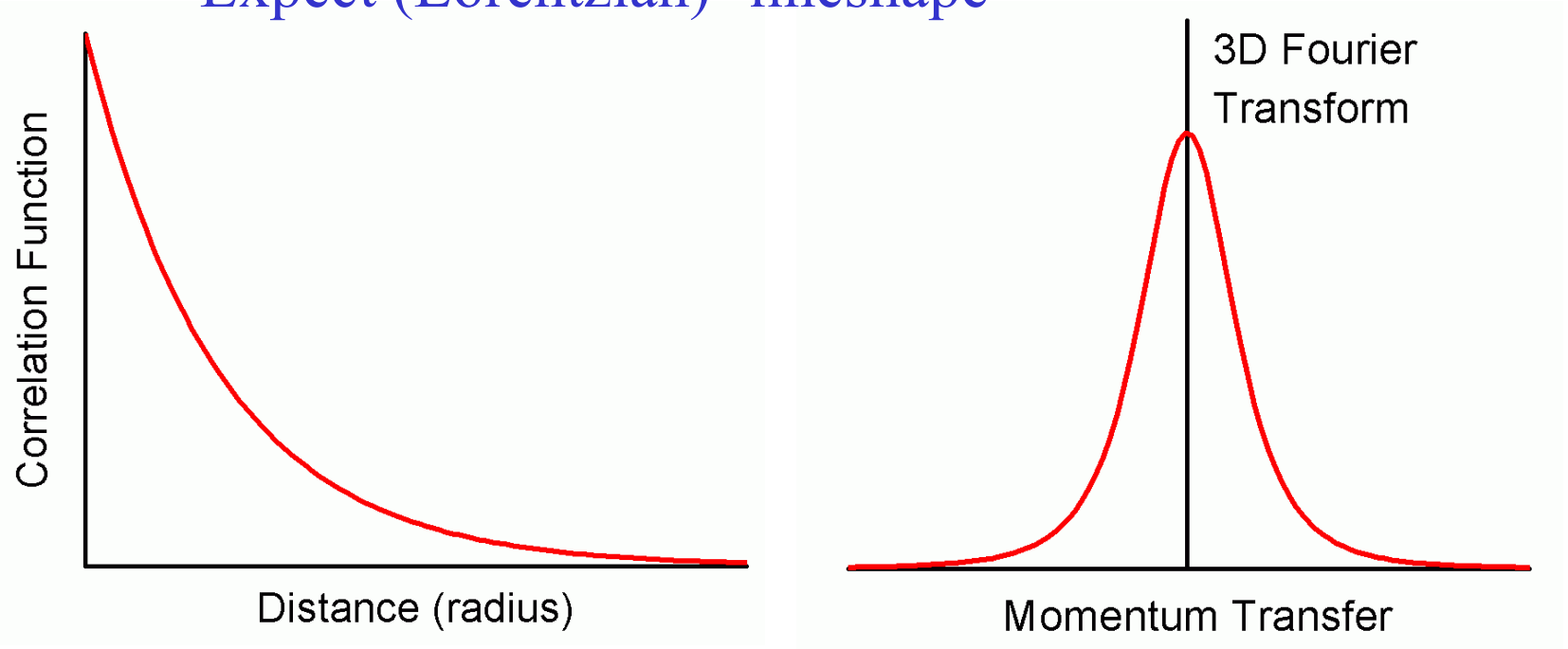

Effect of refraction on lineshape

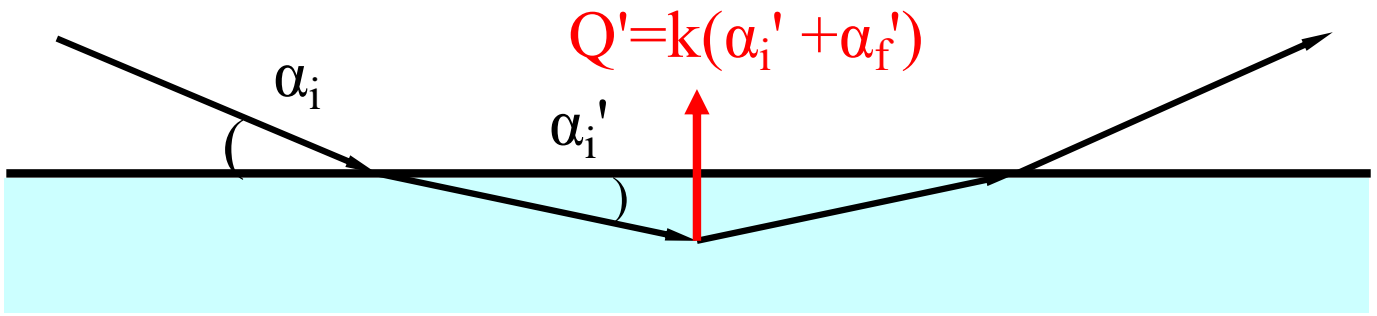

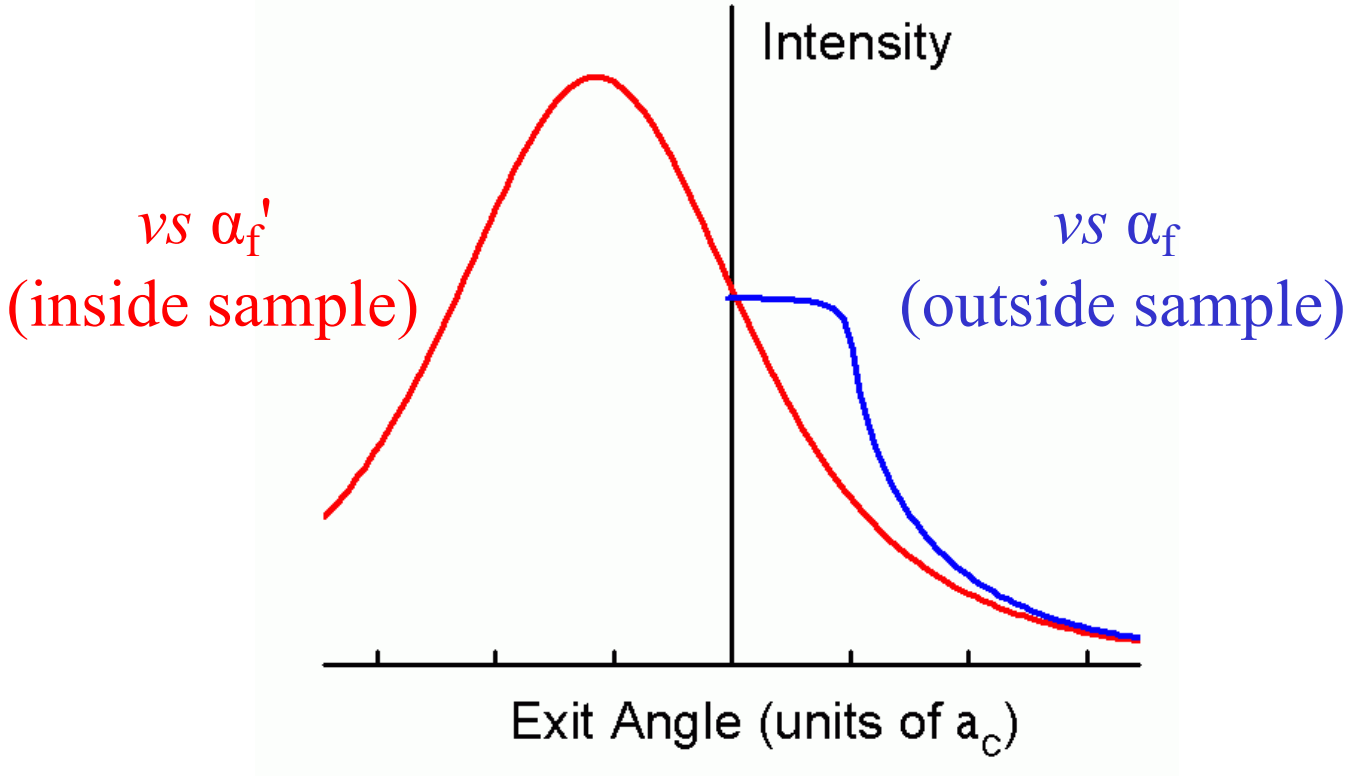

Fits to (Lorentzian)^2 Profiles

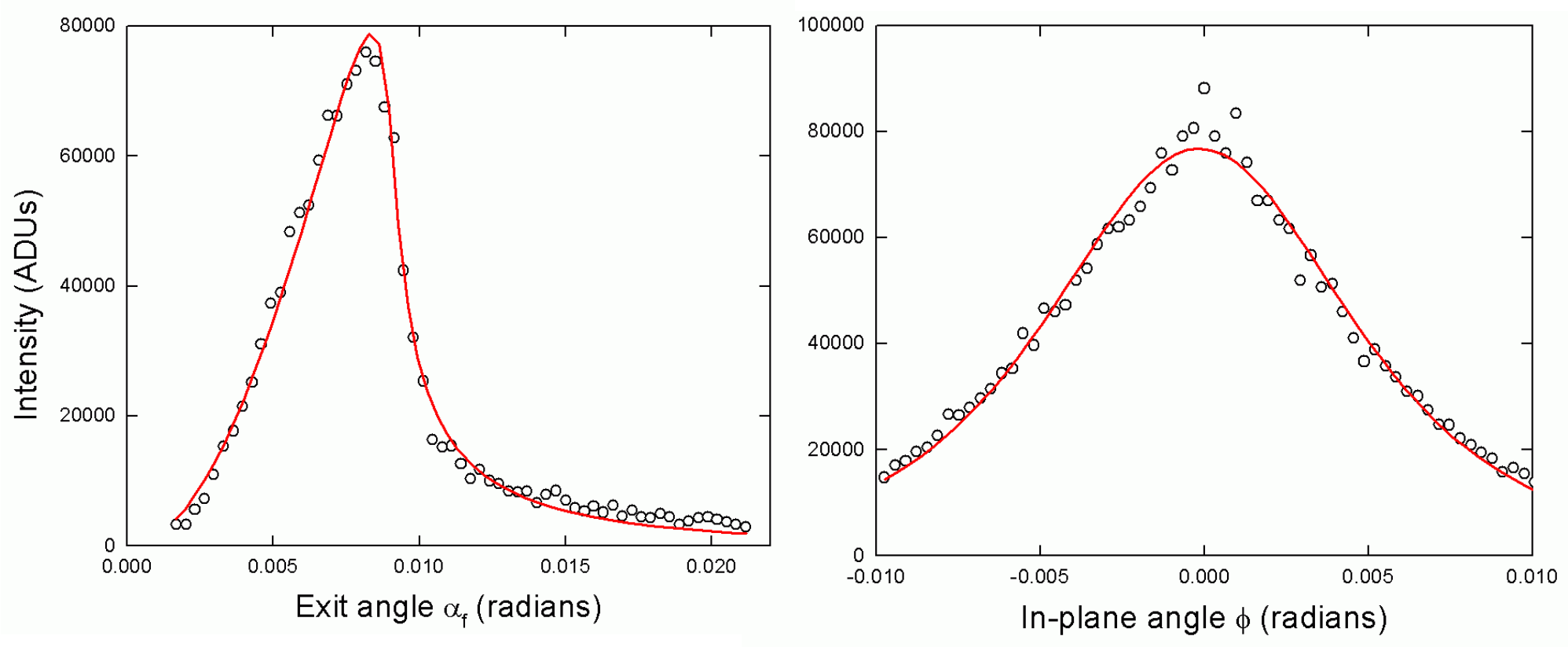

Fit params: center (x,y), amplitude, width=0.0084, α_i=0.011

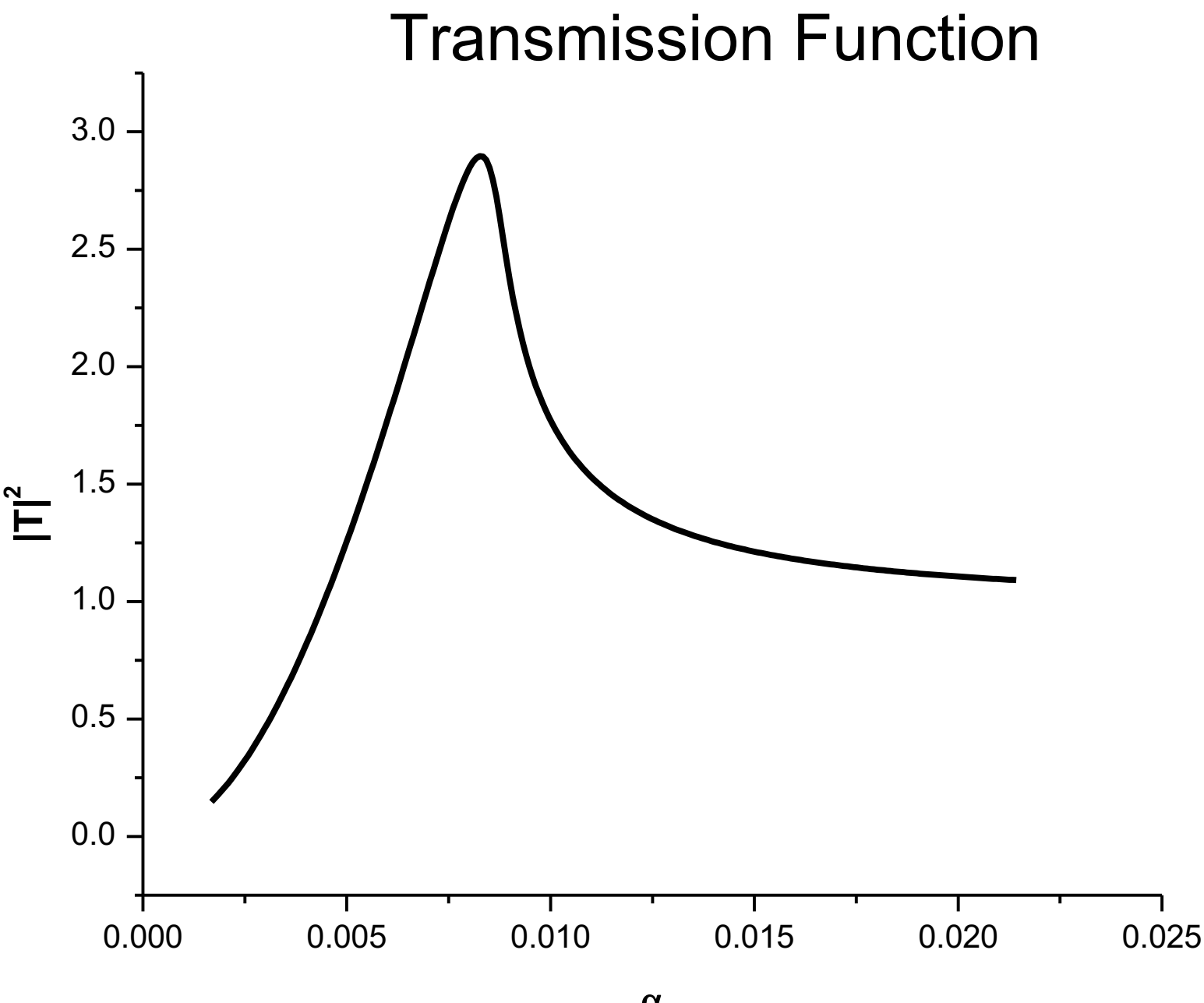
Transmission Function
3.0
2.5
2.0
1.5
1.0
0.5
0.0
|T|²
0.000
0.005
0.010
0.015
0.020
0.025
α

Transmission Function

- Refractive index

$$n = 1 - \delta + i\beta$$

- Snell's law

$$\cos\alpha = n\cos\alpha'$$

$$\alpha' = \mathrm{Re}(\alpha') + \mathrm{Im}(\alpha')$$

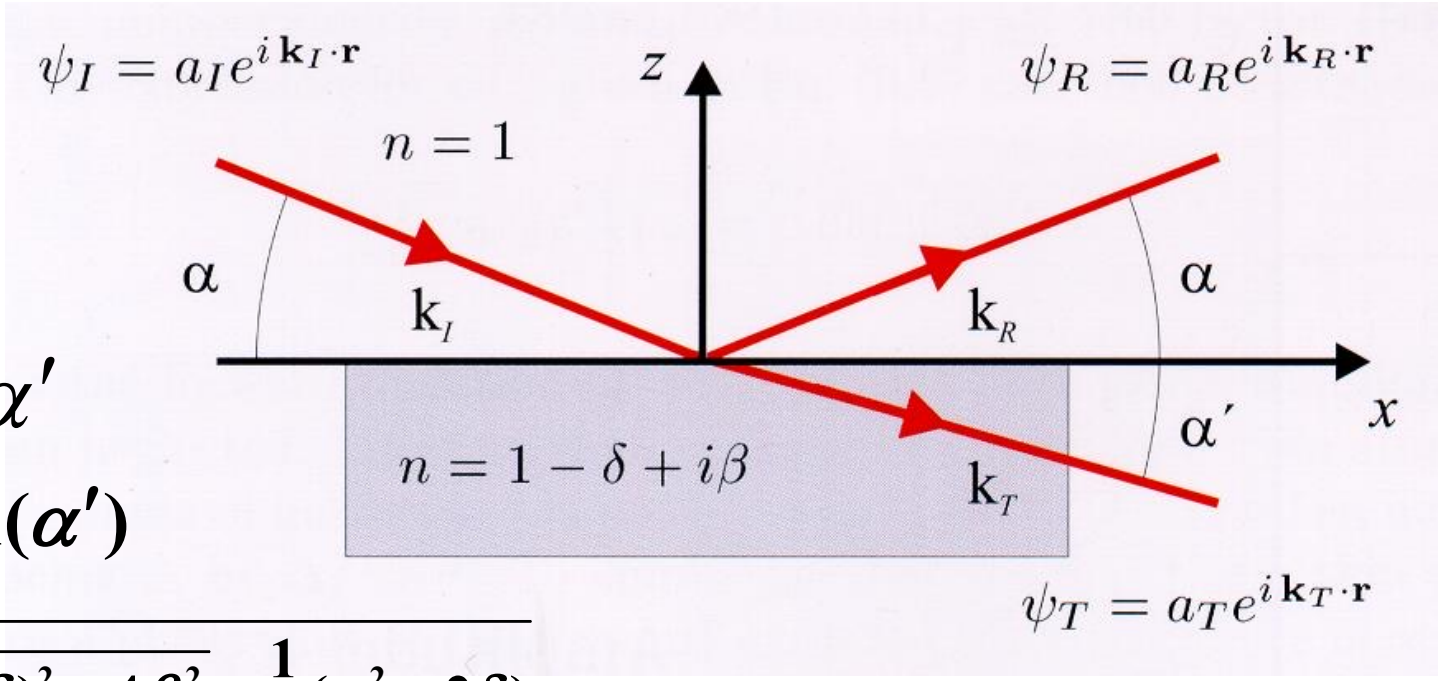

$$\mathrm{Re}(\alpha') = \sqrt{\frac{1}{2}\sqrt{(\alpha^2 - 2\delta)^2 + 4\beta^2} + \frac{1}{2}(\alpha^2 - 2\delta)}$$

$$\mathrm{Im}(\alpha') = \sqrt{\frac{1}{2}\sqrt{(\alpha^2 - 2\delta)^2 + 4\beta^2} - \frac{1}{2}(\alpha^2 - 2\delta)}$$

- Amplitude Transmittivity

$$T = \frac{\alpha_T}{\alpha_I} = \frac{2\alpha}{\alpha + \alpha'}$$

Incidence

$$T(\vec{k}_1) = \frac{2\alpha_i}{\alpha_i + \alpha_i'} = const$$

Exit

$$T(\vec{k}_2) = \frac{2\alpha_f}{\alpha_f + \alpha_f'}$$

Simulations of CCD data

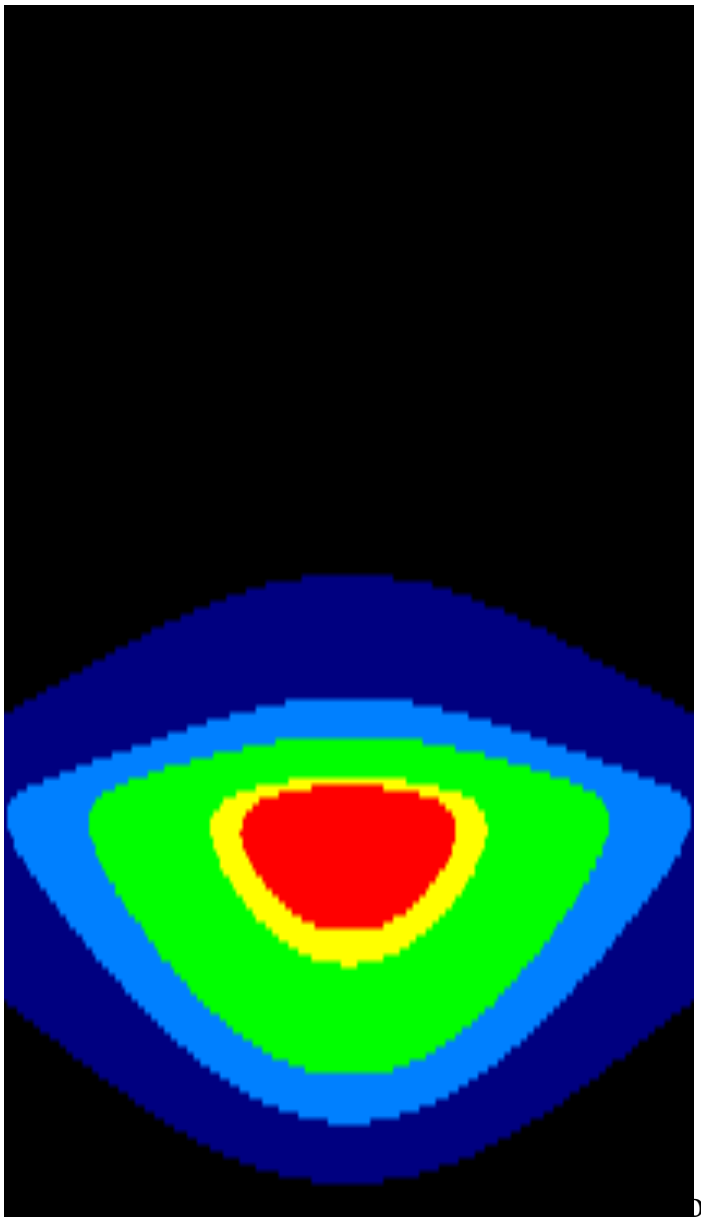

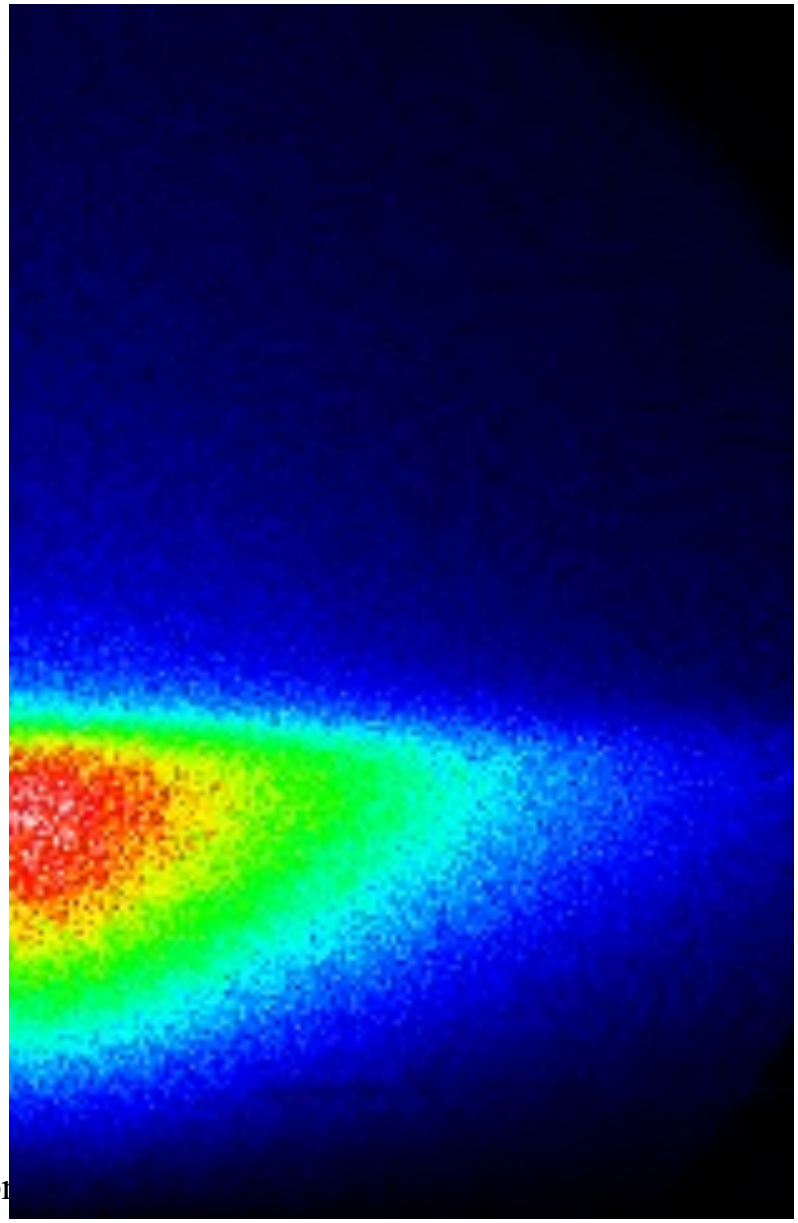

- Distorted-wave Born approximation

$$I \sim \left[\frac{d\sigma}{d\Omega}\right]_{diff} \sim \left|T(\vec{k}_1)\right|^2 \left|T(\vec{k}_2)\right|^2 S(\vec{q})$$

- Assume

$$S(\vec{q}) = \frac{C}{(Q_{2D}^2 + W^2)^P}$$

$$= \frac{C}{((\eta Q_y)^2 + Q_z^2 + W^2)^P}$$

$$or \frac{C}{((\eta\Phi)^2 + (\alpha_i' + \alpha_f')^2 + W^2)^P}$$ with P=2

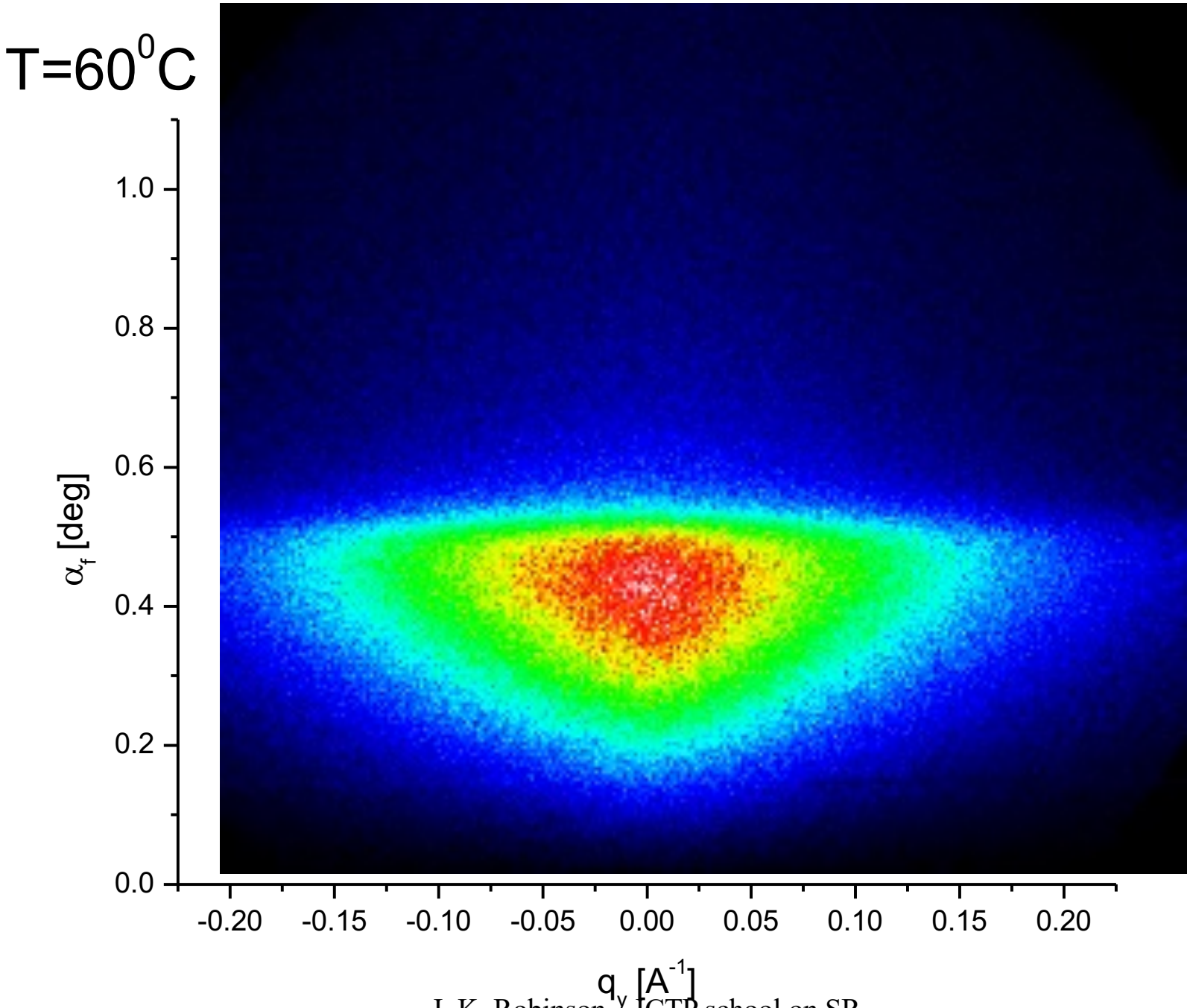
T=60^{0}C
1.0
0.8
0.6
0.4
0.2
0.0
α_f [deg]
-0.20
-0.15
-0.10
-0.05
0.00
0.05
0.10
0.15
0.20
q_y [A^{-1}]

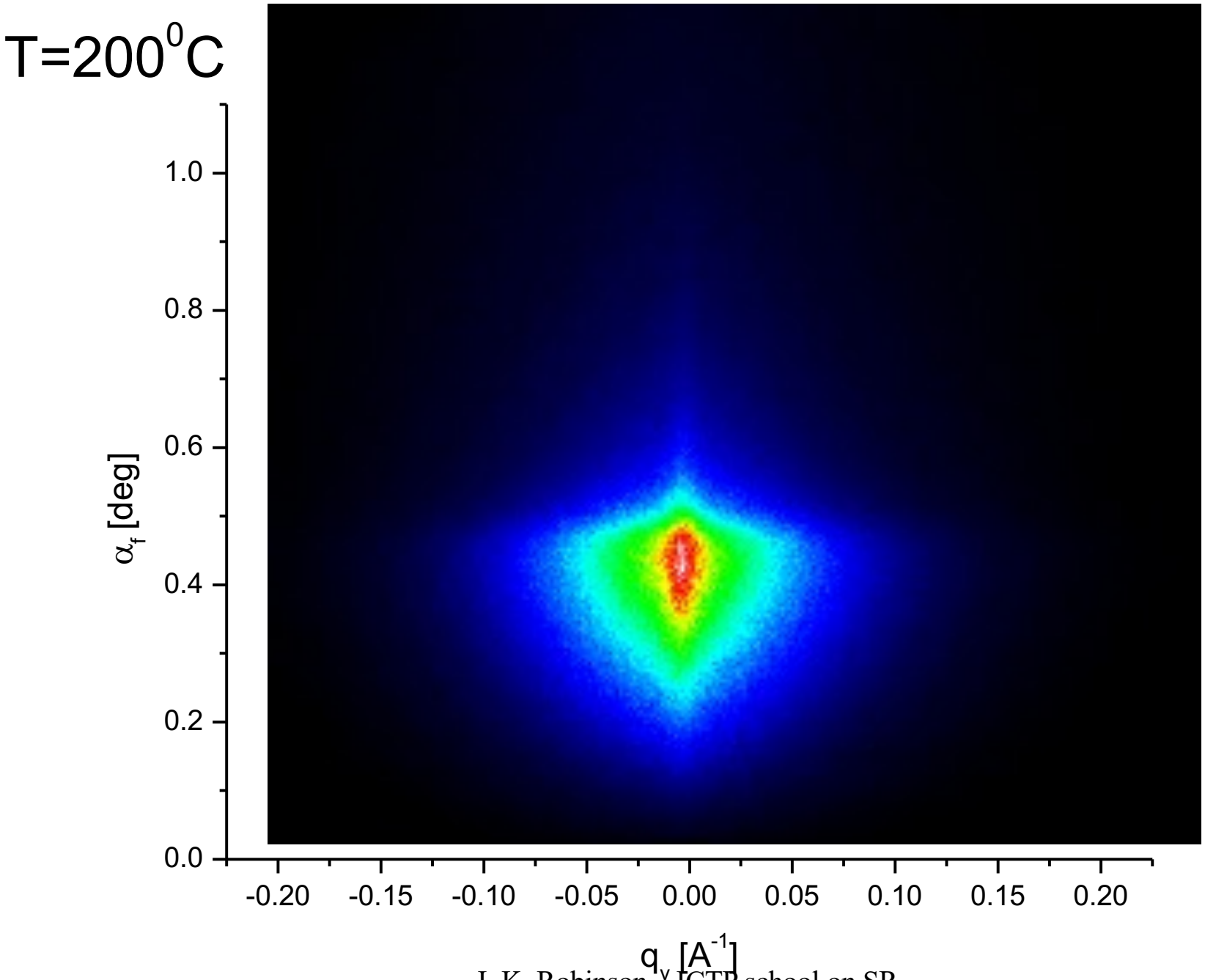
T=200^{0}C
1.0
0.8
0.6
0.4
0.2
0.0
α_f [deg]
-0.20
-0.15
-0.10
-0.05
0.00
0.05
0.10
0.15
0.20
q_y [A^{-1}]

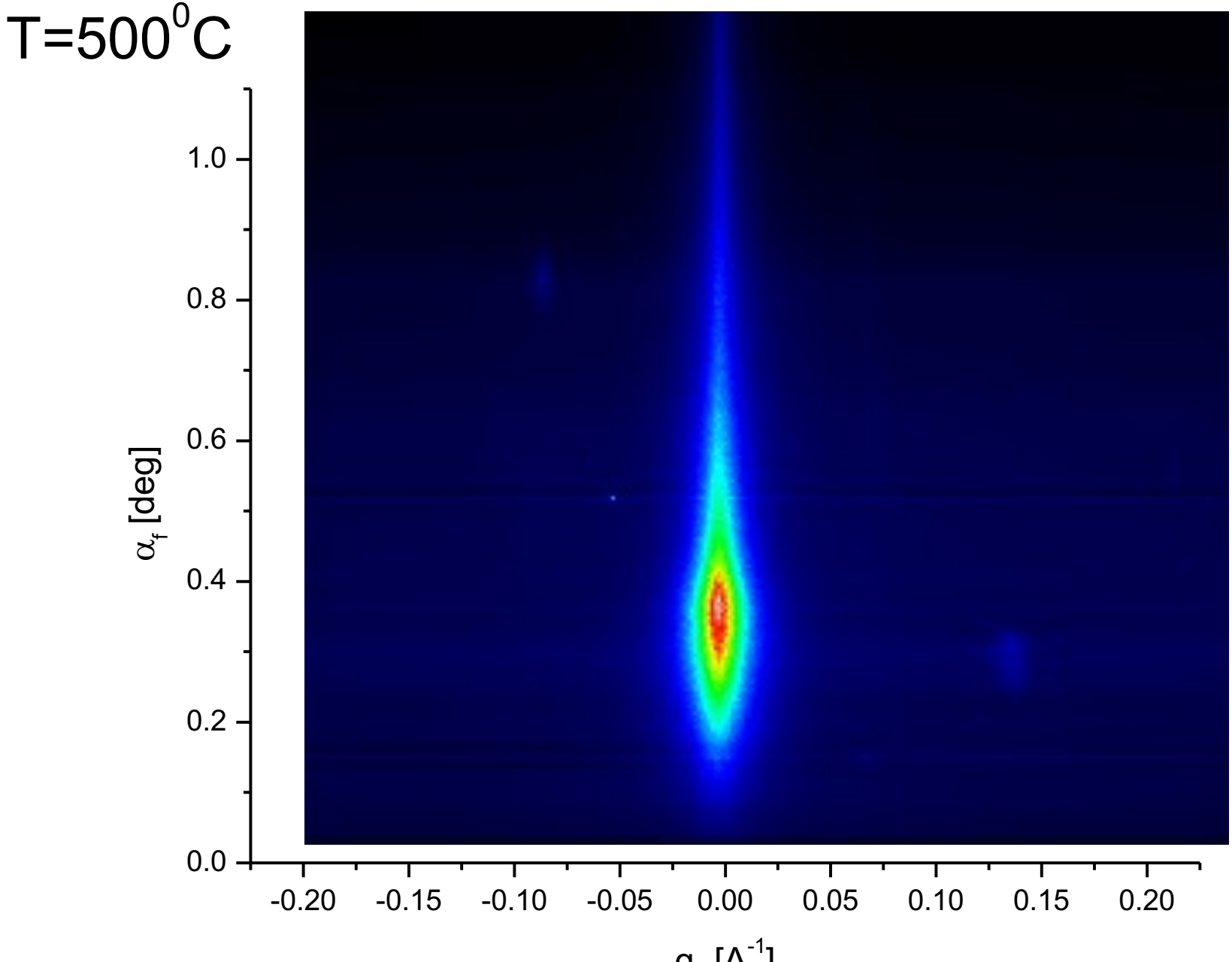
T=500^{0}C
1.0
0.8
0.6
0.4
0.2
0.0
α_f [deg]
-0.20
-0.15
-0.10
-0.05
0.00
0.05
0.10
0.15
0.20
q [A^{-1}]

Future Outlook for GISAXS

- GISAXS explained by refraction + $|T(\alpha)|$
- CGISAXS sees individual grain distribution
- Surface effects are relatively unimportant
- Invert diffraction pattern to an image
- Study evolution grain by grain
- Other metals, kinds of film
- Island to film transition

Conclusions

- Crystal Truncation Rods
- Au quantum nanowires on Stepped Si
- Reconstruction of Pt(110)1x5
- Facetting of Cu(115) to Cu(104)
- Au ‘physisorption’ on Si(111)7x7
- Deep subsurface strain in Pt(111)/CO
- GSAXS and C-GSAXS new methods